RADC-TR-80-115
Interim Report
April 1980

AMOS PHASE IV PROGRAM

AVCO Everett Research Laboratory, Inc.

Sponsored by
Defense Advanced Research Projects Agency (DoD)
ARPA Order No. 2837

Approved for public release; distribution unlimited.

The views and conclusions contained in this document are those of the authors and should not be interpreted as necessarily representing the official policies, either expressed or implied, of the Defense Advanced Research Projects Agency or the U.S. Government.

ROME AIR DEVELOPMENT CENTER
Air Force Systems Command
Griffiss Air Force Base, New York 13441

This report has been reviewed by the RADC Public Affairs Office (PA) and is releasable to the National Technical Information Service (NTIS). At NTIS it will be releasable to the general public, including foreign nations.

RADC-TR-80-115 has been reviewed and is approved for publication.

APPROVED: James W Cusack

JAMES W. CUSACK
Project Engineer

If your address has changed or if you wish to be removed from the RADC mailing list, or if the addressee is no longer employed by your organization, please notify RADC (OCSE) Griffiss AFB NY 13441. This will assist us in maintaining a current mailing list.

Do not return this copy. Retain or destroy.

AMOS PHASE IV PROGRAM

J. Chapman
P. McCormick
AMOS Staff

Contractor: AVCO Everett Research Laboratory, Inc.
Contract Number: F30602-78-C-0061
Effective Date of Contract: 1 January 1978
Contract Expiration Date: 30 September 1980
Short Title of Work: AMOS Phase IV Program
Program Code Number: 8E20
Period of Work Covered: Jan 78 - 31 Dec 78

Principal Investigator: J. Chapman
Phone: 808 877-6594

Project Engineer: James Cusack
Phone: 315 330-3148

This research was supported by the Defense Advanced Research Projects Agency of the Department of Defense and was monitored by James W. Cusack (OCSE) Griffiss AFB NY 13441 under Contract F30602-78-C-0061.

UNCLASSIFIED

SECURITY CLASSIFICATION OF THIS PAGE (When Data Entered)

REPORT DOCUMENTATION PAGE

READ INSTRUCTIONS BEFORE COMPLETING FORM

1. REPORT NUMBER: RADC-TR-80-115	2. GOVT ACCESSION NO.: AD-A088 934
3. RECIPIENT'S CATALOG NUMBER:	
4. TITLE (and Subtitle): AMOS PHASE IV PROGRAM	5. TYPE OF REPORT & PERIOD COVERED: Interim Report 1 Jan 78 - 31 Dec 78
	6. PERFORMING ORG. REPORT NUMBER: AERL TR 1025
7. AUTHOR(s): J. Chapman, P. McCormick, AMOS Staff	8. CONTRACT OR GRANT NUMBER(s): F30602-78-C-0061, ARPA Order-2837
9. PERFORMING ORGANIZATION NAME AND ADDRESS: AVCO Everett Research Laboratory, Inc., Revere Beach Pkwy, Everett MA 02149	10. PROGRAM ELEMENT, PROJECT, TASK AREA & WORK UNIT NUMBERS: 62301E, 28370102, 17 01
11. CONTROLLING OFFICE NAME AND ADDRESS: Defense Advanced Research Projects Agency, 1400 Wilson Blvd, Arlington VA 22209	12. REPORT DATE: April 1980
	13. NUMBER OF PAGES: 227
14. MONITORING AGENCY NAME & ADDRESS (if different from Controlling Office): Rome Air Development Center (OCSE), Griffiss AFB NY 13441	15. SECURITY CLASS. (of this report): UNCLASSIFIED
	15a. DECLASSIFICATION/DOWNGRADING SCHEDULE: N/A

16. DISTRIBUTION STATEMENT (of this Report)

Approved for public release; distribution unlimited.

AERL-TR-1025

17. DISTRIBUTION STATEMENT (of the abstract entered in Block 20, if different from Report)

Same

18. SUPPLEMENTARY NOTES

RADC Project Engineer: James W. Cusack (OCSE) 315 330-3145
Captain G. Dahlen (OL-AB) 808 877-6594

19. KEY WORDS (Continue on reverse side if necessary and identify by block number)

Laser Ranging	Large Optics
IR Radiometry	Adaptive Optics
Telescopes	Imaging
Satellite Observations	Midcourse Measurements

20. ABSTRACT (Continue on reverse side if necessary and identify by block number)

This report summarizes the activities which have occurred at the ARPA Maui Optical Site (AMOS) during the period 1 Jan 78 through 31 Dec 78. These activities have taken advantage of the AMOS facility which was developed by ARPA and now serves as a multipurpose advanced optical testbed. This report contains a complete summary of the development of AMOS, a description of the assets available and summarizes the major accomplishments.

DD FORM 1 JAN 73 1473 EDITION OF 1 NOV 65 IS OBSOLETE

UNCLASSIFIED

SECURITY CLASSIFICATION OF THIS PAGE (When Data Entered)

Ø48459

TABLE OF CONTENTS

LIST OF FIGURES

LIST OF FIGURES

LIST OF FIGURES

LIST OF FIGURES

LIST OF TABLES

1.0 INTRODUCTION

This report describes progress, status and important accomplishments and findings pertaining to the specific tasks that together comprise the AMOS (ARPA Maui Optical Station) Phase IV Program. The period covered is 1 January through 31 December 1978.

The document is divided into four sections. Section 2 gives a brief background of the AMOS facility and summarizes the major accomplishments of previous phases. Section 3 addresses the Phase IV program by first describing the assets available (i.e. the hardware and software systems and capabilities) and then discussing the basic program objectives. This is followed by a summary of significant results and accomplishments achieved during the first year of the Phase IV program and a statement of the important conclusions that can be drawn from these results.

The intent is that Sections 2 and 3 will allow the reader to obtain a basic knowledge of AMOS capabilities and, in particular, a clear understanding of the overall goals and major accomplishments of the Phase IV Program to date.

Section 4 discusses, in detail, progress on specific Phase IV tasks during 1978 and is keyed to the Statement of Work.

2.0 BACKGROUND

The DARPA-sponsored AMOS program has included four phases. Highlights of the first three are given in this section. The fourth is the subject of the remainder of the report.

Phase I spanned the period 1963-1969 and included conception, design, and construction of the basic facility. The University of Michigan was the Phase I contractor. The 1.6 m and twin 1.2 m Telescopes were specified, fabricated, installed and tested. A Control Data Corporation (CDC) 3200 computer, along with first generation pointing and tracking software, was integrated into the facility. Sensors included an IR array for tracking, IR sensor for signature measurements, a low radiance pulsed ruby laser and various imaging devices (e.g. image orthicons and film cameras). The first link to off-island radars was implemented during this period (Kokee Park on Kauai). Although a significant amount of data was obtained on satellites and missiles, Phase I is best described as a period of hardware installation and debugging and development of basic techniques. Phase I, however, clearly demonstrated the potential importance of AMOS and defined directions for the future.

The second phase was from mid-1969 to the end of 1974. Funding came from DARPA via SAMSO. Two contractors were responsible for the program; AVCO Everett Research Laboratory for technical direction and Lockheed Missiles & Space Company for operations, maintenance and development. During Phase II, major improvements were made to test bed and sensor systems. A new

computer system, based upon a CDC 3500/SC-17, was installed which greatly increased AMOS capability and versatility. To augment this hardware, AMOS staff members produced sophisticated new software which allowed simultaneous dual-mount operation along with Kalman Filter-smoothed tracking. Absolute pointing was greatly improved by the development and refinement of mount models. A second radar (Kaena Point on Oahu) was interfaced to AMOS which allowed skin as well as beacon tracking. The original IR tracker was replaced with the state-of-the-art AMTA (Advanced Multi-Color Tracker for AMOS) system which immediately began to provide important signature data. Implementation of AMTA required conversion of the original 1.2 m, B0 Telescope to a B29 configuration (f/20). A high radiance ruby laser was specified, fabricated and installed on what was then the 1.2 m, B30 Telescope. This system was used to obtain ranging data on retro-reflector equipped satellites and to develop techniques and define improvements necessary to fully exploit laser ranging at AMOS. An outgrowth of this effort was the specification and design of a Laser Beam Director facility which was then implemented during Phase III. Improvements in AMOS imaging systems kept pace with the state of the art.

It was during Phase II that AMOS began to routinely provide high-quality data of importance to DoD. Metrics and IR measurements were conducted in support of the MMII, MMIII, HAVE LENT and REVTO programs. IR and visible signatures were obtained on various classes of satellites. Thermal balance

techniques were applied with great success to RORSAT objects. In short, by the end of Phase II, AMOS had successfully made the transition from a university research laboratory to an efficient state-of-the-art DoD measurement facility.

Phase III began in January of 1975 and continued to the end of 1977. AVCO Everett Research Laboratory, Inc. was the sole contractor. Funding again came from DARPA but RADC replaced SAMSO as fiscal agent. Phase III consisted of operations and measurements programs with an overlay of research and development activity.

Measurements continued on MMII and MMIII systems (metrics), HAVE LENT objects (IR masking), and satellites (metrics, signatures). The laser was used for ranging on geodetic satellites and illumination of special targets. Atmospheric characterization hardware was installed and accumulation of a data base was initiated in support of the DARPA Compensated Imaging program. Many special measurement activities occurred during Phase III in areas such as IR and visible radiometry, atmospherics and target signature analysis.

Basic AMOS capabilities were greatly improved during Phase III, as hardware and software modifications continued to be implemented. These improvements were outgrowths of AMOS experience during the first two phases and concentrated heavily on refinement and optimization of existing systems in addition to installation of new and/or modified hardware and software.

Phase III improvements included the following:

- installation of diffraction-limited optics in the 1.6 m Telescope,
- installation/evaluation of the Laser Beam Director facility,
- incorporation of the ruby laser into the beam director,
- new primary mirror support systems for the large optics,
- implementation of beam steering on the 1.2 m Telescopes,
- provision of additional instrument mounting surfaces,
- design and implementation of a contrast mode photometer,
- upgrading of all video imaging systems,
- specification of new acquisition telescopes
- development of long term integration and background characterization hardware for AMTA.

It was also during Phase III that DARPA initiated the transition of a portion of the AMOS facility to ADCOM. Hardware systems involved include the 1.2 m Telescopes along with their sensors and support equipment. The CDC 3500 will be considered as shared equipment, and new hardware and software systems will be

developed to allow timely reduction and transmittal of large amounts of data. The ADCOM portion of the complex will be known as the MOTIF (Maui Optical Tracking and Identification Facility) and is scheduled to become a part of the SPACETRACK network in August of 1979.

By the end of 1977, AMOS had existed for over a decade and had gone through three distinct phases of development. The result was a national asset that can be briefly described as "an advanced electro-optical facility to support critical DoD measurement and development programs operating in a unique environment."

The facility is equipped with state-of-the-art sensors and a sophisticated and versatile computer complex which allows high precision pointing and tracking with the AMOS large aperture optical systems.

3.0 SUMMARY

The AMOS Phase IV program began on 1 January 1978 and ends on 30 September 1980. The objectives of the program have certain important differences from those of the prior three phases. In this section we first describe the systems and capabilities available to accomplish the Phase IV objectives. This is followed by a summary of the objectives themselves. The section concludes with a discussion of important results and accomplishments that have been realized during the first year of the Phase IV program.

3.1 Phase IV Systems

To properly understand the goals and accomplishments of the Phase IV program to date, it is important to have a general knowledge of the hardware and software systems either dedicated or available. These systems are briefly described below:

Facility

AMOS is located on the island of Maui, Hawaii. The observatory facility is situated at an altitude of 3,049 meters (10,000 feet) on the crest of Mount Haleakala. This high-altitude location, in a relatively stable climate of dry air with low levels of particulate matter and scattered light from surface sources, provides excellent conditions for the acquisition and viewing of space objects.

Figure 1 shows an exterior view of the facility. From the left of the figure, the domes are for the 1.2 m Telescopes, the Laser Beam Director, atmospheric instrumentation and the 1.6 m Telescope, respectively.

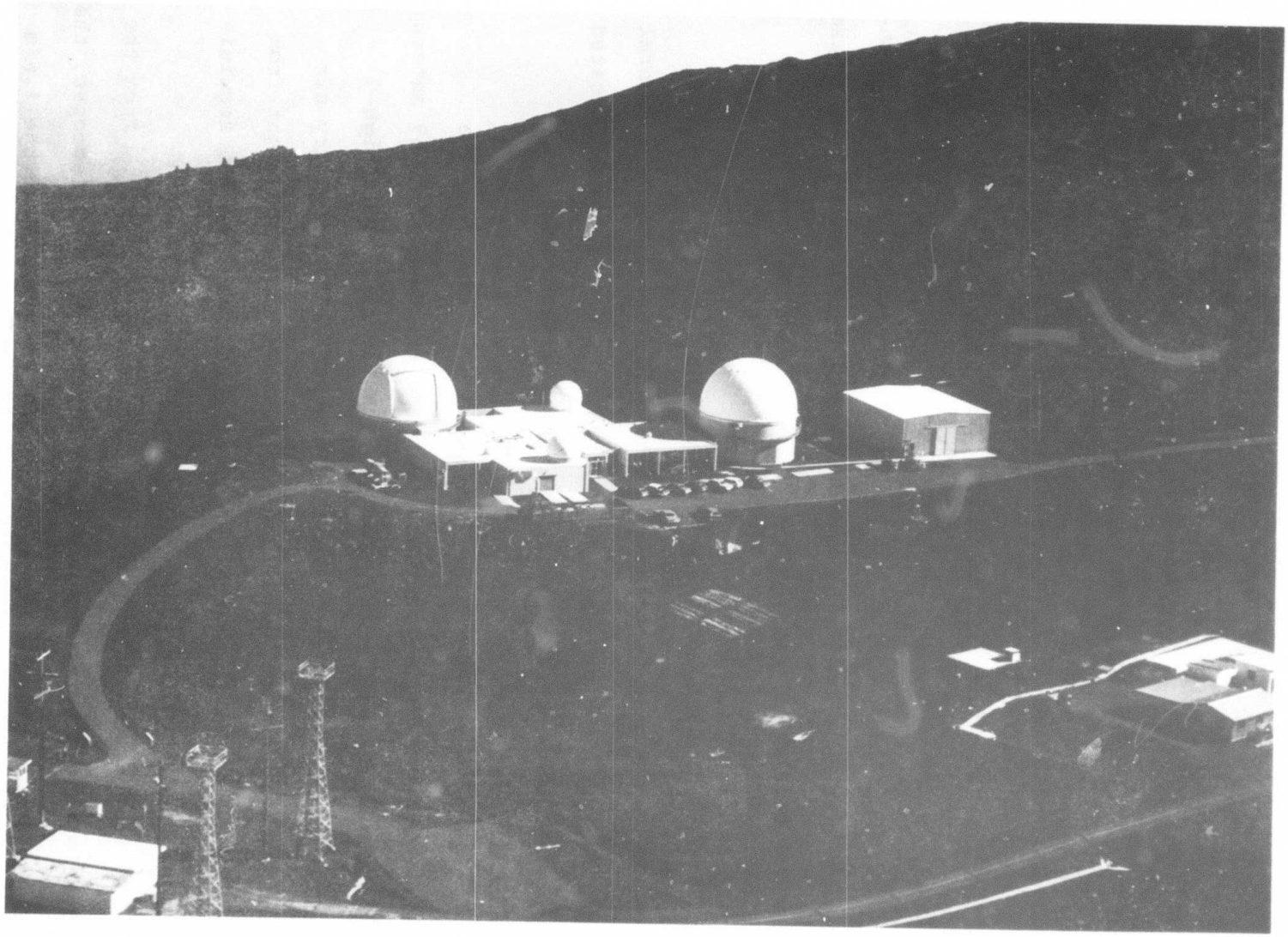

Fig. 1 Exterior view of the AMOS facility.

1.6 Meter Telescope

The AMOS 1.6 m Telescope allows diffraction-limited performance (approximately 0.1 arcsecond resolution) at all mount attitudes above the horizon. The clear aperture is 1.57 m and the effective focal length is 25 m. Two instrument mounting surfaces are available for sensor packages. The rear Blanchard surface will be dedicated to the DARPA Compensated Imaging System (CIS) in 1980. Once this system is installed and operational, system performance should approach the resolution stated above instead of the current 0.5 to 1 arcsecond limit set by typical AMOS "seeing" conditions. The side Blanchard surface supports a classical sensor package which currently includes the laser receiver, a 16 mm film camera, an Intensified Silicon Intensifier Target (ISIT) camera and a visible radiometer. Broadband mirror coatings (Al plus an SiO overcoat) allow spectral coverage from the visible through the LWIR. INVAR metering rods maintain basic intermirror spacing and a computer controlled auto-range system is included. The primary mirror is supported axially with a three-segment airbag and radially with a mercury-filled belt to minimize aberrations and maintain optical alignment.

The mount has fully hydrostatic bearings, a 23-bit shaft angle encoder and is servo-driven by direct current torque motors under computer control. This system allows absolute pointing to about 3 arcseconds rms and tracking to approximately

1 arcsecond rms at slewing velocities up to several degrees per second and accelerations to 2 degrees per second^2.

The AMOS 1.6 m mount, shown in Figure 2, provides a unique and valuable capability for electro-optical research and development programs.

Laser Beam Director

The Laser Beam Director (LBD) was installed during Phase III and provides a versatile pointing and tracking system for use with lasers. The system consists of a 24-inch diameter beam expander (designed for an input beam of 4-inch diameter) mounted on an azimuth turntable and coupled to a 36-inch diameter Beryllium tracking flat. The tracking flat is mounted on an azimuth/elevation gimbal which receives data from the CDC 3500 computer. The pointing and tracking performance of this system is essentially the same as that of the 1.6 m Telescope. The optics are currently optimized for the ruby laser but can be easily modified for other wavelengths.

Versatility was designed into the LBD. During the first year of Phase IV, for example, a special pulsed ruby laser supplied by a user organization was coupled into the system and made available for operations within two days.

A photograph of the LBD is shown in Figure 3. An optical diagram is included in Figure 46.

Pulsed Ruby Laser

The AMOS pulsed ruby laser (λ = 0.694 microns) occupies one channel of the LBD. When operated at 20 pulses per minute,

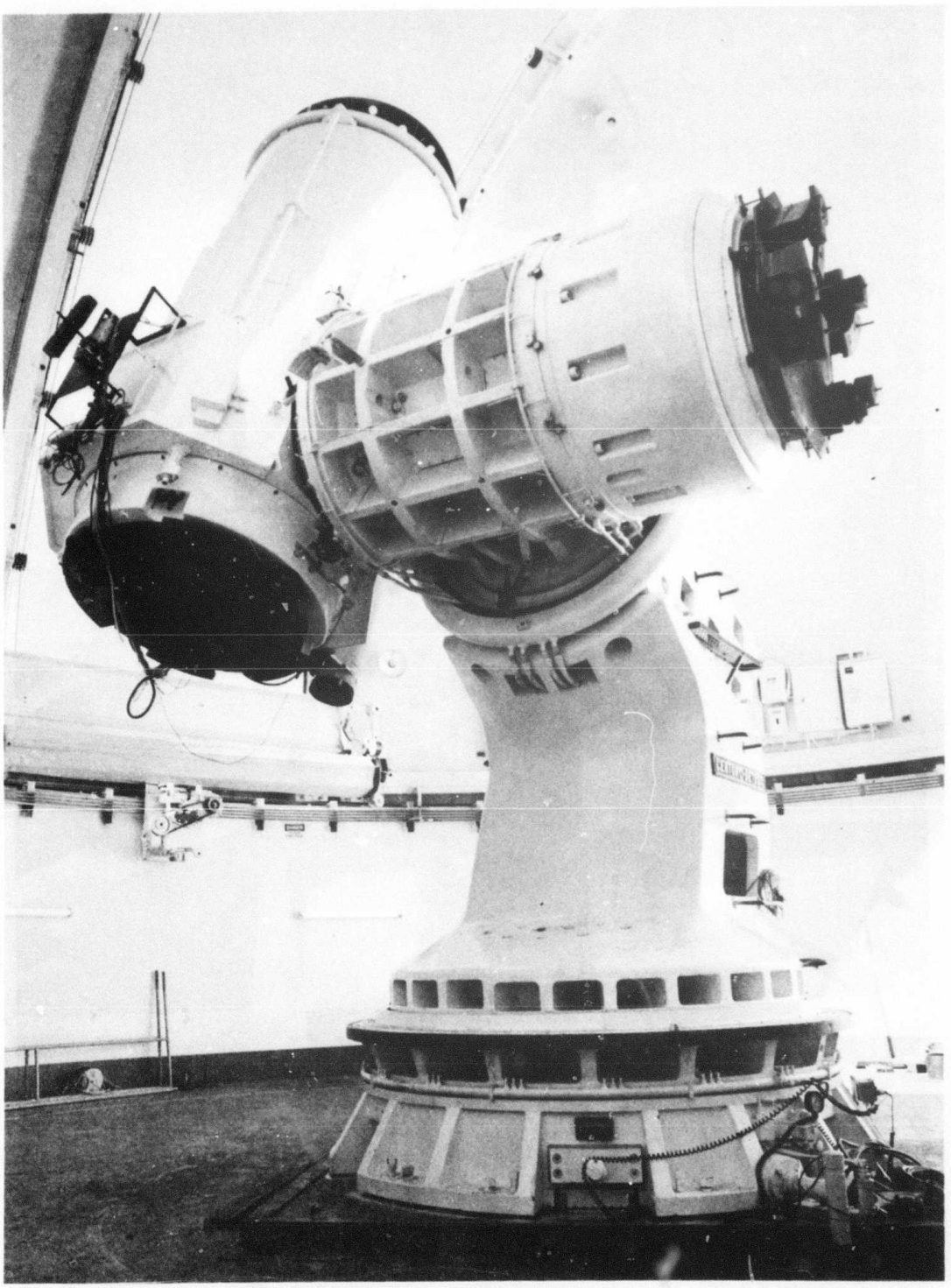

Fig. 2 1.6 meter mount.

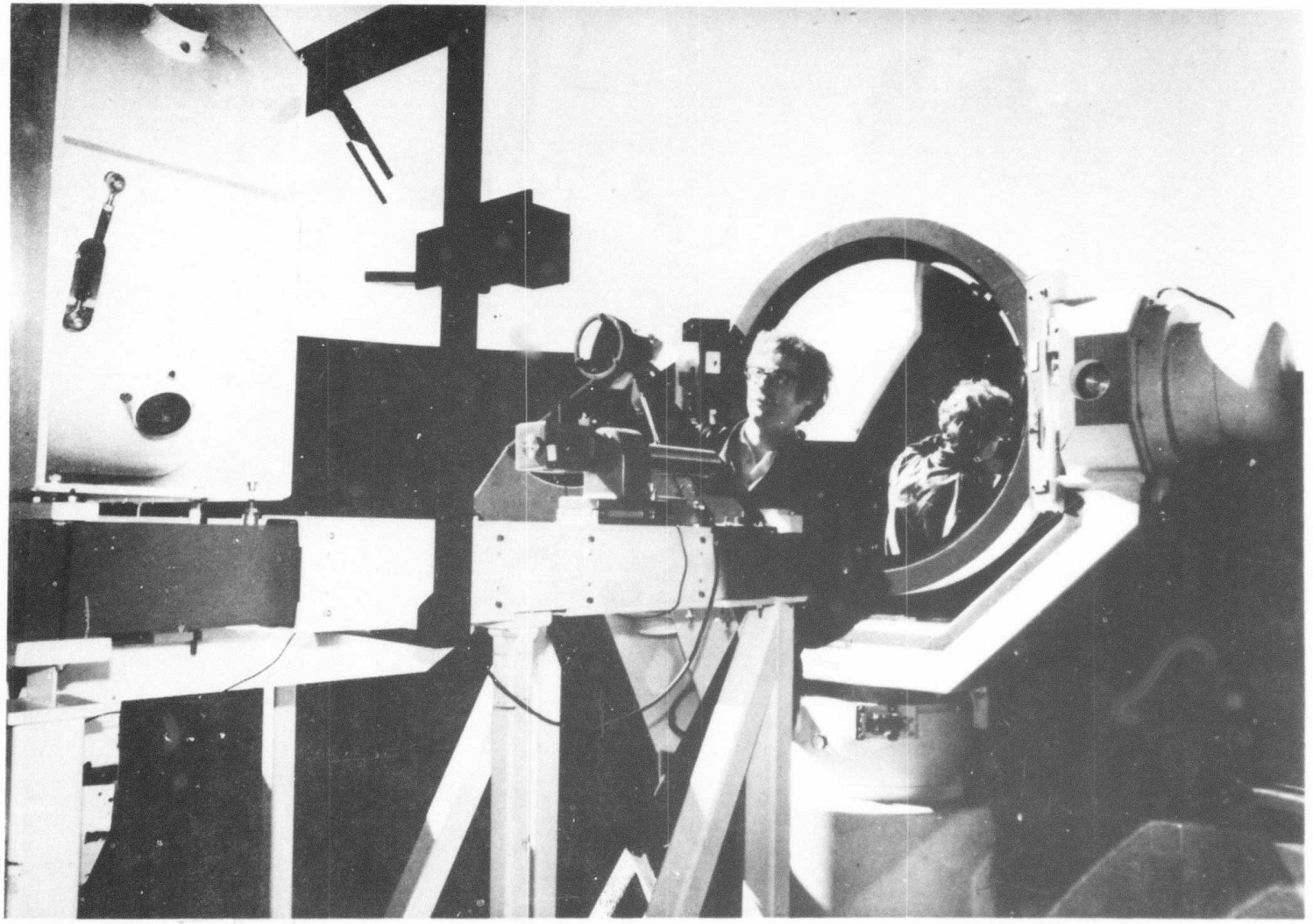

Fig. 3 Laser beam director (6 x beam expander at left gimbaled tracking mirror at right).

the output beam divergence from the 24-inch beam expander can be adjusted to about 2 arcseconds. Q-switched outputs of 10 Joules per 25 nanosecond pulse are used for ranging with precisions of about $\pm$2 m on cooperative targets. Conventional mode operation at the 80 Joule level per 1 millisecond pulse provides an illumination capability. This system is currently being modified for the LBD Phase II Program as discussed in Section 4.10.

Visible Radiometry

A visible-light radiometer is installed on the 1.6 m Telescope and is equipped with various spectral and neutral density filters and adjustable fields-of-view. This system, when operated against a dark night sky, can observe point sources as faint as +18 m_v with a reasonable signal-to-noise ratio. The system is used to measure target radiance and dynamics.

Video Systems

All of the large optical systems are equipped with ISIT cameras (looking through the prime optics) which can be coupled to digital integration and averaging devices. The system installed on the 1.6 m Telescope has been used to photograph a star of apparent visual magnitude +19.5 against a dark night sky. Although these cameras are used primarily to obtain metric data, they can, for example, be used for measurements such as laser illumination.

High Resolution Imaging

The prime sensor for high resolution imaging is a 16 mm film camera located on the side Blanchard surface of the 1.6 m Telescope. This system is currently involved in obtaining a classical imaging data base as a part of the CIS program. Photographs obtained with this hardware are included in Section 4.3.3.3.

LWIR Radiometry

Although the AMTA system will be a part of the MOTIF, it will be available to support Phase IV programs under special tasking.

AMTA consists of a 25-element infrared sensor array mounted directly on the rear Blanchard surface of the 1.2 m B29 Telescope in the west dome. The sensor consists of reimaging optics, servo-driven scan mirror, filter wheel assembly, 25-element Ge:Cd detector array, detector preamplifiers, cryogenic refrigerator dewar, and associated electronics. A beam splitter separates the visible and infrared energy. The visible energy is imaged into a TV camera which serves as an acquisition and pointing aid for the system.

The data is recorded on analog and digital magnetic tape. Recorded are all 25 detectors, a reference calibration, filter position, photometer signal, IRIG B timing and a voice track.

The AMTA sensor permits AMOS to obtain low dispersion spectral data on targets of interest in atmospheric windows between 2 and 21 microns and to perform manual or closed-loop

tracking of targets utilizing real-time position information. The infrared spectral coverage includes 7 bands in the 2 to 21 micron range. The ratio of the signals recorded can be correlated with the temperature of objects of interest. Thermal changes can be determined as the observed body is presented in varying lighting conditions.

Atmospheric Instrumentation

The data output from several atmospheric characterization instruments can be provided to support other data measurements at AMOS. The site supports a continuing Atmospheric Characterization Program whose data can provide information on imaging with a large aperture system in the presence of atmospheric turbulence and allow evaluation of turbulence effects on other types of instrumentation operated at AMOS.

The instrumentation installed at the site includes:

1) Microthermal Probe System
2) Acoustic Sounder
3) Star Sensor
4) Seeing Monitor.

The instrumentation, much of it one-of-a-kind prototype, has resulted from previous studies funded by DARPA/RADC. The sensors were designed to provide information on turbulence at low levels (20 m above AMOS the site), intermediate levels (30 to 300 m), higher levels ranging to the tropopause and finally through the whole atmosphere.

Routine meteorological instrumentation mounted on towers, removed from the basic building structure, record wind speed and direction, ambient temperature and dew point temperature. Atmospheric pressure is obtained from a mercury barometer.

An All-Sky Camera automatically records sky conditions 24 hours per day.

Computer System

The primary function of the AMOS computer system is to provide real-time control of the telescope mounts and Laser Beam Director. The system must calculate, in real-time, target position as a function of nominal ballistic data. It must, in real-time, assimilate radar tracking data and data from a variety of other sensors; compute mount model corrections due to mount anomalies; determine mount position and generate output error signals to the servo systems; respond to real-time perturbations that may be imposed by the test director; and collect and record data for nonreal-time reduction.

The AMOS computer system consists of a medium size general-purpose CDC 3500 computer, an SC-17 sequence controller, a buffer transfer unit (BTU), and 1500 series peripheral equipment.

A 65K-word memory, of 24 bits per word, is utilized with the 3500. The primary task of this computer is to perform real-time trajectory calculations and optimize trajectory determination by application of the Kalman Filter to estimated state vectors updated by observed inputs. Capabilities for processing of multiple state vectors (targets), multiple radars (tracking),

AMOS sensor inputs and external interrupts from the test conductor are also available in this computer. Other functions of the 3500 computer include coordinate transformations, numerical integration, mount model, and other extensive calculations which involve floating point or transcendental functions.

The SC-17 sequence controller is particularly adapted to real-time data acquisition and A/D systems applications. Thus, this unit is the controller of real-time events and processor of operator commands and SC-17 peripheral data which do not require processing by the 3500 computer.

The above paragraphs describe the basic hardware and software systems that are being used to accomplish the AMOS Phase IV Program goals - to which we now turn our attention.

3.2 Phase IV Objectives

The AMOS Phase IV Program consists, in a contractual sense, of various tasks to be accomplished by AERL. Figure 4, for example, shows these tasks in the form of a Work Breakdown Structure which is useful for program management and control purposes.

Certain tasks (e.g. system testing, maintenance, calibration and data reduction) represent well-defined areas of activity designed to maintain the AMOS resource at its current level of performance. All of these activities are essential if the major hardware/software systems are to be operated effectively.

Other tasks represent the real return for DARPA's investment in AMOS. The Measurement Program includes those activities

which, using existing or slightly modified AMOS capabilities, provide state-of-the-art support to Government user agencies. The area of Visiting Experiments encompasses activities that involve an individual or group wishing to use AMOS systems and capabilities to augment their programs. Large System Test Support represents implementation and exploitation of major DARPA programs initiated during Phase III.

A statement of the Phase IV objectives could, therefore, be made by including a description of the requirements for each of the individual tasks. This approach, however, would not clearly reveal the fundamental goals of the Phase IV Program which are far more simply and better stated as follows:

1. EXPLOITATION OF EXISTING CAPABILITIES

   Use the high-quality systems and techniques developed during previous phases to support DoD measurement objectives (visiting experiments, measurement programs).

2. EVALUATION OF NEW TECHNOLOGIES

   Use the inherent AMOS capability and versatility to test, evaluate and bring to operational status various state-of-the-art DoD technologies (DARPA compensated imaging system, advanced electro-optical devices).

3. Improvement of Basic Capabilities

   Continue to improve the performance of test bed and sensor systems and develop new measurement and analysis techniques in order to assure that AMOS keeps pace with the demands of 1 and 2 (improved target state vectors for handoff).

Accomplishment of these three objectives is the real purpose of the AMOS Phase IV Program and any success that is achieved on the individual tasks that comprise the program must be judged accordingly.

3.3 Results, Accomplishments and Conclusions

This section summarizes important results and accomplishments that have been achieved during the first year of the AMOS Phase IV Program.

In order to emphasize the connection between the work actually being conducted during Phase IV and the general goals discussed in Section 3.2, the approach taken here is to combine the results of individual tasks under a few general headings. Section 4 gives detailed descriptions of the individual tasks keyed to the Statement of Work.

Measurement Programs

As emphasized in Section 3.2, one of the basic Phase IV objectives is to fully exploit AMOS capabilities in support of critical DoD measurement programs. This objective was certainly satisfied during 1978.

Two periods (March and October) of measurements were conducted in support of the SAMSO Evaluation Program (SEP). Data obtained during March was reduced and published in two classified reports (AERL-78-167 and AERL-78-179). Data obtained in October was degraded by unfavorable weather conditions and was not reduced. To support these measurements, AERL incorporated a major improvement into the AMTA IR measurement system which has resulted in a 30-fold reduction in scan noise (Section 4.3.1.1).

Three Western Test Range (WTR) launches were supported by AMOS to obtain data for the U.S. Army Ballistic Missile Defense (BMD) program. The prime sensor was the AMTA IR measurements system operating in the 8-9 micron and 10-13 micron spectral bands. Primary interests were target signatures and determination of target color temperature. Data and conclusions are contained in a classified report (AERL-78-398).

Two planning meetings were held during 1978 to discuss the HAVE LENT IV and HAVE LENT V measurement programs. HAVE LENT IV is currently scheduled for the Fall of 1979. Essentially, all AMOS measurement systems will support these experiments which involve high-altitude aerosol releases from sounding rockets launched from the Barking Sands test range on Kauai.

AMOS began a very important new measurement program in the Fall of 1978 to obtain data for the Air Force Weapons Laboratory (AFWL). The overall AFWL goals are: (1) development of an IR adaptive optical system to compensate for atmospheric turbulence,

(2) solution of shared aperture problems that arise when using a single system for transmission and reception of radiation and (3) solving the problem of predicting and correcting for turbulence to be encountered by the transmitted beam.

A major contribution at AMOS to the AFWL program will be to demonstrate the use of an IR detection system to acquire targets without visual or radar assistance. In addition, an IR signature base is being obtained to further define the detection probability for a given search system and scenario.

Measurements began in support of the AFWL program in November 1978. Sky radiance measurements (which can be related to real-time atmospheric transmittance) were completed by the end of the year and a report is being prepared. Figure 14 shows an example of sky radiance data obtained with the AMTA system. Sky granularity measurements were initiated in December 1978. The basic thrust of this work is to investigate the possibility of achieving clutter cancellation in real-time for an appropriate IR sensor, thereby reducing the observation time required to achieve a given measuring precision by as much as a factor of 100. The AMTA system is being used to obtain data to confirm or refute theoretical predictions for scaling atmospheric radiant structure.

A third type of measurement activity being conducted by AMOS for the AFWL program involves satellite acquisition statistics and target signatures. These measurements are divided into three phases with an enhanced capability incorporated into AMTA

for each phase. The first phase will develop an IR target signature data base for a group of selected targets and provide a history of offset tracking information. The offset data will be used, in part, to define the field-of-view requirements for an automatic search system. The signature data will assist in defining the required integration time for the search and provide design information for future, more complex, IR detection systems.

The second phase will investigate the utilization of AMTA as a target tracker. The scanning secondary mirror will eliminate the cavity noise normally generated by the internal scan mirror system. Outputs for the twenty-five detectors will be displayed on one of the AMOS TV networks for utilization by the Video Auto Tracker. A tracking accuracy of about 15 arcseconds is expected.

An automatic search routine will be incorporated into the third phase of measurements. Tracking accuracy will be improved by an order of magnitude by incorporating a modification to the target scan pattern and by the addition of post-detection processing. The post-processing will be accomplished by a dedicated microcomputer. For the brighter satellites, it will be possible to define target position on the array with finer than pixel-limited resolution and provide tracking precision in the realm of 1 to 2 arcseconds.

In summary, significant measurement support to DoD programs was provided by AMOS during 1978. Data obtained by the AMOS

sensors will be of great value in making long-term decisions regarding the directions that these and other programs will take in the future.

Visiting Experiments

Another area that received significant attention - and produced important results - during 1978 involved support to visiting experiments at AMOS. Two experiments (Sandia Laser Experiment and Atmospheric Characterization Program) were performed and a third (AFWL IR FLIR Measurements) was initiated. Also, the possibility of several new experiments was explored through briefing contacts. These possibilities include a Patrick AFB Laser Experiment, a SAMSO CW Laser Experiment and measurements of an Instrumented Test Vehicle.

The Sandia Laser Experiment was first initiated in the Summer of 1975 during which time the capability to successfully point a ruby laser beam (using the AMOS Laser Beam Director) at a satellite during the daytime hours was demonstrated. The objective of the program was to establish a calibration of the satellite on-board sensor over the entire diurnal cycle using laser excitation. Since the satellite could not be visually acquired during the daytime, pointing was accomplished by means of known orbital elements and an accurate mount model.

The actual calibration was accomplished during the period between July 12 and July 22, 1978. Due to the particular pulse waveform requirements imposed by the satellite sensors, a special cooled ruby laser system supplied by Sandia was used in

the experiment. Beam forming and pointing was accomplished using the AMOS Laser Beam Director system.

In addition to successful accomplishment of the basic experimental goals, several valuable results were obtained that will lead to improved AMOS capabilities in the future.

During the course of the daytime measurements, it was discovered that the Laser Beam Director was experiencing severe pointing drifts. It was also noted, by observation of the return from the retro-reflectors, that the beam expander system was tending to defocus in the presence of solar heating. The pointing drift problems, also a result of solar heating (particularly on the gimbal system), were circumvented in real-time by frequent reference to bright stars which could be observed in the daytime on the Boresight TV. The observed stellar offsets were then added to the satellite tracking commands.

The ultimate solution to the problem, however, is to provide protective shielding for both the 24-inch collimator and the gimbals of the 36-inch tracking flat. Since the collimator is not moved during satellite tracking, the entire expander system can be enclosed in a solar reflecting tube which will serve to maintain a uniform temperature throughout the collimating and beam folding optics. Additionally, the shaft angle encoders and bearings of the tracking flat can easily be protected from direct solar illumination through the use of shields. Further protection could be included by restricting the dome slot width, particularly for the tracking

of synchronous satellites. These improvements will be incorporated prior to the Patrick AFB experiment.

The program also provided an opportunity to obtain a measure of the far-field intensity pattern of the Laser Beam Director system. With the availability of a feedback link, which provided a direct measure of the relative magnitude of the target irradiance, it was possible to obtain a rough map of the beam pattern. Section 4.3.2 includes samples of the data obtained. The significant point here is that the satellite sensors provided valuable information on the laser far field intensity profile. This will be extremely useful in predicting returns from non-cooperative targets and in tailoring the Beam Director optics to achieve the optimum beam pattern for such targets.

During the period 17 July to 11 August 1978, a visiting experiment was conducted in support of an existing Atmospheric Characterization program. The experiment was designed to meet the following four objectives: (1) Obtain data to characterize the angular dependence of seeing; (2) Investigate the short-term statistics of seeing; (3) Characterize the noise in the AMOS Model II Star Sensor; (4) Process existing data previously collected with the Real-Time Atmospheric Monitor (RTAM).

Brief descriptions of each of these tasks, the measurements implemented and the results are given in Section 4.3.2.

As part of the AFWL IR Measurement program, a visiting experiment will be conducted at AMOS during the months of April

and May 1979. A FLIR (Forward Looking Infrared) sensor and associated adaptive optics package will be mounted on the rear Blanchard surface of the 1.6 m Telescope. The package will be used to demonstrate the acquisition and tracking of satellites, particularly in the daytime, and to investigate the capabilities of an infrared adaptive optics system.

In preparation for this experiment, modifications are being made to the 1.6 m Telescope and to room 26 of the Observatory which will house the system control electronics. A six-inch diameter Germanium lens will be installed in the optical system of the f/16 telescope to convert it to an afocal system as required by the FLIR. The requirements for the system control electronics which will be housed in room 26 are similar to the demands of the ITEK Compensated Imaging System which will be installed in this same room in 1980. The modification schedule for room 26 is being accelerated for this visiting experiment.

Compensated Imaging Support

Success of the Compensated Imaging System (CIS) is of prime importance to the Phase IV Program. When proven and operational on the 1.6 m Telescope, the CIS will represent a major technological breakthrough. This capability will provide, in principle, imagery of orbital and suborbital objects with an angular resolution approaching the diffraction limit of the systems' foreoptics. In the case of the AMOS 1.6 m Telescope, this is about 0.1 arcseconds which represents an order-of-magnitude improvement over the average limit imposed by atmospheric seeing.

Perhaps of equal importance is that the CIS will be the first field demonstration of a fully adaptive optical system. Such optics have been considered for a variety of applications; hence, an operational CIS will have wide ranging impact.

Current AMOS support to the CIS program includes: (1) site preparation, (2) interfacing with CIS contractors, (3) performance of special measurements and tests to assure compatibility of the new hardware with AMOS and to aid in CIS design decisions and (4) development of classical imaging and atmospheric data bases to allow performance evaluation and optimization when the CIS hardware arrives on-site in 1980. Significant progress was made in all of these areas during 1978.

Vibration tests (Section 4.3.3.2) were conducted on the 1.6 m Telescope to aid Itek in their design of mechanical structures for the CIS telescope-mounted components.

The 1.6 m Telescope was loaded with weight (over 5,000 pounds) to simulate the CIS hardware. The telescope was then tested for step response and velocity and acceleration performance (Section 4.3.3.2). These tests are of critical importance since the telescope-mounted equipment has increased significantly in weight as Itek's system design has progressed. Moments of inertia now exceed those originally specified for the 1.6 m Telescope. Although performance has not yet been significantly degraded, concern does exist and testing will continue in parallel with the design effort.

By the end of 1978, AMOS engineers - working with CIS contractors and appropriate subcontractors - had completed designs of the extensive facilities modifications that are required to support the CIS system (Section 4.3.3.5). These modifications include installation of special wiring and air conditioning systems as well as alterations to existing buildings. All work is scheduled to be completed early in 1979.

Major accomplishments in the area normally defined as classical imaging, i.e., imaging without adaptive optics, were achieved during 1978. To support this program, AMOS engineers designed and fabricated a versatile sensor package which was subsequently installed on the side Blanchard surface of the 1.6 m Telescope. Also, computer-controlled motion of primary/secondary mirror spacing (to account for focal plane offsets due to non-infinite target ranges) was implemented on the 1.6 m Telescope. These new hardware capabilities, when combined with the diffraction limited optics of the 1.6 m Telescope and new measurement techniques developed during the Summer of 1978, resulted in excellent resolved images of several near-earth satellites (section 4.3.3.3).

The atmospherics instrumentation systems that had been developed and evaluated during the Phase III Program were brought to an operational status during 1978. By the end of the year, joint classical imaging/atmospherics measurements

were being conducted. These measurements will continue during 1979 to obtain the required data base for the CIS program.

Target State Vectors

During the latter part of Phase III, a program was initiated to determine system performance parameters and hardware necessary to generate improved target state vectors by including laser range data. The goal was to provide a hand-off vector to down-range sensors. This activity included range measurements with the AMOS LBD/Ruby Laser system and development of a model to budget permissible errors, thereby defining necessary improvements. During Phase IV, these improvements are being implemented at AMOS and a real-time hand-off will be demonstrated.

This program is called LBD Phase II and is described in detail in Section 4.10. Some of the important results to date are summarized here.

Laser ranging and angular pointing data obtained at AMOS were reduced and used in conjunction with a model developed by AERL to evaluate measurement error and observation scenario effects on hand-off accuracy. The measurement errors were determined to be about ± 2 arcseconds (one standard deviation) in angles and about ± 2 meters (one standard deviation) in range. Propagated down range, these uncertainties result in a maximum predicted error ellipsoid axis of the order of 30 meters, 3σ, at 90 kilometers (300 kft) target altitude. This result is well within that required by overall program goals.

The ranging data used in the analysis were obtained on the

retro-reflector satellite GEOS-C. The return from this target, using the AMOS Ruby Laser as the transmitter and the 1.6 m Telescope as the receiver, is the order of 10^6 photoelectrons per laser pulse. When the same system is used to range on a 1 m^2 Lambertian-type target at 1600 km range, the return is only a few photoelectrons per laser pulse. Actual hand-off of a typical target of interest, therefore, presents a far more difficult problem than obtaining an updated state vector on GEOS-C.

In order to accomplish the hand-off demonstration, several upgrades to the laser receiver/detector system are being implemented. This work began in the Summer of 1978 and includes installation of more sensitive detectors on the 1.6 m Telescope along with development of a computer-controlled range gate and a multiple-target ranging receiver. The latter improvement will allow low level returns to be processed even in the presence of noise. New software is being developed for these new hardware systems. In addition, a major software effort is required to include range in the Kalman filter and to provide the required hand-off state vector to the down-range sensor.

By the end of 1978, all of the above work was progressing satisfactorily and on-schedule. The actual demonstration of real-time hand-off is scheduled for July/August of 1979.

Systems Support and System Testing

Although not as exciting, perhaps, as the measurement and experimental programs discussed in the preceding paragraphs, the activities termed systems support and system testing are

no less important to the accomplishment of overall program goals. The two categories obviously augment each other. Problems observed during measurement programs generate a period of system testing which, in turn, normally leads to a system improvement that consequently further increases AMOS measurement capabilities.

Systems support and testing activities are discussed in detail in Sections 4.1 and 4.2. Two important examples are (1) provision of new acquisition telescope systems for both of the large telescopes and (2) development of the computer-controlled auto-focus capability referred to previously. The requirement for more sensitive (+16 m_v against a dark night sky) and versatile acquisition telescopes was generated by current and planned measurement programs. The systems are scheduled for installation early in 1979. The need for a computer-controlled auto-focus capability on the 1.6 m Telescope arose from the stringent requirements of the Classical Imaging effort. This capability was implemented during 1978.

Conclusions

The first year of the AMOS Phase IV Program has seen significant progress in the areas of measurements, visiting experiments and system development.

Data was obtained during the year that is of great value to various DoD programs. This data has included LWIR and visible radiometric signatures of space objects, high precision metric information (both angles and range) and images that

approach the diffraction limit of the 1.6 m Telescope.

Special support was given to outside users in the area of visiting experiments. The state-of-the-art AMOS systems were completely successful in achieving the individual program goals.

In parallel with these measurements and experiments, major improvements were and/or are being implemented in the LWIR, laser, software and test bed systems. As the new capabilities inherent in these improvements become available, AMOS will be able to provide additional measurement support to the DoD community and continue to satisfy the basic program objectives.

4.0 PROGRESS ON PHASE IV TASKS

The following sections discuss, in detail, progress on specific Phase IV tasks during 1978 and are keyed to the contract Statement of Work.

Figure 4 shows the Work Breakdown Structure (level three) which is used internally by AERL to monitor the progress and status of individual tasks.

4.1 Systems Support

The basic requirement of the Systems Support task is to assure that all existing AMOS systems are operational, calibrated, and optimized for conduct of measurement and experimental programs. This task is concerned with areas of system testing, evaluation and optimization that are not necessarily covered in a routine manner or by established procedures as are, for example, system maintenance and periodic testing. In short, a major goal of this task is to assure the integrity of all AMOS systems.

A second, equally important, goal of the Systems Support task is to expand and develop existing AMOS capabilities such that AMOS can continue to respond to the evolving requirements of new measurement and experimental programs. This is accomplished by conducting tests and performance evaluations on existing systems, identifying directions for improvement and, after approval by RADC, implementing these improvements.

Although hardware and software systems are of equal importance from the standpoint of mission success, they require

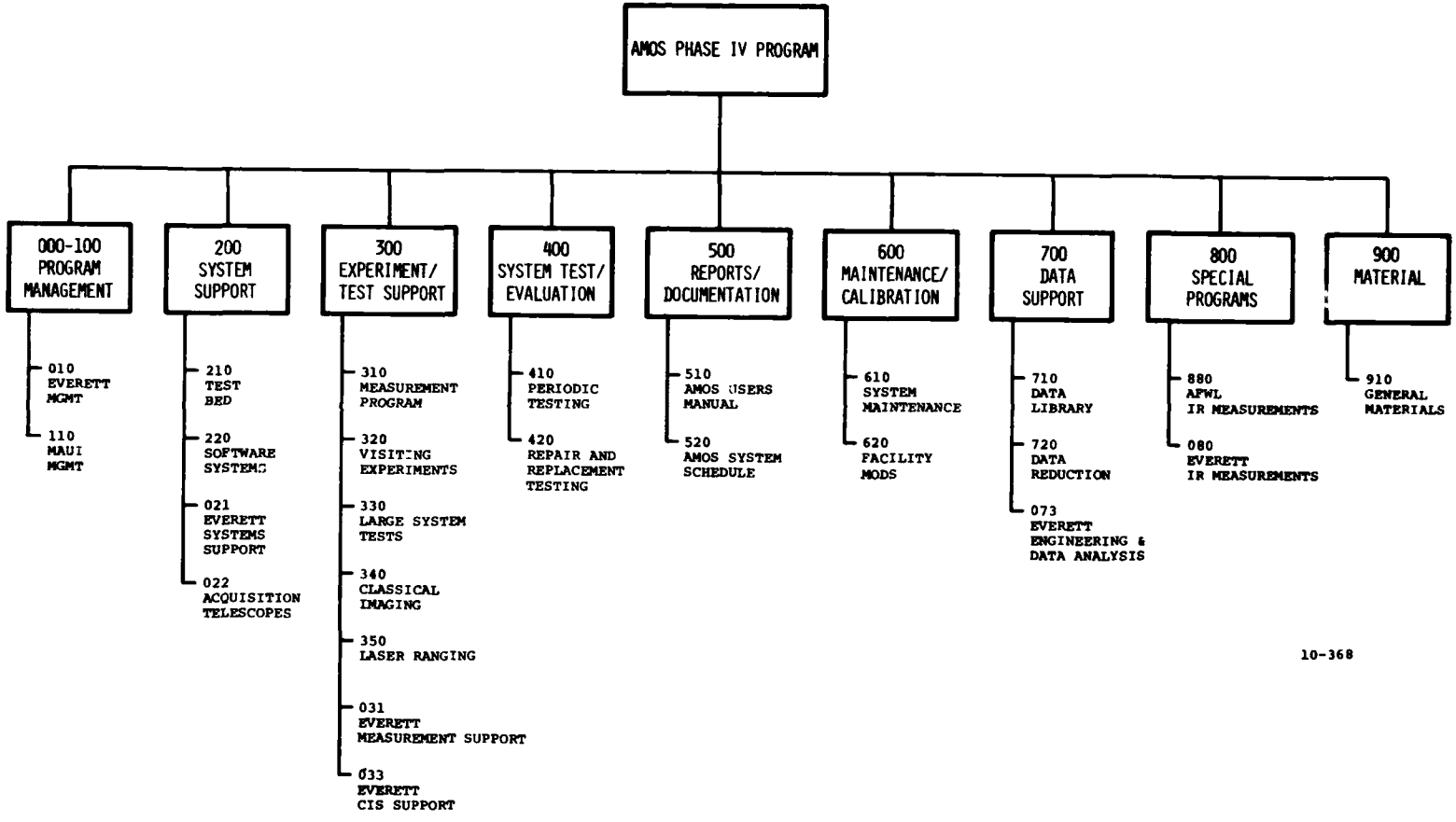

Fig. 4 AMOS Phase IV Work Breakdown Structure.

slightly different methods of approach within the context of the Systems Support task and, therefore, are treated separately here.

4.1.1 Hardware Systems Support

As stated above, the Systems Support task involves both the optimization of existing system performance and the development of new capabilities. An excellent example of the latter is the implementation of new AMOS Acquisition Telescope Systems (AATS) for the 1.6 m and 1.2 m mounts. During the past several years, based upon current and planned program requirements, it became clear that the existing AMOS Acquisition Telescopes were not adequate. The 10-inch system on the 1.6 m Telescope had a single 1° field-of-view. The 18.6-inch system on the 1.2 m Telescope mount had only two fields-of-view (3° and 23'). Both systems exhibited a large amount of flexure as a function of attitude and both were inadequate from the standpoint of sensitivity. Under the Teal Amber contract, AERL performed systems analyses to determine the required performance specifications and operational characteristics for the new Acquisition Telescope System. The resultant specifications were based upon both known and anticipated program requirements, and experience obtained by the AMOS staff over the past several years in the general area of acquiring and tracking various classes of man-made space objects. The basic requirements are given in Table 1. Procurement specifications for the telescopes and their associated TV cameras were prepared and submitted to appropriate

Table 1. AATS - basic performance requirements.

System Utilization	Field of View	Sensitivity	Background $(m_v/sec)^2$
Low orbit, high angular velocity, bright targets	3°	+ 11	+ 17.5
High orbit, low angular velocity, dim targets	0.5°	+ 16 (+17 design goal)	+ 21
		+ 14	+ 17.5
Precision handoff	0.1°	+ 16 (+17 design goal)	+ 21
		+ 14	+ 17.5

* m_v = Apparent Visual Magnitude

vendors for technical and cost proposals. Purchase orders were placed with the Boller & Chivens Division of the Perkin-Elmer Corporation for the telescopes and with Quantex Corporation for the video systems.

A baseline analysis was subsequently performed which included investigations of both single and two-telescope configurations. Based upon consideration of system complexity, performance, technical risk, size and weight, a two-telescope configuration was selected for the AATS. The AATS system diagram and optical schematic are shown in Figures 5 and 6 respectively. The system includes a filter wheel, motor-driven secondary mirror, sun shutter, reticle projectors and associated control electronics and displays. A remotely controlled motor-driven flip mirror changes the optical path to the TV camera from the 22-inch diameter to the 8-inch diameter telescopes. In like manner a motor-driven, remotely controlled 5X magnifier changes the 22-inch diameter telescope 0.5° FOV to a 0.1° FOV. Optical, thermal and structural analyses were performed. Of particular interest was the result of the encircled energy analysis, which indicated that the configurations selected satisfied the specified requirements, except at the edge of the field for the 0.1° FOV (illustrated in Table 2). The AATS telescope designs were accepted, parts fabricated and both systems assembled.

Preliminary acceptance testing of the AATS telescopes began on March 16, 1978 at the Perkin-Elmer Applied Optics

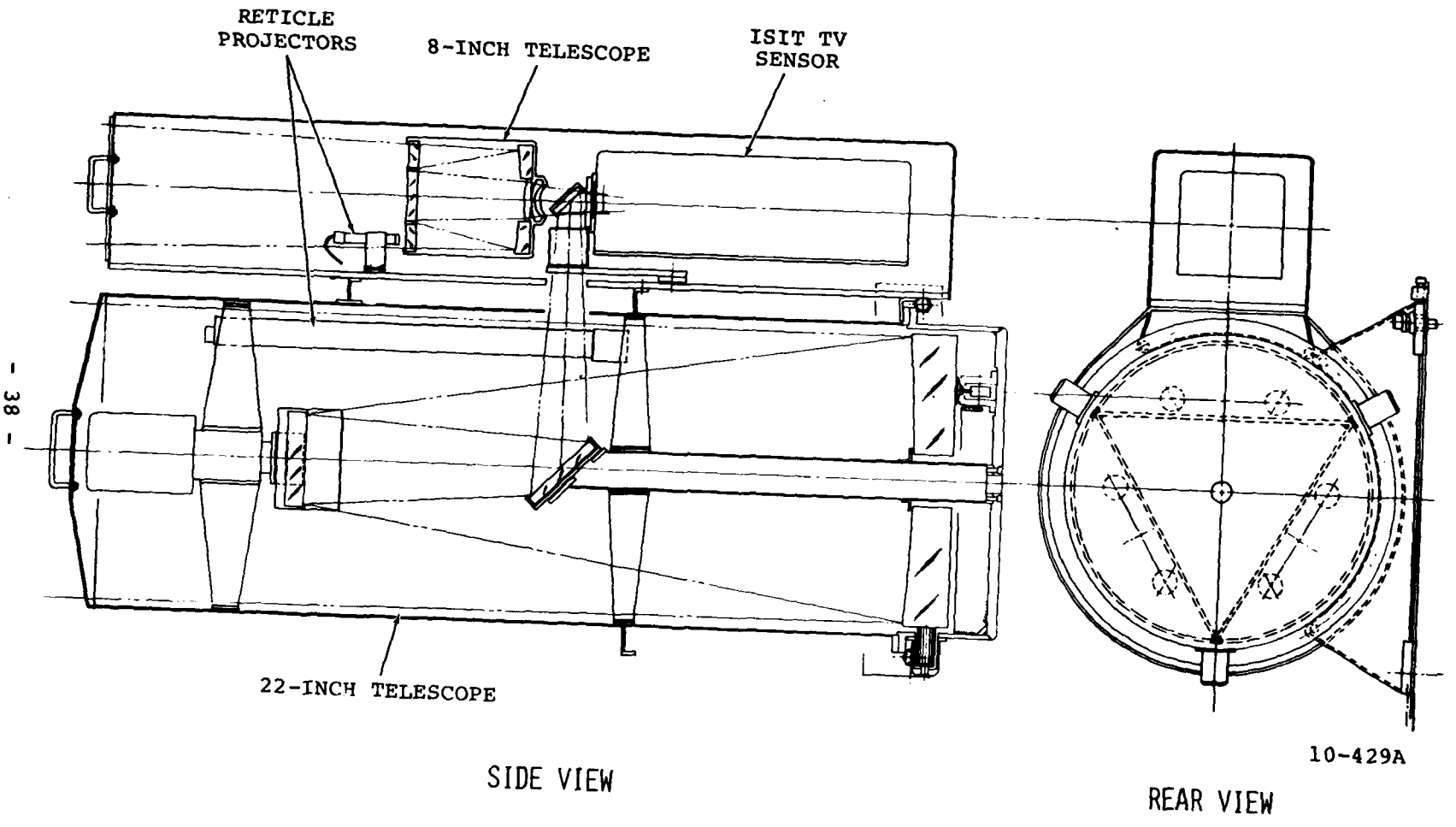

Fig. 5 AMOS acquisition telescope system.

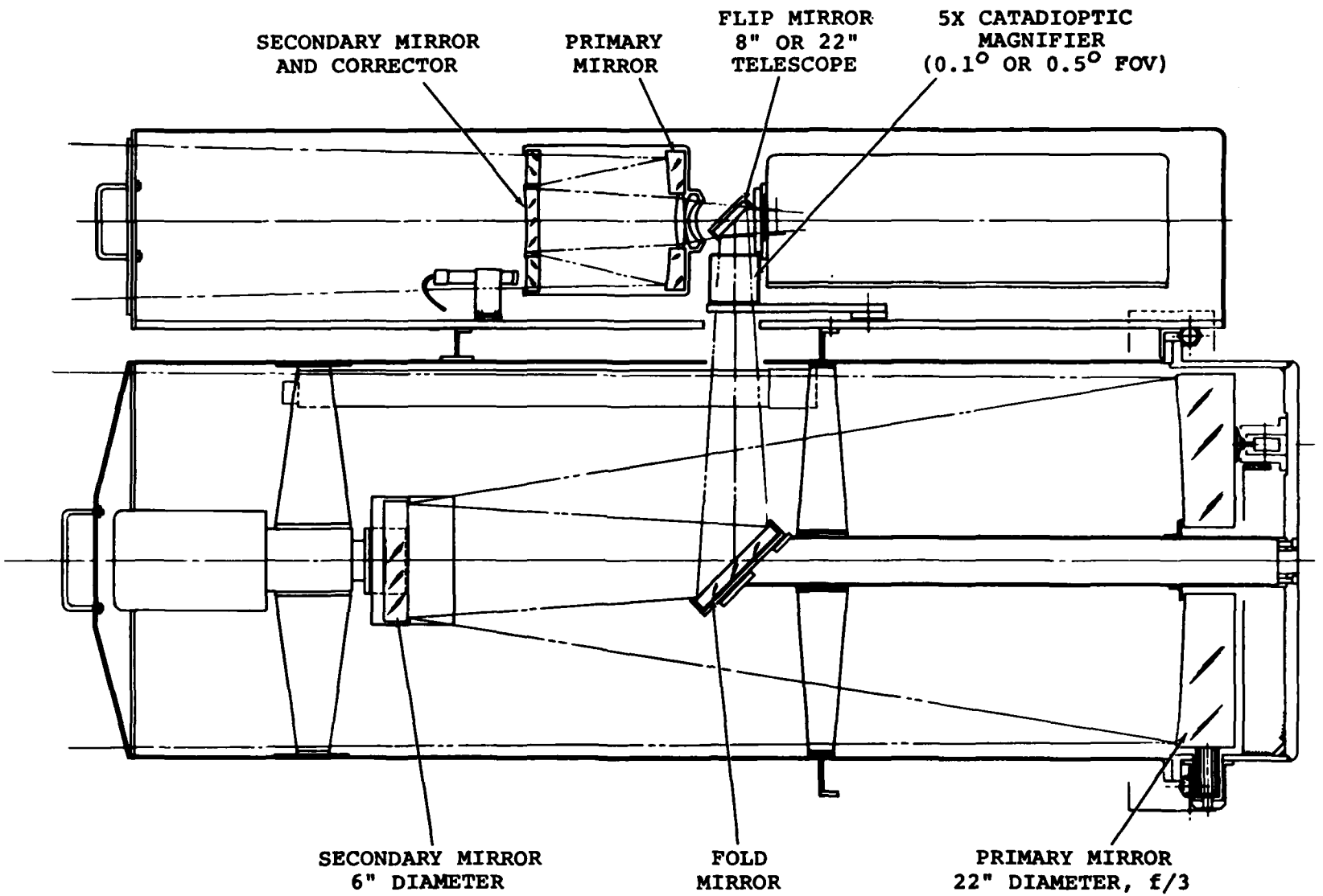

Fig. 6 AATS optical diagram.

10-430

Table 2. AATS encircled energy analysis.

Specification Optical Performance Requirement	Results of Image Quality Analysis
3.0° FOV 85% of the energy within 65μm diameter or less across the field	3.0° FOV For a 65μm diameter On axis - 97% of the energy 0.5° - 97% of the energy 1.0° - 97% of the energy 1.5° - 96.7% of the energy
0.5° FOV 85% of the energy within a 30μ dia or less over the central (± 0.05°) of the field and 65μm dia or less over all other portions	0.5° FOV For 30μm diameter On axis - 88.9% of the energy 0.1° - 90.4% of the energy For 65μm diameter Edge of field - 92% of the energy
0.1° FOV 85% of the energy within a 150μm diameter across the field.	0.1° FOV For 150μm diameter On axis - greater than 85% of the energy 0.025° - 83% of the energy 0.035° - 85.7% of the energy 0.05° - 82.6% of the energy

Division (AOD), Costa Mesa, California. Problems developed at the initiation of the testing. Although the 22-inch telescope is an all-reflective design, the system produced an apparent longitudinal chromatic aberration and excessive scattering in the 0.5° FOV. Efforts to focus the system for energy concentration measurement produced partial concentrations of red and blue separated axially by as much as 0.020 inches but with no zero-order white patch. The nominal depth of focus for the 0.5° FOV system is $\pm$ 0.003 inches. Thorough investigations were made of both systems, the test set-up, and the test equipment. During the testing, the aperture of the 22-inch diameter telescope was effectively reduced to 12 inches and the color problem was eliminated. When the aperture was increased to 16 inches, the color problem began to reappear. After going through a complete evaluation, it became evident that the prime candidate for the color problem was the multilayer, high efficiency, dielectrically enhanced mirror coating. Discussions were held with Liberty Mirror Inc., the coating vendor, as well as with coating experts across the country. The Liberty Mirror No. 758 coating contained approximately 27 layers and was approximately 4 microns thick. To definitely prove that the coating was the cause of the color problem, the mirrors were removed from one of the 22-inch diameter telescopes, the coating stripped off, the mirror recoated with aluminum without a protective overcoat, reassembled, aligned, and tested. The color problem was gone as was the excessive scattering.

Further analysis by Perkin-Elmer AOD showed that the presence of longitudinal color effects in the image formed by a primary mirror coated with a dielectric-enhanced aluminum coating can be predicted theoretically by assuming that the coating distribution is nonuniform across the aperture. The distribution of energy in the region of the prime focus of a spherical mirror can be computed by calculating the radial variations in amplitude and phase due to a given coating nonuniformity and, subsequently, obtaining the Fourier transform of this radial distribution at the prime focus. Figure 7 shows the optical configuration which was explored theoretically when an f/3 primary mirror is coated with an aluminum film/ dielectric stack which increases the reflectivity over the 0.4 to 1.0 micron region. It was found that monotonically increasing or decreasing changes in coating thickness from center to edge produced an almost identical focal shift for two different colors, but did not produce any longitudinal chromatic aberration. When a coating distribution which has a turning point such as that shown in Figure 7 is analyzed, a large focal plane splitting occurs for red and blue light. Figure 8 shows the intensity distribution (normalized to that of a perfect mirror) along the optical axis (z axis) for a coating distribution which first decreases by 3% (.97) at the 2/3 radius point and then increases to a value of 1.03 at the edge of the clear aperture. This nonuniformity produces a 20 micron chromatic aberration at the prime focus. Larger amounts are obtained

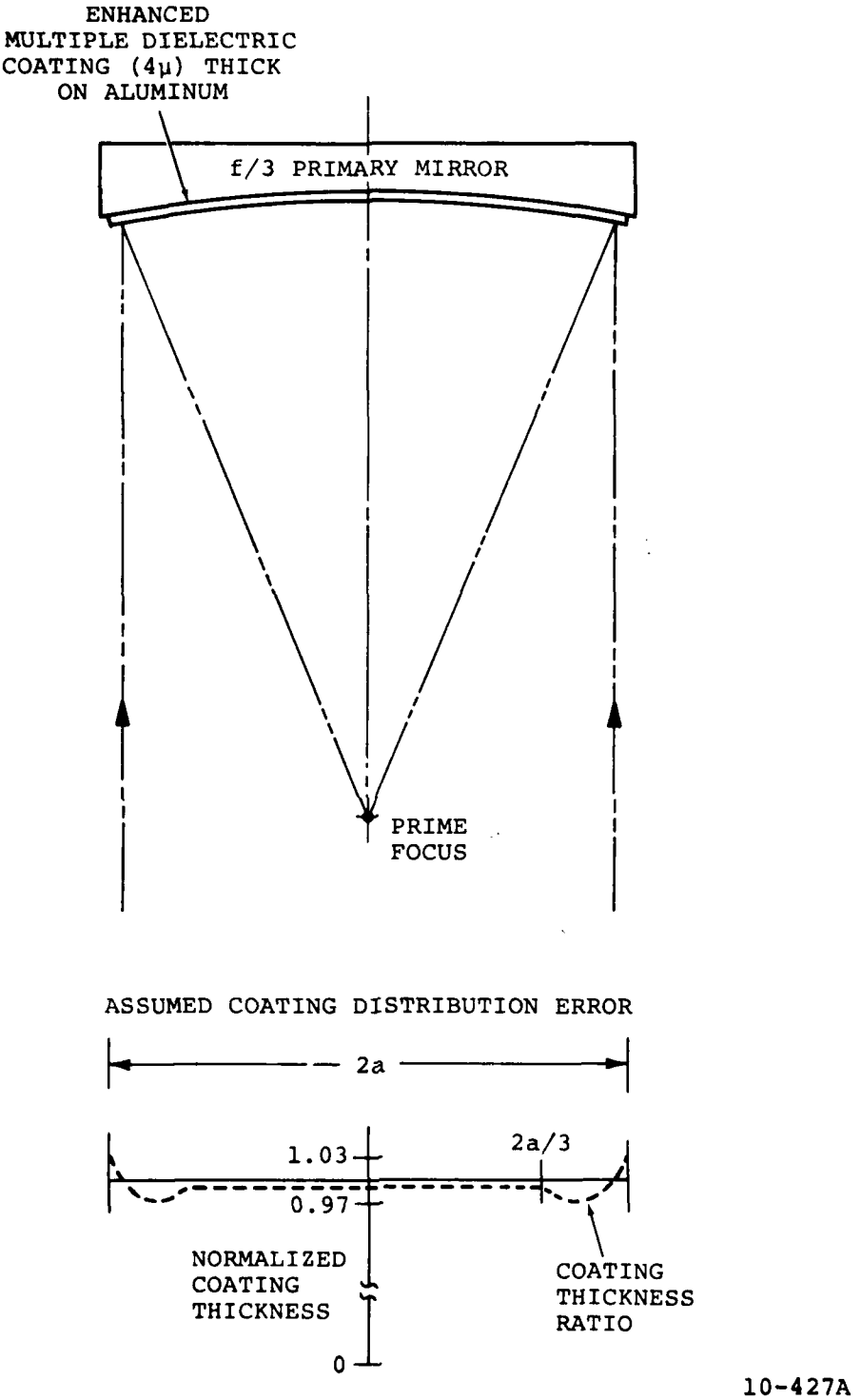

Fig. 7 Optical configuration and assumed coating distribution error. Coating thickness falls by 3% after the 2/3 radius point and increases to 3% thicker than nominal at the edge of the aperture.

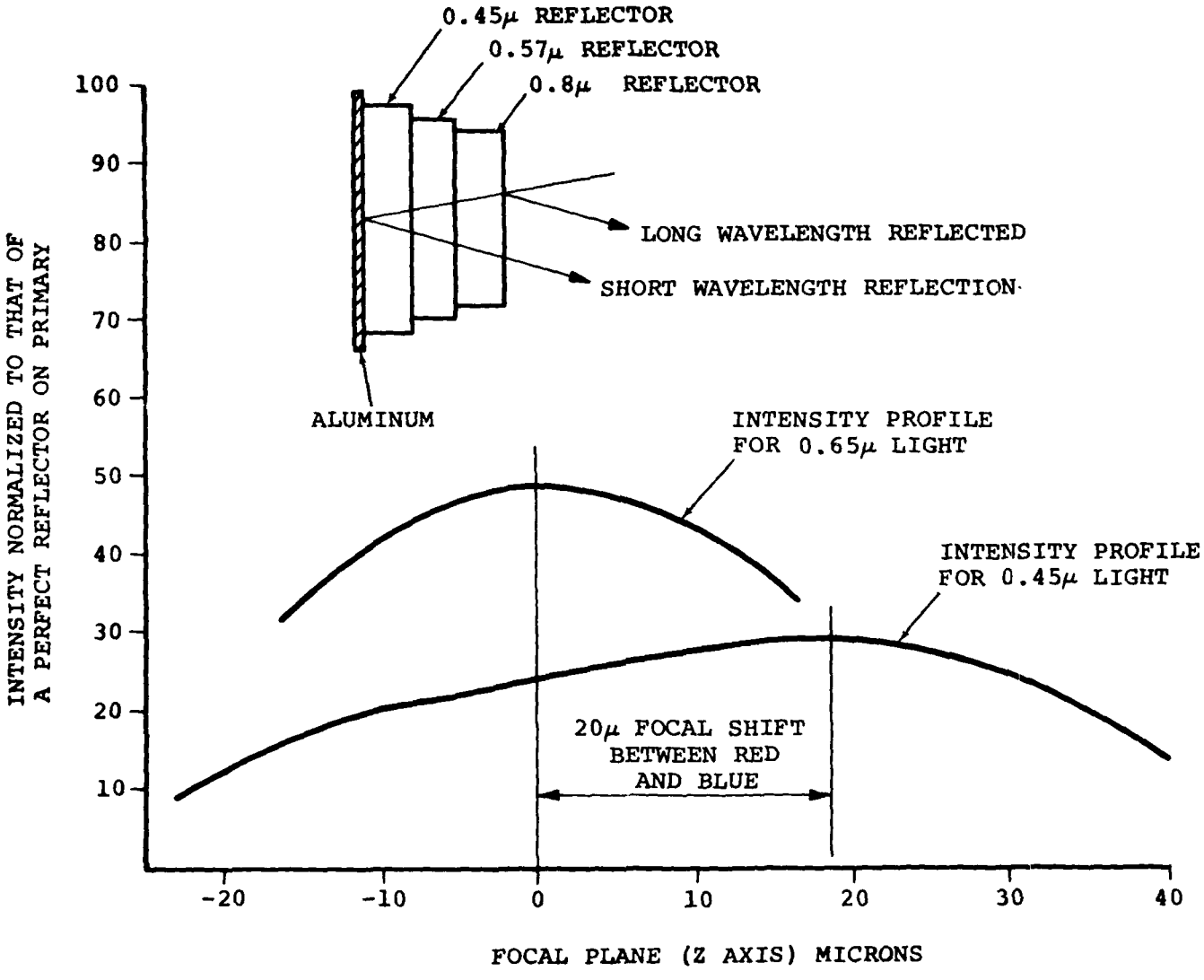

Fig. 8 Computed intensities at the prime focus for red (0.65μ) and blue light (0.45μ) reflected from a 4μ thick dielectric enhanced aluminum reflector.

for further small changes in coating thickness distribution. Such a chromatic aberration at the prime focus of a telescope is greatly magnified by the secondary mirror. Consequently, it is possible to obtain large focal shifts at the secondary focus of a telescope which utilizes enhanced dielectric coatings of substantial thickness.

The next step was the evaluation and selection of a replacement mirror coating. Various vendors were contacted, their coating characteristics evaluated and finally one developed by the coating department at Perkin-Elmer, Norwalk, Connecticut was selected as the replacement. The coating selected consists of five layers (Al, MgF_2, ZrO_2, SiO_2, ZrO_2) with a total thickness of 0.4 microns. The primary, secondary and tertiary mirrors of the 22-inch diameter telescope and the flip mirrors were stripped and recoated.

Problems of a different nature developed with the 8-inch diameter (3° FOV) telescopes. The imagery of one telescope was good on-axis but poor off-axis and the focal plane location was out of tolerance. The telescope was disassembled and the optical elements and mechanical parts inspected. All were found to be within tolerance except for the front corrector. Its thickness was 0.009 inches out of tolerance, but this condition could not cause the poor imagery problem. The telescope was reassembled and carefully aligned. The images were good both on-axis and off-axis, and the focal plane location was within 0.001 inches of the theoretical value. The assembly has

been potted and is ready for final installation in one of the AATS.

As currently scheduled, factory acceptance testing of the AATS optics will take place at Boller & Chivens in February, 1979. Installation at AMOS is scheduled for March and the systems should be operational in April.

The AATS Television Sensor System consists of the camera head (mounted in the AATS), a camera control unit (CCU) and the Quantex DS-20 Digital Image Memory/Processor. The camera head, which is a modified Quantex QX-12 camera, contains a 40 mm Varo 8605/1 Image Intensifier fiber-optically coupled to a 40 mm RCA C-21202 SIT tube, two high voltage multipliers, a preamplifier, deflection amplifiers and voltage regulators. There is also a motor-driven mechanical focus assembly which can move the image intensifier/tube combination $\pm$ 0.64 cm. The camera control unit performs the video processing and video control functions. All of the controls other than the mechanical focus are located in the DS-20 unit. Five DS-20 controls that effect the camera operation are video gain, sensor gain, beam, focus and integration time. The mechanical focus controls are located on the CCU front panel. The DS-20 Digital Image Memory/Processor is used for image capture, image processing and display tasks. It uses an A/D converter, a random access memory and an arithmetic unit, all under microprocessor control, to perform digital video processing functions in real-time. It has a 512 x 512

memory and an A/D converter sampling rate of 10 MHz with a resolution of 6 bits.

The two TV camera systems and spare sensor assembly (potted image intensifier/SIT tube combination) have been acceptance tested and delivered to AMOS.

4.1.2 Software Systems Support

Successful accomplishment of Phase IV tasks requires the use of existing computer software. If, however, a special performance evaluation is undertaken, and data reduction and analysis can be expedited by use of the computer, then the Software Systems Support task is utilized to formulate a new code to produce the desired results.

During 1978, for example, it was necessary to modify and supplement laser ranging software to allow on-site, post-mission performance evaluation and to provide the proper output format for input to an error model. The upgraded capability thereby provided now exists as part of the permanent test bed software.

Software algorithms were also developed during 1978 which greatly enhanced the AMOS capability to obtain resolved images of near earth space objects whose range changes significantly during photographic missions. A target at a finite range (R) will be imaged a distance ΔB beyond the infinity focal position of the telescope. The term ΔB can be expressed as $\Delta B \simeq f_c^2/R$, where f_c is the effective focal length of the telescope. In order to compensate for this effect (it is assumed that the

sensor remains fixed), the secondary mirror must be moved a distance $\Delta I \simeq f_c^2/M^2R$. ($M \simeq$ secondary magnification = 5.63).

The 1.6 m Telescope was originally provided with a manually controlled, secondary mirror motor-drive system to translate the mirror along the optical axis. This secondary drive has the following basic performance characteristics:

FUNCTION	ΔI^*	ΔB^{**}
Single Step	1 micron	31.7 microns (0.0012 in.)
Slow	3.1 microns/sec	98.3 microns/sec
Fast	31 microns/sec	983.6 microns/sec
Total Travel	$\pm$2 centimeters	+63.4 centimeters

* ΔI = change in inter-mirror spacing, I

* ΔB = change in back working distance, B

For example, for a target with a minimum range of 200 Km, the secondary would move a distance of 9.8×10^{-5} meters (equivalent to 98 discrete steps) away from the primary and back again. This is equivalent to 3.1×10^{-3} meters (0.122 inches) at the focal plane. Clearly, for any realistic target, the ability to correct by a few hundred discrete steps around the infinity focus position is more than adequate.

The depth of focus (δ) for a system, is $\pm 2.44\lambda F^2$. If we take $\lambda = 0.55$ microns and F = 16 we get $\delta = \pm$ 343 microns = $\pm$ 0.013 inches (equivalent to about $\pm$ 11 discrete steps at the secondary). Therefore, the allowed tolerance for any given position command is several counts of the secondary drive system.

Ranges beyond which correction is not required can be determined by assuming $f_c^2/R<2\lambda F^2$ which gives R>2200 kilometers.

Even though the required corrections are small (and occur at relatively slow rates), the manually operated system was unacceptable. The solution was to accomplish real-time focussing using the CDC 3500 computer which stores nominal range data as a function of time for the target being tracked. To summarize, the hardware/software systems for auto-range compensation during imaging missions must be able to correct for targets closer than about 2,200 km. Maximum corrections from the zero position (infinity focus) are the order of 100 steps of the drive mechanism and the correction rates are very slow. Tolerances are 3 or 4 steps. Correction is in accordance with the approximate relationship: $N \simeq 20000/R$ steps where R is in kilometers.

In order to implement the above capability into the 1.6 m Telescope, a software development task was initiated and completed during 1978. The software is used in conjunction with hardware developed during the Phase III contract.

Operation of the auto-focus system is as follows:

1) The 1.6 m Telescope is pointed to a star and manually focussed by the experimenter. (An automated focussing capability should be implemented in the future). This step is necessary to account for temperature induced focal shifts.

2) The main console operator activates the Auto-Focus (AF) computer read sequence from the Alphanumeric Keyboard (ANK) panel.

3) The computer reads and stores this focus position. This is the bias offset for infinite focus for the package and dome conditions prior to a mission.

4) The dome operator switches focus control from manual to computer.

5) The bias offset is now output from the computer to the focus interface. This will hold the focus at infinity as long as the computer remains in sidereal mode.

6) When the computer is switched to ballistic mode, the AF subroutine computes focus corrections based on predicted range of the target.

AF output = Bias offset - (20,000/Range)

where: Range is in Kilometers

(Bias offset is the pre-mission focus setting for infinity).

7) When the computer is switched back to sidereal mode, the AF bias offset will be output to the AF interface to drive the focussing back to the infinity focussing point for post-mission calibration.

8) The AF bias offset may be changed anytime during calibration by switching focussing to manual, resetting it,

activating the read sequence and switching back to computer focussing.

Based on those events the computer functions required are:

1) ANK input to activate reading of the AF position when at infinite focus.
2) Computation of AF position biased by the number just read.
3) Output of the infinite focus AF number when in sideral mode.
4) Output of the range corrected and biased AF number when in ballistic mode.

The above capabilities were operational on the 1.6 m Telescope by the end of 1978 and are now being used in the classical imaging data base programs. (See section 4.3.3.3).

4.2 System Testing

AERL conducted tests on the AMOS subsystems during 1978 to assure that they continued to have the performance capabilities required to support research and development programs. This testing falls into two general categories - periodic and repair/replacement - which are discussed below.

4.2.1 Periodic Testing

Periodic testing and performance evaluation of existing equipments may occur in various ways. In the case of equipment which is in regular operation in the acquisition of data or in regular operating support of that equipment, the monitoring of data quality or of other evidences of system performance (e.g.,

pointing accuracy or image quality of a telescope) will give a running indication of the condition of the system in general and provide clues as to a specific area or component requiring attention. Baseline performance has been established for all major AMOS systems and related support equipments and, therefore, they are evaluted against their respective baselines.

Periodic tests of system performance are required for two primary reasons. First, anomalous system behavior will be uncovered by a review of data (e.g., pointing drift as a function of time or temperature). When problems are discovered, tests are conducted, and the analyzed data used to determine a remedial course of action. Secondly, certain tests are required to evaluate potential interface problems which are not specifically identified with a particular visiting experiment or special program.

Additional special testing would center on the many equipments and components (mostly optical) which are used in experimental applications and instrument packages, the quality and performance potential of which are not completely known. Precise calibration and evaluation of these components will significantly increase their value to the Observatory.

Data obtained as a result of periodic tests is used to update maintenance schedules and test procedures.

4.2.1.1 1.6 M Telescope Primary Mirror Support System Testing

A significant amount of periodic testing was performed during 1978. In the interests of brevity only one example

will be discussed here. The example is, however, covered in detail since it clearly demonstrates the level of complexity involved in assessing optimum performance of the AMOS systems.

Pointing shifts and hysteresis of the order of 10 arc-seconds had been observed for certain North declination angles (near 65°) during evaluation of the new mount model for the 1.6 m Telescope. It was determined that radial decentration of the primary mirror was occurring, which was qualitatively consistent with the observed pointing errors.

Tests revealed several problems:

1) The primary mirror was taking from several seconds to a few minutes to stabilize radially after the telescope had been pointed from one section of the sky to another. In addition, the mirror frequently went through a transient movement of several thousandths of an inch during telescope motion between positions, and was more pronounced along the E-W axis than along the N-S axis.
2) The mirror failed to return to within 0.002-0.003 inch of its previous radial position. However, since 0.001 inch of radial displacement alone causes a 1 arcsecond shift in pointing, this in itself could not produce the effects observed.
3) The mirror showed a general tendency to sink below its average position when being supported by the mercury belts.

4) The radial mirror position was quite erratic when the telescope went through zenith.

Investigation of the (mercury belt) radial support system resulted in the discovery that the mineral oil - used to fill the volume not occupied by mercury - was contaminated by particulate matter.

Further examination revealed that the mercury and oil combination moved sluggishly in the belt and that oil bubbles became trapped within the mercury, requiring tens of seconds to percolate out.

Draining of the belt was hindered by a mass of sludge that appeared to consist of small globules of mercury in the oil, a sediment of red mercury oxide, and possibly dirt from inside the belt. The belt was cleaned by flushing with toluene and was then allowed to air dry.

With the air pump shut down, and the mirror support air bag deflated, the entire weight of the mirror was found to be supported by the 1.250 inch diameter back-up pads, rather than by the five inch diameter defining pads. In addition, the plane defined by the defining pads was apparently up to 0.050 inches out of parallelism with the Blanchard plate.

In effect, the axial position of the primary mirror was being defined by the air bags. The mirror position and the resulting pointing performance of the 1.6 m Telescope then became a function of the air pressure and telescope attitude. The axial shift or tilt of the primary mirror normally would

have been detected by observation of the mirror position read out indicators as observed from the dome control console. It was found, however, that the push rods used in the indicator system had machining marks along their surface which prevented free movement in their guides. The rods were removed, polished and reinstalled.

The defining and back-up pads were adjusted so as to be parallel to the Blanchard surface. The back-up pads were then adjusted so that the defining pads would define the mirror position while in operation but not carry the entire weight of the mirror when the air bag system is shut down.

All pads were adjusted to position the mirror above the air bag so that each defining pad carries 15-20 pounds of mirror weight in operation without retaining clip pressure.

Following this, the belt was refilled with mercury only (the volume not occupied by mercury contains air). Test results indicate that the sinking tendency is now controlled. Mirror excursions during rapid motion of the telescope are still present, but the transients settle out much faster with the mercury/air combination than with the mercury/oil combination.

Axial support system tests indicated that there was little or no tendency for the mirror to tip when the telescope was rolled toward the horizon. However, during the course of working with the mirror it appeared that the mirror was hanging-up at times for reasons not fully understood. The sensitivity of

the axial position indicators was such that this movement was not being detected. The indicators were replaced (for testing purposes) with 0.0001 inch dial indicators.

Push tests on the rear defining pads indicated excessive readings for the weight supported by those pads, followed by too small a reading after release of the front retaining clips. Variations encountered during these tests further indicated some sort of hanging-up inside the cell. Measurements of mirror position also indicated that the mirror might be resting on two of the small outer back-up pads (East and Southwest) and on the larger inner defining pad at the North-west location.

Measurements of mirror parallelism in relation to the Blanchard plate, while adjusting the two rings of support pads, strongly indicated that, at most, only one of the defining pads was ever in contact with the mirror at any given time.

The retaining clips were then tightened down to a total force of approximately 35 pounds. At this point an all-attitude test revealed that the lower edge of the mirror was tilting away from the Blanchard plate at large zenith angles (75°), with the SW edge being worse by a factor of three. This indicated a discrepancy between the centroid of the mercury belt buoyancy and the centroid of the mirror. Lowering the mercury belt at the SW edge by 0.020 inches reduced the imbalance on that edge by a factor of three. Further lowering of the belt all round by 0.15 inches reduced the tilt of the NW sector to nearly zero but produced no further improvement in SW, and

none in E. This would indicate some sort of friction or hanging-up of adjustments inside the cell.

A night-time pointing check, using an old mount model, yielded pointing hysteresis of up to 15 arcseconds. The worst case being in the Southwest quadrant of the sky rather than the Northeast where the original discrepancy showed up.

A check of reference pad loads showed that the E and SW loads had fallen to 26 pounds and 18 pounds respectively, indicating that these two sectors may have settled during excessive mount motion encountered during the all-attitude tests.

Retightening all three retaining clips to about 40 pounds reduced the pointing hysteresis to 1 to 4 arcseconds, again worse in the South than in other areas. This performance was deemed satisfactory for current high priority measurement activities. Further work on the mirror support systems is scheduled for March, 1979.

4.2.2 Repair/Replacement Testing

Upon repair and/or replacement of operating elements in the basic AMOS systems and related equipment, AERL performed testing and evaluation to ensure that proper operation had been restored. Upon successful conclusion of the testing, the system was then certified for use in obtaining valid and reducible data.

A specific example of this category of testing is the replacement of the defective 1.6 m azimuth drive motor which is discussed in detail in section 4.2.2.1. The replacement

effort required a specific engineering approach to be developed. The motor was originally installed prior to mount assembly but required replacement without the major cost and time impact that mount disassembly would have entailed. Following replacement, detailed testing was performed before the 1.6 m system could again be placed in an operational status.

It is important to point out that, in all but the most trivial cases, repair/replacement testing involves significant effort and participation by senior AMOS personnel. In the case of the defective torque motor for example, it is not enough to merely replace the motor and show that the mount can move in azimuth. An extensive test program is required to assure that the overall performance of the 1.6 m complex has not been degraded.

4.2.2.1 Replacement of the 1.6 M Telescope Azimuth Torque Motor

Replacement of the defective torque motor was accomplished during the Spring of 1978.

Preliminary efforts included writing the procedure to be used to accomplish the repair.

The next phase was to procure parts for, and then construct, the lifting platform and the motor stand. The basic system that was used in lowering and raising the heavy parts was a lifting platform, whose height was controlled by turning four nuts on four 1" diameter threaded rods. The threaded rods also served as lateral guides. The rods screwed into the telescope base, and they were supported at their lower ends by a tube and

jam-nut arrangement. Two chain hoists, suspended from large screw eyes attached to the telescope base, were also used to aid in manipulating the heavy castings and the torque motor.

In order to replace the torque motor, it was necessary to cut all cables going through the azimuth axis, and install in-line connections. Some connections existed and some required installation of plugs and jacks. Other conductors were connected at an array of terminal strips on a panel in the pedestal room. This cabling and connector effort was done in phases to allow normal telescope use as long as possible before the telescope-disabled phase of the torque motor replacement began. As soon as all cables had disconnect/reconnect provisions, and the platform was installed in the pedestal room, the actual disassembly commenced. Cables were first de-energized and disconnected and wiring was then removed from the various components on the bottom of the base casting. The hydraulic swivel was removed and lines plugged. The torque motor disassembly proceeded quickly with the removal of the tachometer generator (stator and rotor), resolver mounting plate, and torque motor cavity bottom cover.

It was apparent during disassembly that there had been enough hydraulic oil seepage to coat all inner workings with oil and that considerable cleaning of components would be necessary before reassembly. Figure 9 shows a view of the damaged torque motor while still in the motor cavity.

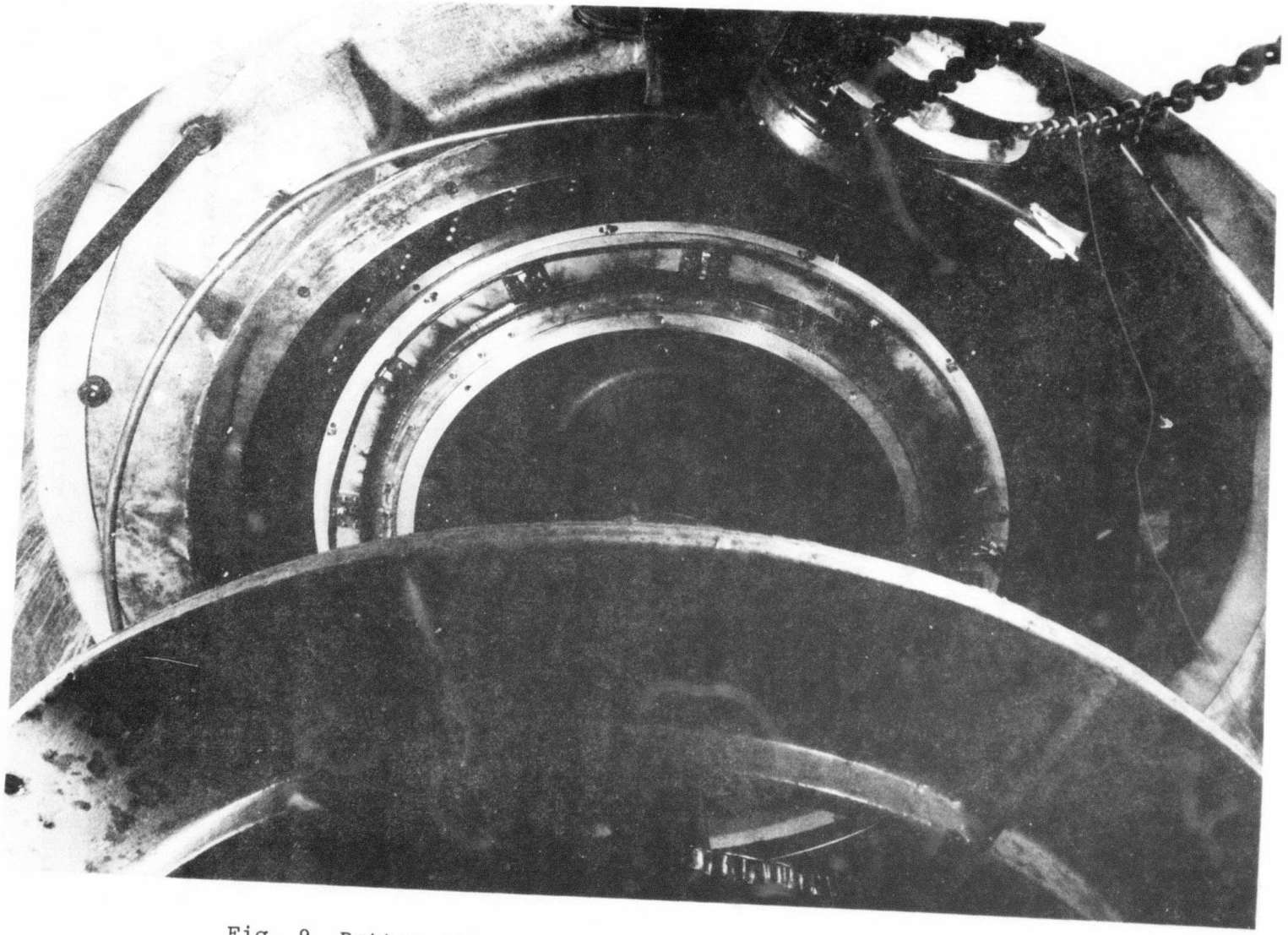

Fig. 9 Bottom view of damaged torque motor before removal.

As soon as the damaged torque motor was removed, efforts were directed to cleaning the motor cavity, and the elimination of future oil-spills. All questionable hydraulic fittings up on the telescope were repaired and accumulations of oil in various bolt holes were removed. An unsuccessful attempt was made at removing a large telescope base attachment bolt, where oil drips were evident, to apply thread sealant. As an alternative solution, a drip-pan was attached between adjacent casting webs to direct oil drips away from the top of the torque motor.

Silicone rubber dams were attached to the bottom surfaces of these casting webs to cause oil seepage to drip off the webs outside the motor diameter rather than flow all the way down the webs towards the torque motor.

A neoprene shield (or umbrella) was designed and fabricated to protect the torque motor from other sources of contamination. It was affixed to the top of the motor before it was installed in the motor cavity.

During attachment of the new motor to its cavity, a minor mechanical discrepancy was discovered in that the attachment bolts and nuts for the stator's permanent magnets were not recessed in the stator body as was the case with the old motor. It was necessary to slightly lower the motor assembly to insert the attachment screws through the flange and then bring up all the screws at about the same time, a fraction of a turn at a time, so that they would not run into the magnet attachment bolts and nuts. Figure 10 is a photograph of the new torque

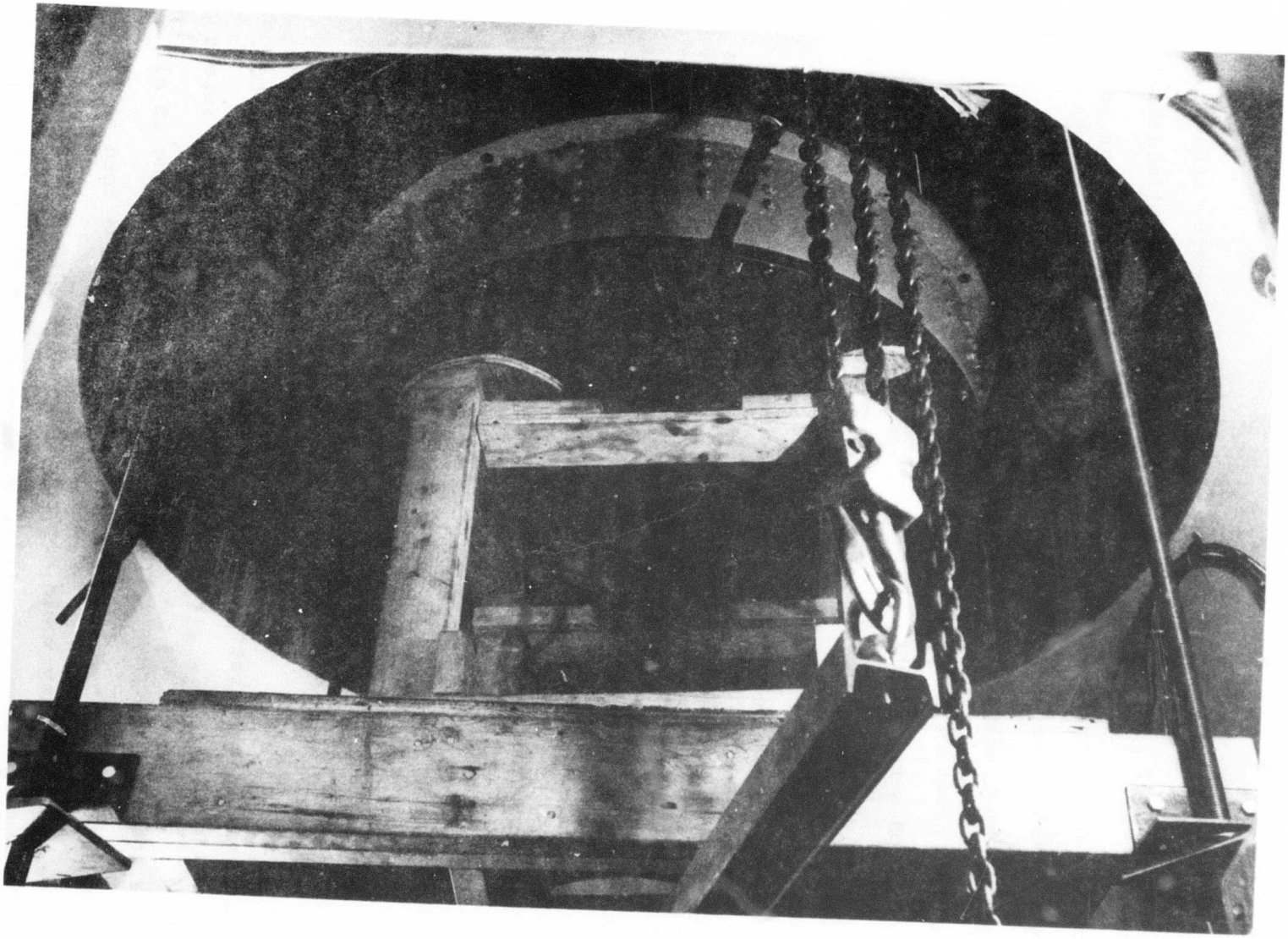

Fig. 10 New torque motor before installation.

motor on its stand. The threaded rods are visible at the right and left edges of the picture.

As soon as the new motor was attached to the telescope, its magnetic keeper-ring was removed and an initial electrical check performed. The motor's DC resistance and torque vs. current characteristics were within specifications, and telescope reassembly proceeded.

The most difficult task of telescope reassembly was the Shaft Angle Encoder (SAE) alignment. Figure 11 gives a view of the SAE stator attachment plate after installation of the new motor.

The first step in the realignment procedure was to mechanically center the SAE rotor using a microscope as an optical aid. Then the SAE stator was installed and the electrical alignment procedure was begun.

The electrical alignment procedure is necessary to obtain sufficient accuracy to adjust rotor to stator parallelism as well as rotor and stator centering. The final alignment adjustments are critical, in that shims must be selected to 0.0005 inches and adjusting screws must be set and locked to similar tolerances.

After SAE inductosyn plate alignment, the remaining electro-mechanical components were installed and cables were returned through the azimuth axle. Final tasks to be completed before telescope performance evaluation were: check out of the azimuth control modes, i.e. synchro and manual; and correlation

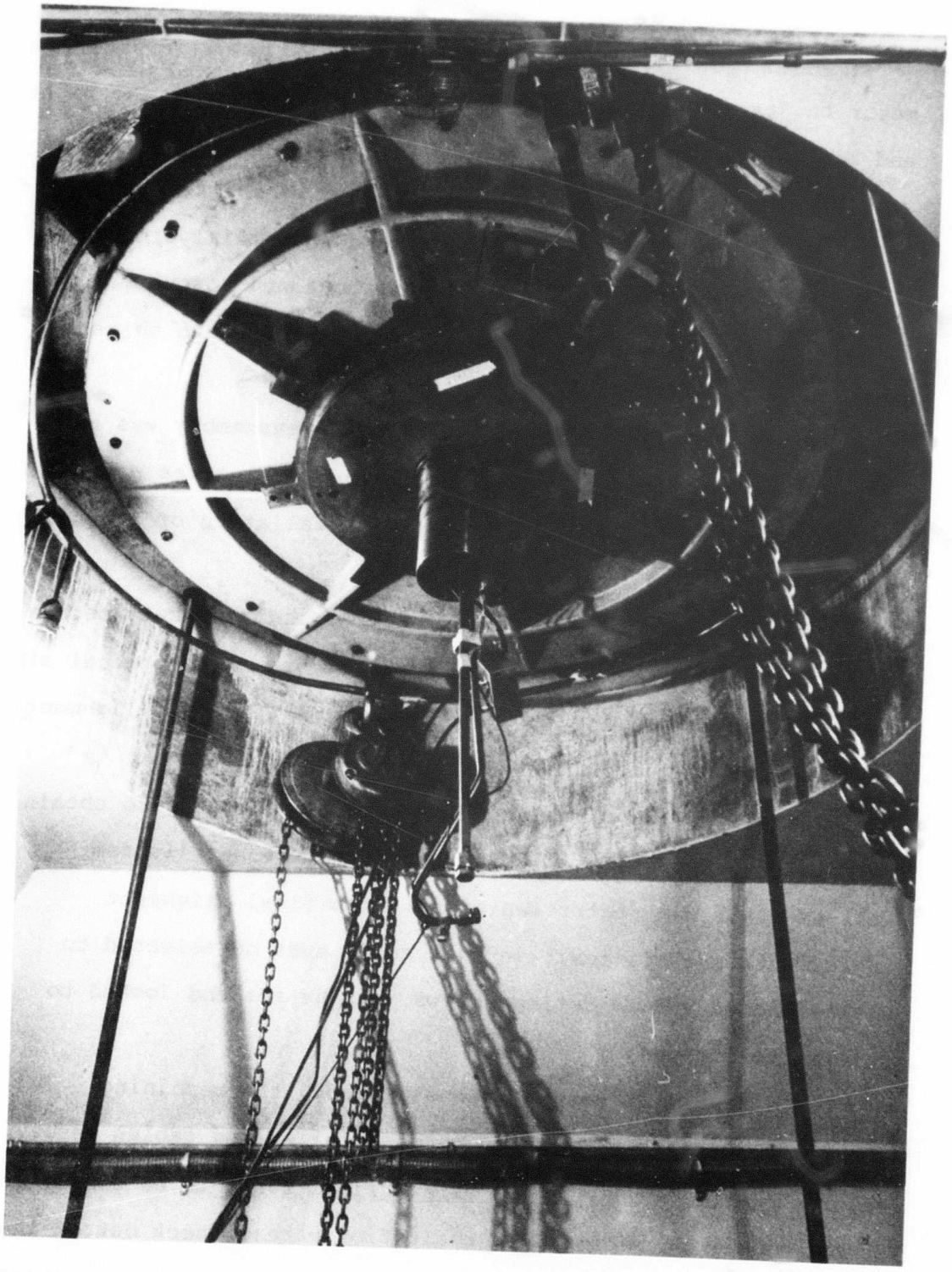

Fig. 11 Reinstalled motor and shaft angle encoder stator plate.

of the SAE fine and coarse transducers (inductosyn plates and resolver respectively).

After all of the above work had been completed, 1.6 m Telescope performance was evaluated (i.e. pointing and tracking tests) and the system was once again operational.

4.3 Program Support

Program support includes Measurement Programs, Visiting Experiments, Large System Tests and the Laser Beam Director Program. The first two categories represent exploitation of inherent AMOS capabilities, developed over previous years, to support various DoD programs. The third represents implementation and evaluation of new DARPA-sponsored technologies at AMOS. The fourth is concerned with improvements of existing AMOS hardware and software to fulfill specific DoD requirements.

4.3.1 Measurement Programs

The measurement programs utilize existing or slightly modified AMOS systems and instrumentation to obtain data requested by government agencies. Most of these programs were not specifically identified at the initiation of the current contract but evolved during the course of the year's activity as a result of direct contact with their sponsoring agencies. Measurement programs are conducted by resident AMOS staff members in contrast with visiting experiments which involve user personnel in the role of Principal Investigator. Measurement programs which utilize existing AMOS hardware systems in a more or less routine manner and are covered by an existing Mission Instruction

and Operation Plan (MIOP) are directly assigned to the Operations Crew who then proceed to obtain the required data in accordance with the weekly schedule. The data, along with relevant calibration and system configuration information, becomes a formal AMOS Data Package which is qualified and, upon direction of DARPA/RADC, transmitted to the user agency. Measurement programs which require modifications to AMOS systems and/or procedures to accomplish their goals are assigned to an AMOS Principal Investigator for implementation. He is responsible for preparing a MIOP (CDRL 002), assuring that the modifications are implemented in accordance with schedules and priorities, and serves as Test Director during the actual conduct of the measurements. After qualifying the data package and verifying that it does indeed satisfy the program requirements, he - after receiving necessary approvals - transmits the data to the user. As required, other outputs of Measurement Program activities include Flash Reports (CDRL 019) and Quick Look Reports (CDRL 011).

During 1978, the following measurement programs were conducted or initiated: 1) SAMSO Evaluation Program, 2) AFWL IR Measurement Program, 3) BMD Missile Measurements, and 4) HAVE LENT IV and V Measurements.

4.3.1.1 SAMSO Evaluation Program

Background

The SAMSO Evaluation Program (SEP) was initiated during the DARPA Phase III contract. The objective of the program

was to obtain the visual and infrared signature of a specific satellite and observe yearly changes, if any. Several agencies with measurement capabilities were involved in the program. McDonald Observatory (University of Texas) performed photometric measurements while Catalina Observatory (University of Arizona) and AMOS gathered infrared signature data. Earlier participants in the program also included the Cloudcroft, and the GEODSS ETS sites in New Mexico.

Summary of Measurements

Two periods of measurements were conducted in 1978. The first was during the first and second weeks of March. The second was from 23 October through 2 November. Data resulting from the March series was reduced and summarized in two SECRET reports (AERL-78-167 and AERL-78-179). The quality and quantity of the raw data resulting from the 1978 Fall series did not compare favorably with the March set and was not reduced. The Fall measurements were plagued by unfavorable weather conditions resulting from a local storm system and a major computer (CDC 3500) failure which delayed the measurements two nights.

The infrared measurements of the SEP target are difficult to perform, requiring long observation times and ideal weather conditions. The measurements are particularly difficult to conduct from the AMOS location because of the satellite's position with respect to Maui. The measurement elevation angles are less than 45 degrees which results in increased atmospheric attenuation as compared to the other sites and also reduces the

allowed observation time (before target eclipse by the earth's shadow) by a factor of three to four. As a result, the variance in the reduced data was somewhat larger than that obtained by the Catalina Observatory although the measured magnitudes agreed closely.

Nodding Secondary Mirror

In preparation for the SEP measurements a major improvement was incorporated into the AMTA IR measurement system which resulted in a 30-fold reduction in scan noise. The scan noise artifact had been inherent in the AMTA system since its delivery in 1973. It is caused by the scan mirror being located in close proximity to the detector array. Two major factors contribute to the observed scan noise; 1) the light pipes used in conjunction with the AMTA focal plane array exhibit a high degree of directionality, and 2) the mirror, rotating through a relatively large angle, reflects radiation from material of various temperatures and emissivities existing within the cavity onto the detector array. Moving the scan mirror to a greater optical distance (e.g. the primary or secondary mirror of the telescope) reduces this artifact. Scanning the primary mirror or the entire telescope at a rate allowing modulation of the target image above the 1/f detector noise is impractical due to the enormous mass involved. Indeed, even scanning the eight pound secondary mirror at the desired 45 Hertz rate proved difficult. However, a secondary mirror scan rate of 23 Hertz with acceptable waveform was achieved and used in the March

measurement series. Modifications were made to the system prior to the Fall series to enable a 45 Hertz rate and thus improve the system sensitivity by further reducing the 1/f noise contribution. The higher frequency was obtained by utilization of drivers with improved torque capability.

Figure 12 shows a photograph of the B29 Telescope secondary mirror and the push-pull galvo driver arrangement used in the experiment. The system is capable of only square-wave movement and only at toggle amplitudes as pre-adjusted by mechanical stops located on the mirror housing. However, the system did prove that noise reduction could indeed be achieved, and a new improved version is presently under design for the AFWL IR Measurement Program (see Section 4.3.1.2) which will provide not only square-wave scanning with remotely controllable amplitudes, but will also allow scanning with linear, constant velocity waveforms.

4.3.1.2 AFWL IR Measurement Program

Background

The AFWL IR Measurement Program was initiated in November of 1978 as a result of several meetings between AERL and AFWL at both AMOS and the Air Force Weapons Laboratory, Kirtland AFB. The capabilities of AMOS, particularly of AMTA and the 1.6 m Telescope, will be used to fulfill some of the objectives of the program.

Major technology areas for the overall system are threefold: 1) development of an IR adaptive optical system to

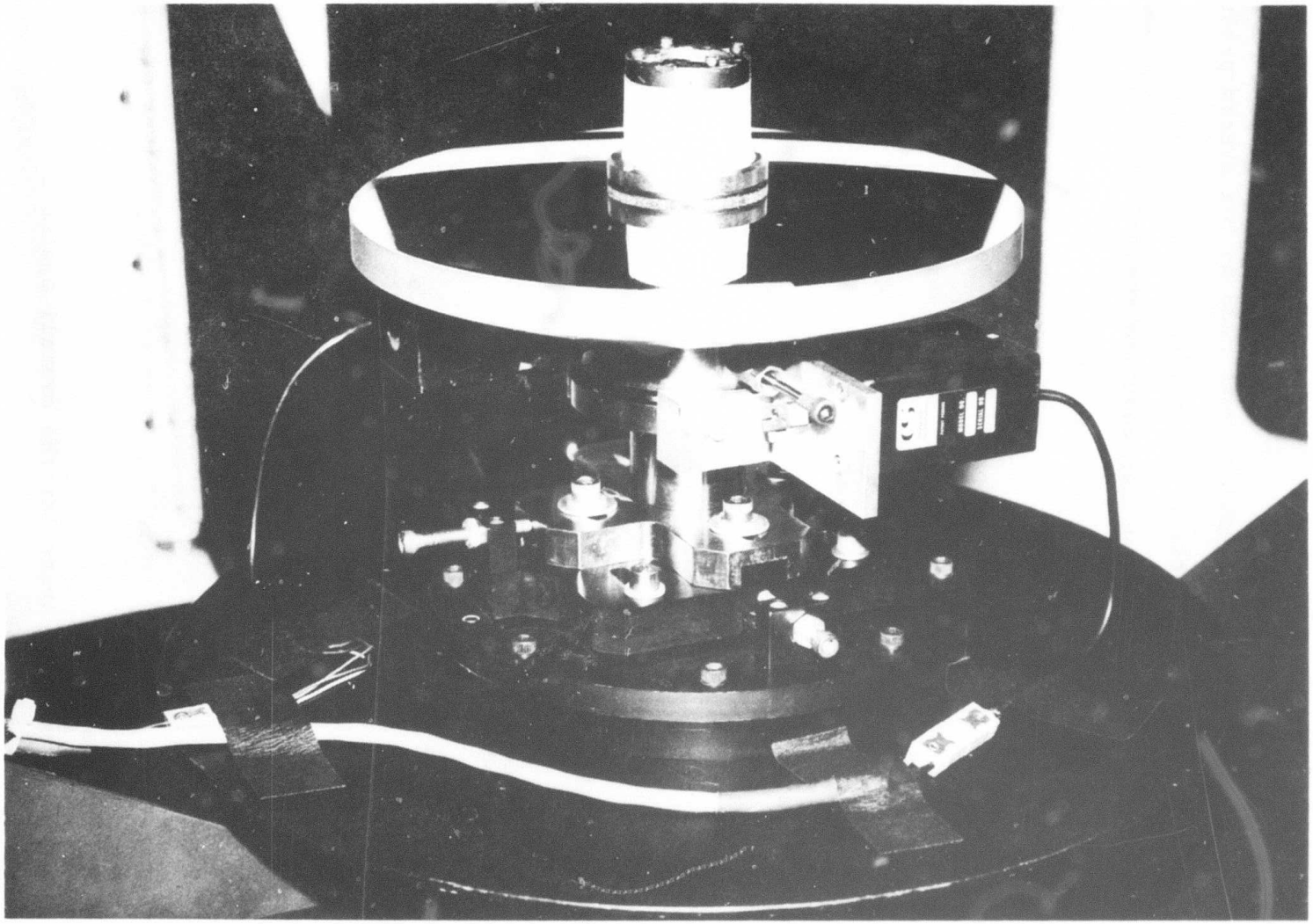

Fig. 12 B29 nodding secondary mirror used for SEP measurement program.

compensate for atmospheric turbulence, 2) solving the problems associated with the utilization of a shared aperture, and 3) solving the look-ahead problem of predicting and pre-correcting for the turbulence to be encountered by a transmitted beam.

The major contribution of AMOS to this program will be to demonstrate the ability to acquire satellites using only an IR detection system (without visual or radar assistance) and orbital elements supplied by NORAD. In addition, an IR signature base will be established to further define the detection probability for a given search system and scenario. As part of the program, the AFWL will provide a complete IR sensor package for test on the 1.6 m Telescope. This particular portion of the experiment will be performed under the Visiting Experiments Program and is discussed further in Section 4.3.2.

Program Outline and Schedule

A functional block diagram of the AFWL IR measurement program being conducted at AMOS is shown in Figure 13. Three series of Satellite Acquisition and Signature Measurements are to be performed using the AMTA sensor. Prior to each set of measurements, improvements will be made to the system to enhance its acquisition and tracking capabilities. As an end result, AMTA will provide initial target acquisition for hand-off to the AFWL FLIR sensor package.

The program was started with a combination of sky radiance and satellite acquisition measurements during the second week of November and continued until the end of December, at which

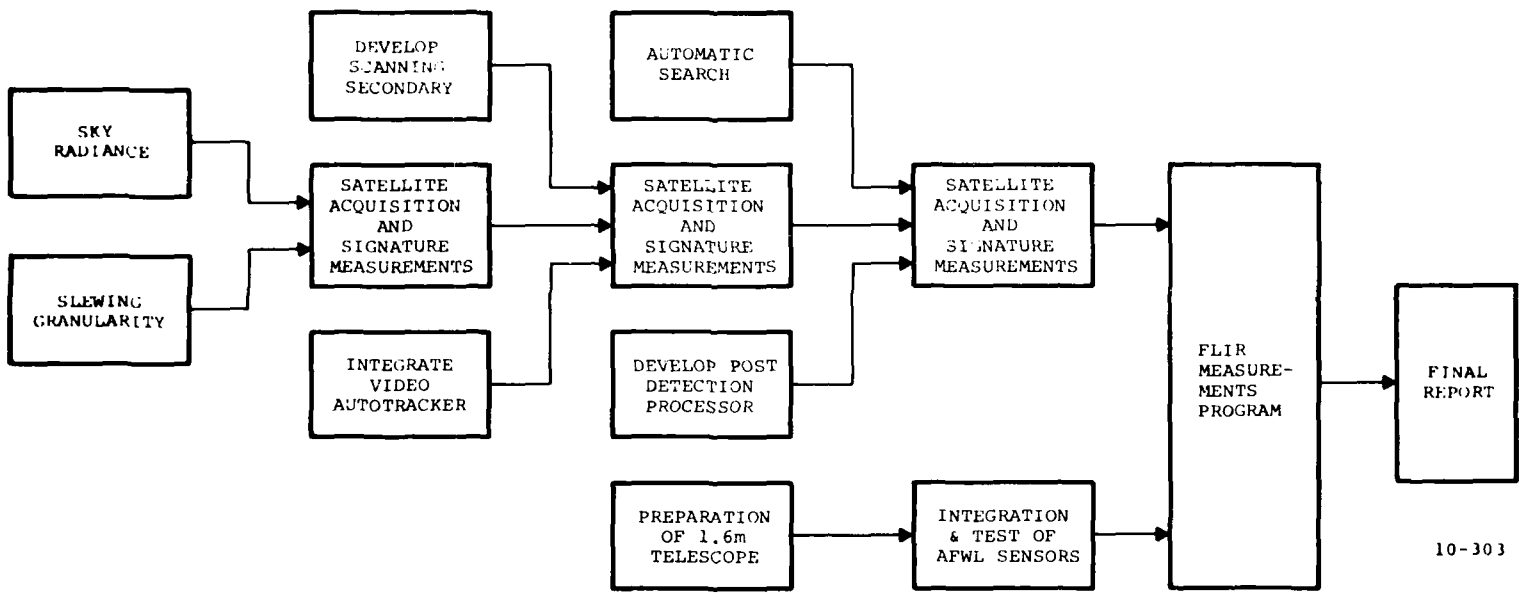

Fig. 13 Functional block diagram of the AFWL IR measurement program.

time the 1.2 m Telescopes were disassembled for refurbishment. A limited number of granularity measurements were performed in December, and it is expected that additional measurements will be performed at the conclusion of the refurbishment exercise. Preparation for the arrival of the FLIR was started in early November. All modifications will be complete by April 1 in time for its expected arrival.

Sky Radiance Measurement

Calculating a satellite's infrared radiant intensity signature from irradiance measurements requires a knowledge of the atmospheric attenuation at the time of the measurement. Two methods are generally used to obtain a measure of the attenuation; 1) star measurements, or 2) analytical models (e.g. LOWTRAN). Neither method provides a real-time measure of the transmission and both can be in considerable error in the presence of clouds. It has been demonstrated[1] that sky radiance measurements made with the AMTA sensor can be related to atmospheric transmittance thereby providing a viable technique for deriving transmittance during a real-time target measurement.

The technique is accomplished by processing the dc output of the AMTA system at the same time the ac component is being used to obtain target signature or tracking information. The recorded dc voltage is converted, by calibration, to sky radiance within the selected spectral region.

---

(1) IR Atmospheric Measurements, Final Technical Report, Nov 1977, AVCO Everett Research Laboratory, Inc., F30602-75-C-0235. RADC-TR-77-385 (A049054)

Figure 14 shows a plot of sky radiance data for filter 5 (8-13 microns) as a function of telescope elevation angle over the range of one degree to 90 degrees (Zenith). By knowing the effective temperature of the air producing the irradiance, it is possible to compute the atmospheric emissivity and in turn the transmission of the atmosphere. A plot of the derived transmission is shown in Figure 15. The plot for a clear sky is very nearly a straight line when plotted on log-log paper. For a sky with considerable structure, possibly due to clouds, the curve deviates considerably from that of a straight line. For a homogeneous sky, the transmission can also be computed from models (e.g. LOWTRAN 3), also shown in Figure 15. The primary advantage of obtaining transmission by radiance measurements lies in the ability to obtain line-of-sight data in real-time during the satellite track. This is particularly important in the case of a non-homogeneous sky or rapidly changing weather patterns. An accurate measure of the transmission is, of course, required to obtain corrected target signature data and two color temperature measurements.

Sky Granularity Measurements

AMTA, like most LWIR radiometric sensors, operates in the contrast mode. That is, the desired information is embedded in the apparent brightness difference between two closely spaced fields-of-view one of which includes the object being observed. Moreover, the atmosphere is not a homogeneous radiator. For example, when a telescope tracks a satellite,

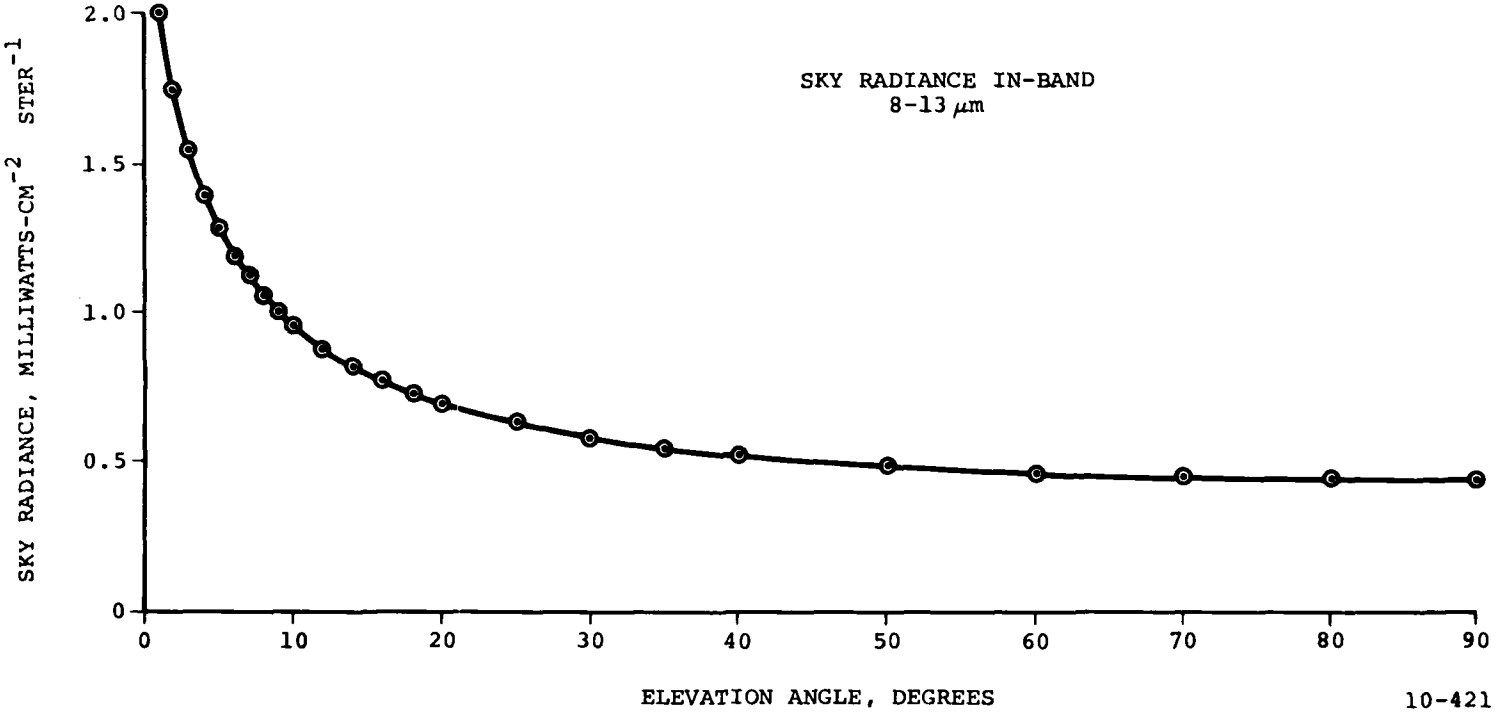

Fig. 14 Measured sky radiance in AMTA filter band 5 as a function of telescope elevation angle.

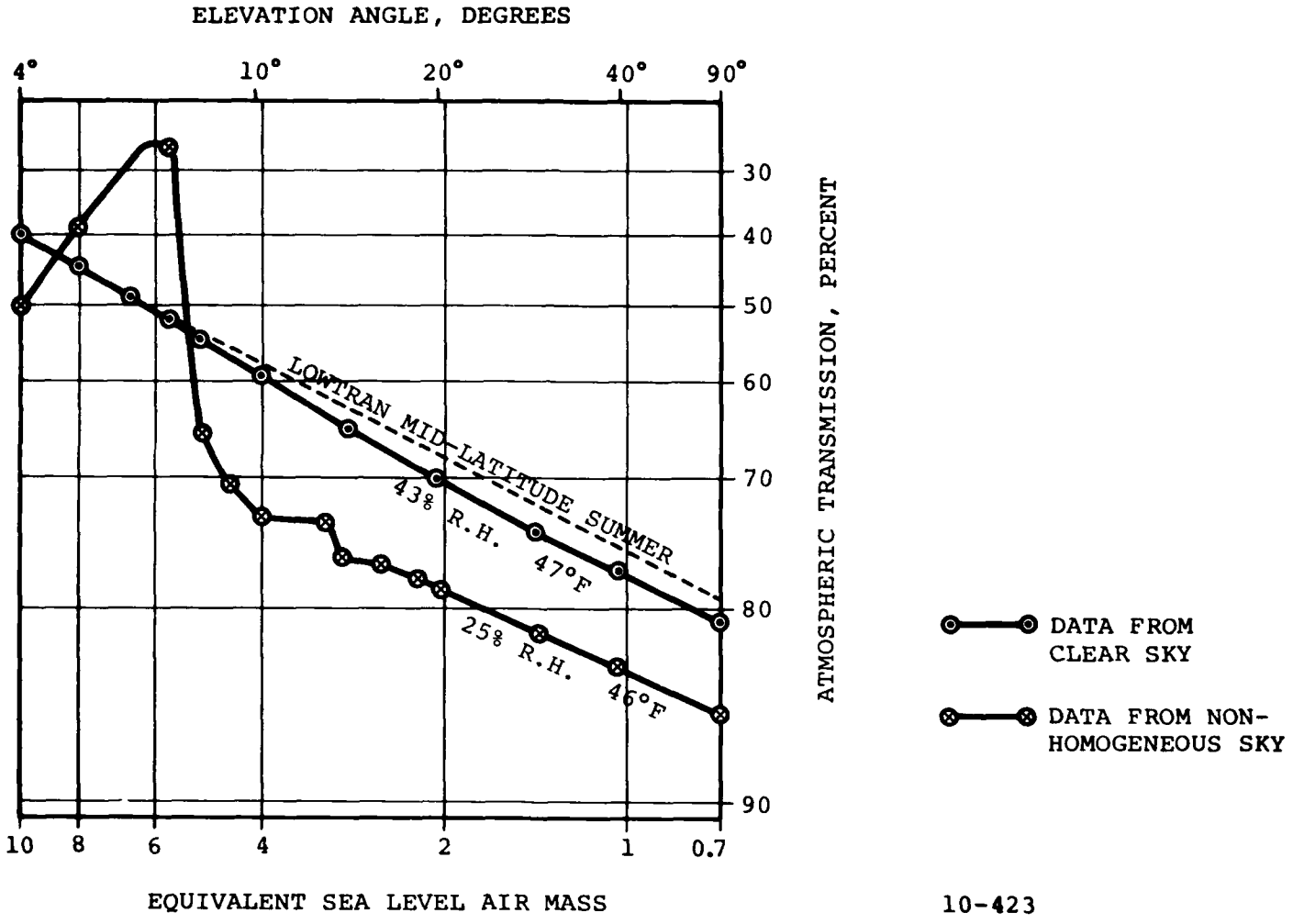

Fig. 15 Atmospheric transmission as calculated from sky radiance measurements.

the apparent motion of thermal structure within the intervening radiant atmosphere produces a noise-like detector output which competes with the target signal. The interfering signal, or clutter, generally exceeds background photon arrival rate fluctuations and is probably responsible for the fact that many well developed LWIR sensors fail to achieve, in the field, the measuring precision predicted from smooth background-limited performance.

It has been suggested that high pixel-density detector focal planes, made possible by CCD technology developments, will permit measuring the interfering pattern and thereby provide the information necessary for automatic clutter cancellation in real-time. Measurements made at AMOS indicate that complete clutter cancellation might reduce the observation time required to achieve a given measuring precision by a factor of 100. To test this hypothesis, there is a need for field data to confirm or refute theoretical predictions for scaling atmospheric radiant structure.

Granularity data for calculating the frequency density distribution of such sky noise is being collected in all LWIR atmospheric windows using the AMTA sensor. The data is being reduced to a (noise spectral density) spectrum with the aid of a Nicolet 660 Fast Fourier Transform Analyzer.

Satellite Acquisition and Signature Measurements

The actual satellite measurements are divided into three phases with an enhanced capability incorporated into AMTA for

each successive phase. The first phase will develop an IR target signature data base for a group of selected targets and provide a history of offset tracking information. The offset data will be used, in part, to define the field-of-view requirements for an automatic search system. The signature data will assist in defining the required integration time for the search and provide design information for future, more complex, IR detection systems.

The second phase will investigate the utilization of AMTA as a target tracker. The scanning secondary mirror will eliminate the cavity noise normally generated by the internal scan mirror system. Outputs for the twenty-five detectors will be displayed on one of the AMOS TV networks for utilization by the Video Auto-Tracker. A tracking accuracy of up to approximately 15 arcseconds is expected.

An automatic search routine will be incorporated into the third phase of measurements. Tracking accuracy will be improved by an order of magnitude by incorporating a modification to the target scan pattern and by the addition of post-detection processing. The post-processing will be accomplished by a dedicated microcomputer. For the brighter satellites, it should be possible to define target position on the array with finer than pixel-limited resolution and provide tracking precision in the realm of one to two arcseconds.

AMTA Modifications

The precision track requirements for the AFWL Program will

require that certain modifications be made to the existing AMTA system. These modifications include the development of a linear scanning secondary mirror system, up-dating the AMTA display for use by the Video Auto-Tracker and the development of a post-processor to provide automatic search and precision fine track capability.

Linear Scan Secondary

Based on the success of the nodding secondary used in the SEP measurements to reduce cavity induced scan noise, further improvements are being incorporated into the secondary mirror system. The improvements will provide a capability to remotely control the amplitude of the scan and allow the use of more complex waveforms including a square waveform superimposed on a linear search pattern.

The mirror will be driven by two modified Infomag model 517 linear motors operating in a push-pull mode. The two motors will be driven by a 525 watt Torque Systems model PA-601 servo amplifier to produce up to 100 inch-pounds of torque. The system will include both position and velocity sensing feedback to provide a rapid, linear response. The mirror will pivot about a Bendix flex bearing. The advantages of this type of bearing are its long-life, frictionless operation and zero lubrication requirements.

A sketch of the system and the B29 secondary mirror is shown in Figure 16.

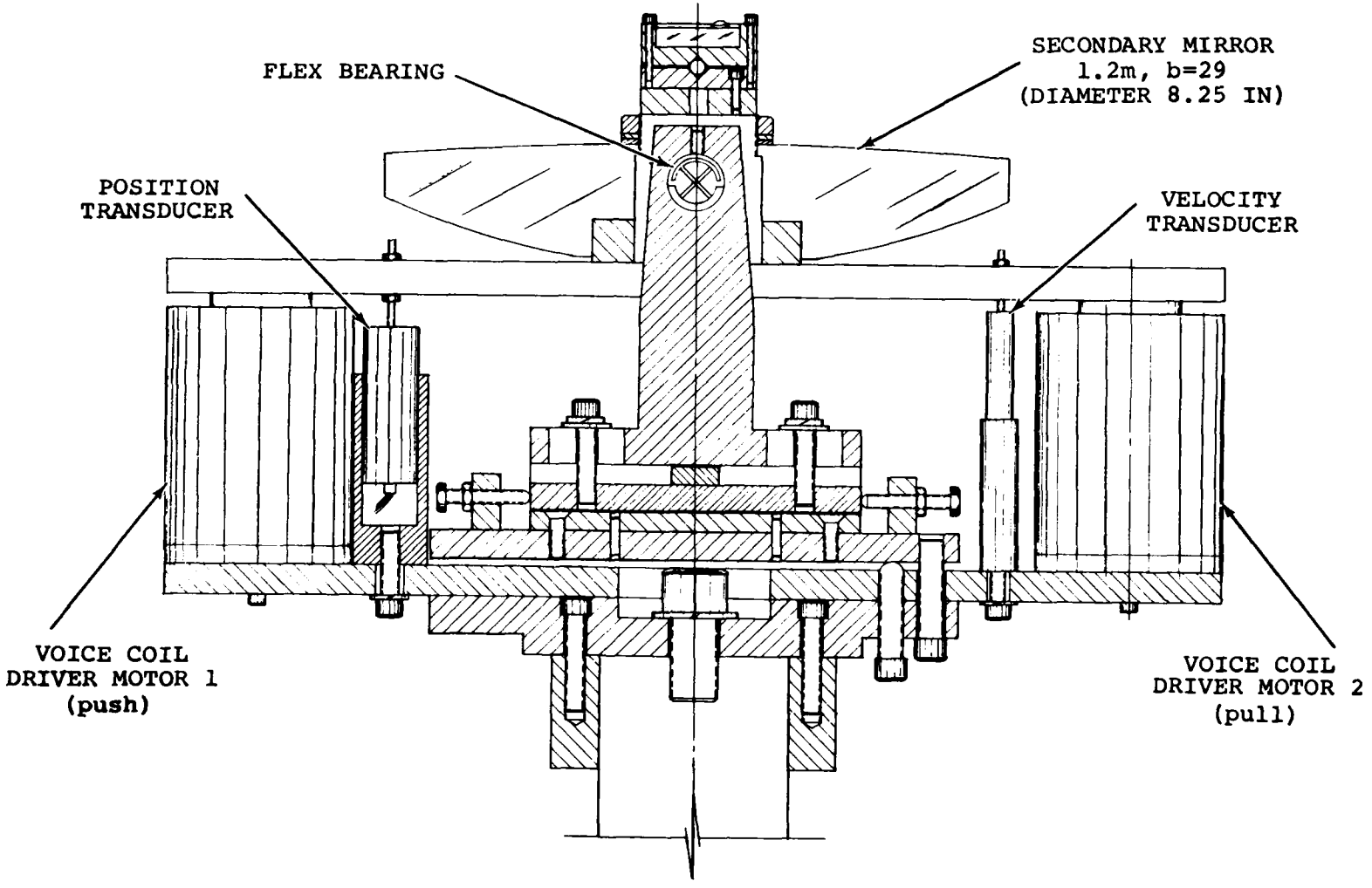

Fig. 16 Schematic drawing of linear scan secondary mirror system for AMTA.

Video Auto-Tracking

Provisions for displaying the outputs of all 25 detectors were originally incorporated into the AMTA system. The system also included a scan converter so that these outputs could be displayed on the Observatory's TV monitors. The capability was never used due to the inherent scan noise which overwhelmed the low level target generated signals. However, with the incorporation of the scanning secondary, the system is now compatible with the existing Video Auto-Tracker system. With minor modifications, this system can be used to drive the telescope. The tracking accuracy will be limited by the coarseness of the 25 element detector array (on the order of 15 to 30 arcseconds). The system, however, will provide valuable data for the following phase in which added processing will provide increased tracking precision.

Detection Processor

An Intel microprocessor system has been purchased which will be programmed to control the AMTA automatic search and precision track system. Outputs from all 25 detectors will be digitized, filtered and processed to identify the presence of a target. Once detected, coarse error signals will be provided to the telescope so as to drive the detected target to the intersection of four detectors forming a quadrature array. Precision error signals are then derived by differencing opposing detectors. The system will then centroid track the target to an expected accuracy on the order of 1 to 2 arcseconds.

A schematic of the conceptual system is shown in Figure 17. During the active tracking, the target will be toggled alternately between the quadrature array and the center of a fifth detector located at the center of the array. The output of this fifth detector will be processed for target signature information.

The microprocessor will also control the search operation for initial target acquisition. The search pattern will be optimized based on outputs of the first and second phase of the Satellite Acquisition and Signature Measurements. At this stage of the program, the early results of the offset analysis indicate (not unexpectedly) that the polar axis offsets (representing time errors) for a satellite generally exceed the declination offset errors by a factor of 3 to 5 times. In addition, the magnitude of the offsets tends to correspond to the age of the elements (e.g., if the elements are old, one should expect larger offset errors). Figure 18 shows a plot of acquisition offsets as measured for a number of low altitude satellites. The offsets are coded with respect to the age of the elements as indicated.

4.3.1.3 BMD MISSILE MEASUREMENTS

Measurement Program

As a result of the U.S. Army's Ballistic Missile Defense (BMD) program and their continued interest in obtaining Mark 11 and Mark 12 infrared signature data, AMOS was tasked to collect data on at least three Western Test Range launches. Data from

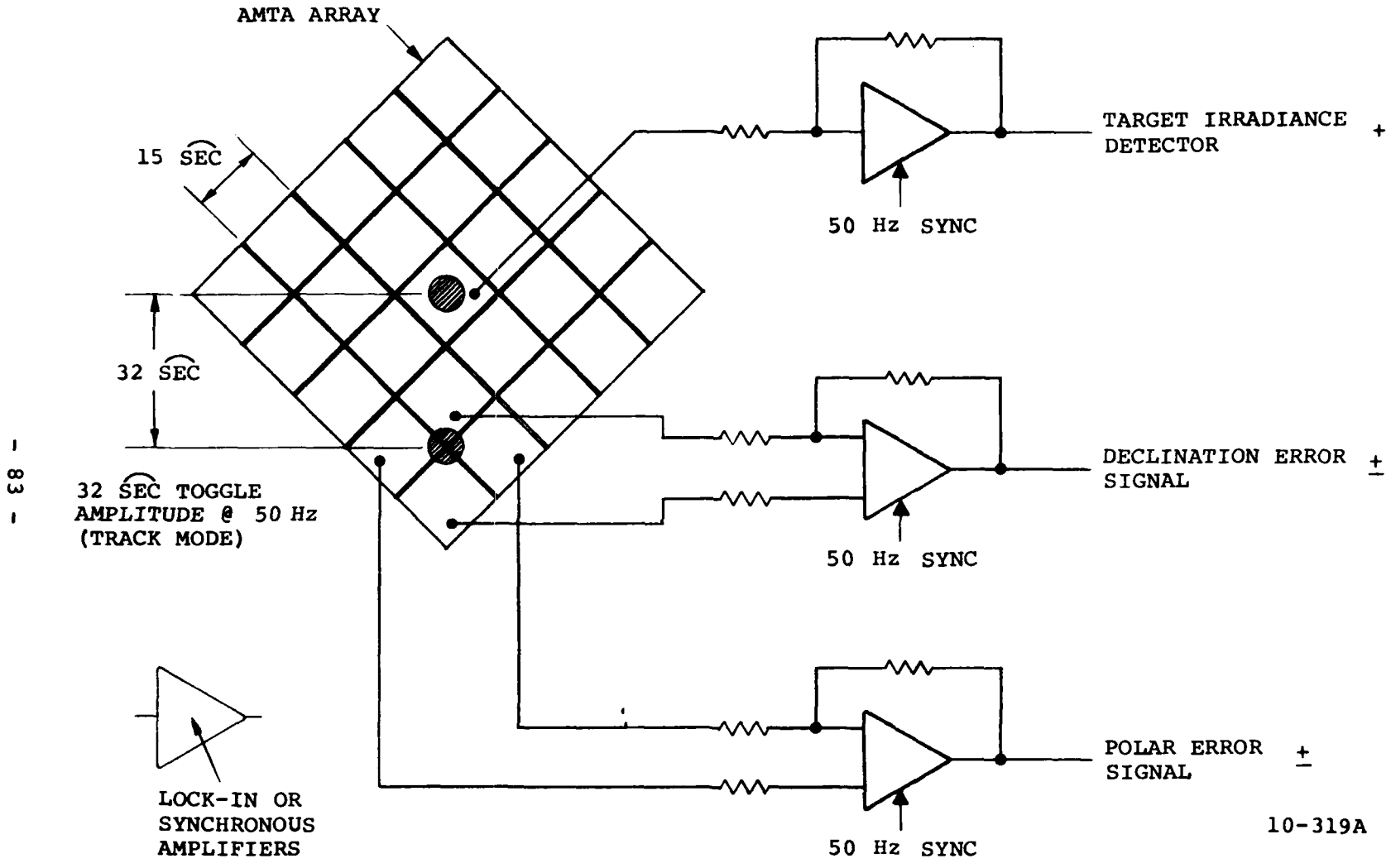

Fig. 17 Schematic of AMTA tracking and signature measurement concept.

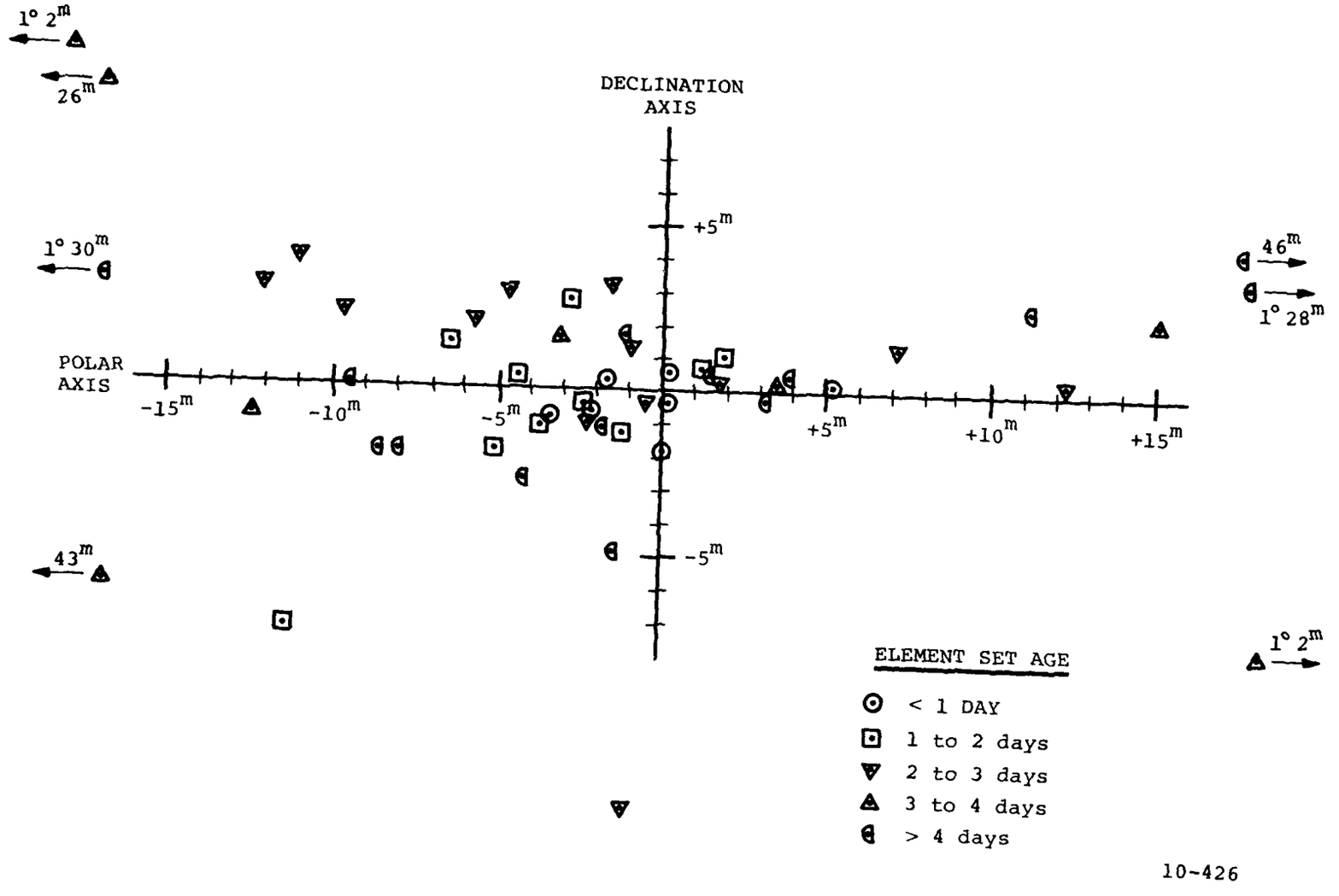

Fig. 18 Measured acquisition offsets for 52 low altitude satellites.

these launches is also of interest to the Army's Homing Overlay Experiment (HOE). Primary interests are radiometric signatures in the 8-13 micron band and target temperature data based upon two color measurements.

Normally when two-color measurements are used to derive target temperature, spectral bands are selected which are widely separated and yet have significant target irradiance values. For AMTA, these bands have been historically filter 5 (8-13 microns) and filter 6 (16-22 microns). However, because of the large variability in atmospheric transmission in the filter 6 band (due primarily to atmospheric water vapor) the use of these bands can easily lead to erroneous temperature calculations unless an accurate determination of transmission is made. For the particular measurements conducted under this program, filter bands 3 and 4 were used to obtain the effective target color temperature. These bands cover the 8 to 9.2 micron and 10.2 to 12.9 micron spectral regions respectively. Although they are not separated as much as the filter 5 and 6 bands, the transmission in 3 and 4 is more equally affected by water variations and, provided the signatures exhibit a sufficiently high signal-to-noise ratio, they will permit a well defined calculation of temperature.

Data Reduction

Data was collected on three WTR missile launches which resulted in Flash and Quick-Look reports from AMOS. Two of the measurements (launches of 28 June and 26 July) were forwarded

to AERL/Everett for further data analysis. Although cloudy weather was encountered during both of those measurements, it was possible to derive valid signature data and reasonable two-color temperatures. The data and conclusions are summarized in AERL 78-398, a SECRET document.

4.3.1.4 HAVE LENT IV & V

Program Plans

Tentative plans have been made for two HAVE LENT type measurements which will involve AMOS support. HAVE LENT IV is planned for the Summer of 1979 whereas HAVE LENT V will probably occur in the Summer of 1980. Both experiments involve high altitude aerosol releases from sounding rockets launched from the Barking Sands test range on Kauai. Both experiments require LWIR measurements with the AMTA sensor. Of the two experiments, HAVE LENT V will present the greatest challenge to the capabilities of AMOS. Angular tracking rates for this experiment will exceed 1°/second. Less than 10 seconds of total time will be allotted for a two-color IR measurement. HAVE LENT IV more nearly simulates the previous launches in the series and the measurements will follow nearly the same scenario established in 1975 (HAVE LENT III) with the exception that a larger scan amplitude will be used to obtain a better measurement once the aerosol cloud size exceeds the angular field-of-view of a single AMTA detector.

Program Status

Two planning meetings have been held to discuss the new

HAVE LENT programs and a third meeting devoted to the HAVE LENT IV experiment will be held in February of 1979. Preliminary test plans for the two programs have been written by staff members of the MIT Lincoln Laboratory Countermeasures Technology Group. These plans have been reviewed by personnel at AMOS and will form the basis for future meetings and, finally, the AMOS MIOP.

4.3.2 VISITING EXPERIMENTS

The visiting experiment program was established to assist approved agencies and individuals in utilizing the unique capabilities of the AMOS Observatory.

A qualified systems interface engineer or scientist is assigned to each visiting experiment. In the early stages of experiment planning he makes contact with responsible personnel in charge of the proposed experiment and identifies and documents the user's requirements. The experimental definition and requirements result in the preparation of a MIOP which, after DARPA/RADC approval, becomes the governing document for the conduct of the program. Included in the MIOP is a brief description of the experiment and its objectives, a description of the sensors involved and their calibration, a scenario for the operation of the experiment, and the requirements for data collecting, data reduction and reports. The assigned scientist or engineer serves as the planning and communications focal point for the visiting experimenter, representing the official source of information who plans, schedules, and expedites the

experimental program at AMOS. He is also responsible for the design and fabrication of any interface hardware necessary to the conduct of the experiment. Where possible, existing facilities are configured to meet the program needs. It is also his responsibility to ensure that the experiment is performed safely and does not place the experimenter or any AMOS facilities in jeopardy.

During the initial year of the Phase IV contract, two experiments (Sandia Laser Experiment and Atmospheric Characterization Program) were performed, and a third (AFWL IR Measurements) was initiated. Also, the possibility of several new experiments was explored through briefing contacts. These include a Patrick AFB Laser Experiment, a SAMSO CW Laser Experiment and measurements of an Instrumented Test Vehicle.

4.3.2.1 Sandia Laser Experiment

Background

Planning for the Sandia Laser Experiment was actually initiated in the Summer of 1978 when the capability to successfully point the AMOS ruby laser beam at a satellite during the daytime hours was demonstrated. Since the satellite could not be visually acquired during the daytime, pointing was accomplished by means of known orbital elements and an accurate mount model.

The basic objective of the program was to establish a calibration of the satellite on-board sensor over the entire diurnal cycle using laser excitation. The calibration was accomplished

during the period between 12 July and 22 July 1978. Due to the particular pulse waveform requirements imposed by the satellite sensors, a special cooled ruby laser system supplied by SANDIA was used in the experiment. Beam forming and pointing was accomplished using the AMOS Laser Beam Director system.

Conduct of Experiment

Preparation for the experiment began in early July of 1978 with the arrival of a liquid-nitrogen-cooled ruby laser system from Sandia Laboratories, Albuquerque, New Mexico. The special ruby laser and its associated pulse timing control system was needed to meet the satellite sensor requirements which included a four millisecond pulse duration. The laser was set up on an optical table located adjacent to the AMOS ruby system. Alignment and calibration were performed using a HeNe laser which was directed through the ruby rods to the beam forming system and then returned by the 36-inch diameter flat used in an autocollimation mode.

The system was collimated by viewing the return from three retro-reflectors positioned around the perimeter of the out-going beam on an ISIT TV camera. System boresight was established using a star. Pointing was additionally verified by nighttime firings at the target satellite. A telephone communication link, using the AMOS/Wheeler lines, was set up with the satellite control station on the mainland. Through this link it was possible not only to verify a hit in near real-time but also to obtain a rough measure of the magnitude of the hit.

Laser firings were scheduled to cover the full diurnal period, but were broken up into 7.5 hour shifts separated by a 22.5 hour period between completion of one shift and the beginning of the next. Each shift was to include two data sets of 20 hits which required two to three hours to complete. This arrangement would allow a full 24 hour coverage of the satellite (the satellite is in earth synchronous orbit) in a one week period and allow a single crew to accomplish the work.

The first laser firings were attempted on the evening of 12 July when the satellite could also be visually observed. Although positive hits were detected, the existence of cirrus clouds above the observatory limited the percentage of hits to about 50%, insufficient for a successful data run. The next data run, which did produce one successful measurement set, was performed on July 14. The scheduled second set for that day was not completed, again because of a build up of cirrus clouds.

It became obvious that the measurement program would exceed the allotted time period unless modifications were made to the schedule. It was decided to support the program on weekends and to extend the 8 hour shifts through the use of "mini-teams" using both AMOS and Sandia personnel.

The actual schedule is graphically presented in Figure 19. In addition to the weather problems that were encountered, equipment problems occurred within the beam director, the laser timing system, and the laser flash lamp system. The program

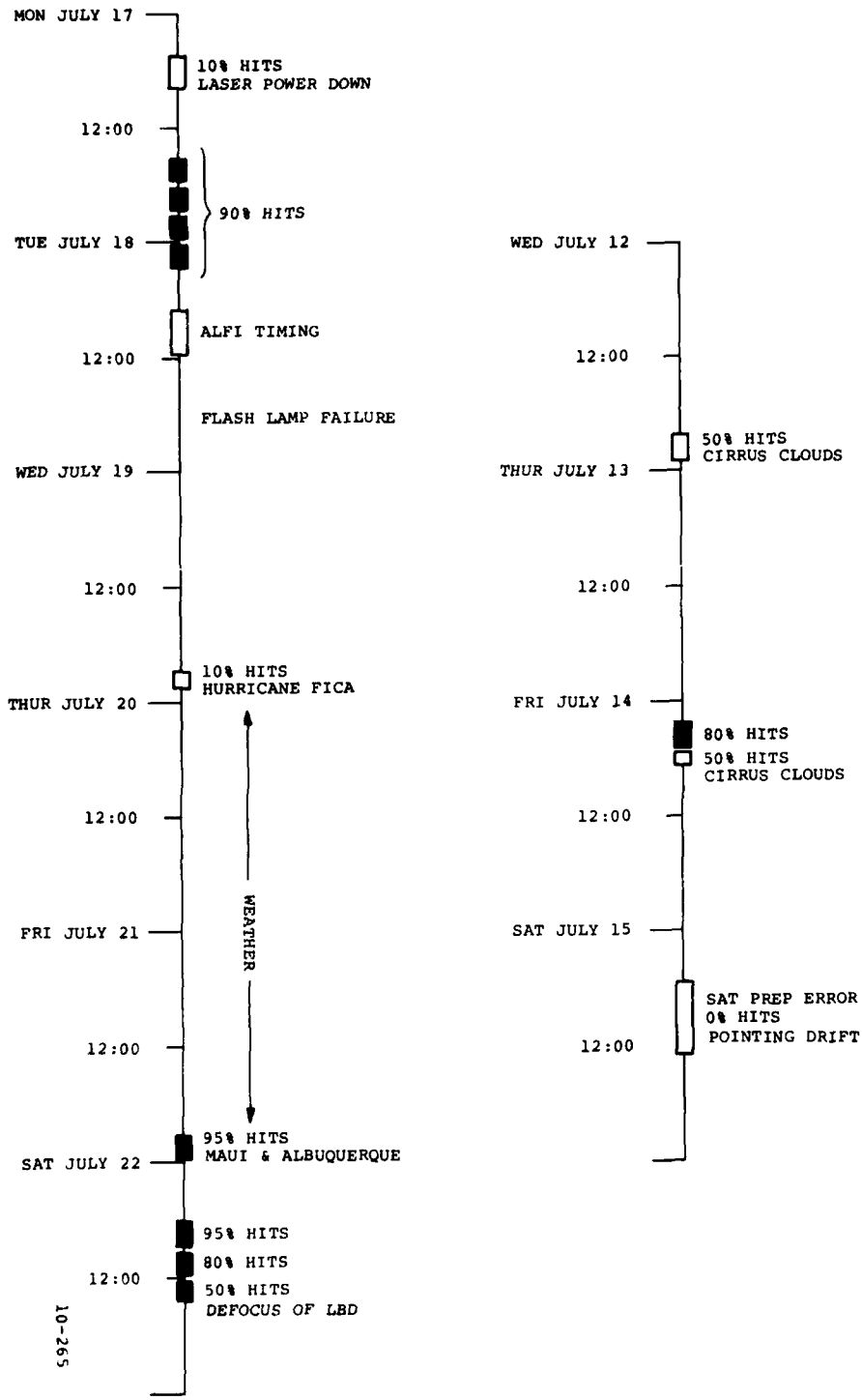

Fig. 19 Time chart of the actual firing schedule used in the Sandia experiment.

was successfully completed with the last measurement set on 22 July.

Pointing Drift

During the collection of the daytime data, it was discovered that the Laser Beam Director was experiencing severe pointing drift. It was also noted, by observation of the return from the retro-reflectors, that the beam expander system was tending to defocus in the presence of solar heating. The pointing drift problems, also a result of solar heating (particularly on the gimbal system), were circumvented in real-time by frequent reference to bright stars which could be observed in the daytime. The observed stellar offsets were then added to the satellite tracking commands.

However, the ultimate solution to the problem is to provide protective shielding for both the 24-inch collimator and the gimbals of the 36-inch tracking flat. Since the collimator is not moved during satellite tracking, the entire expander system can be enclosed in a solar reflecting tube which will serve to maintain a uniform temperature throughout the collimating and beam-folding optics. Additionally, the shaft angle encoders and bearings of the tracking flat can easily be protected from direct solar illumination through the use of shields. Further protection could be included by restricting the dome slot width, particularly for the tracking of synchronous satellites.

Beam Pattern Experiment

The program provided an opportunity to obtain a measure of the far-field intensity pattern of the laser beam director system. With the availability of a feedback link, which provided a direct measure of the relative magnitude of the hits, it was possible to obtain a rough map of the beam pattern as shown in Figure 20. The plot indicates that the beam had a half-angle divergence of about 25 arcseconds at the target and also exhibited a high peak at the beam center.

To better understand the radial amplitude variations a photographic mask (with scaled down dimensions of the aperture of the Laser Beam Director) was illuminated first with converging and then with diverging light from a Helium Neon laser. After appropriately scaling the geometry, scans were made of the laser far-field intensity profile corresponding to 25 arcseconds diverging (Figure 21) and 25 arcseconds converging (Figure 22) beams. Figure 22 shows a close similarity to the data taken on 18 July. The narrow central peak explains why a small angular change around the boresight resulted in a large amplitude change in the reported magnitudes.

The secondary peak around 10 arcseconds on the data can be attributed to the near-field intensity profile. Near-field burn patterns showed that the laser beam was underfilling the aperture of the Beam Director.

The rather strong focussing shown here was detected during the Sandia Experiment and was corrected somewhat by adjusting

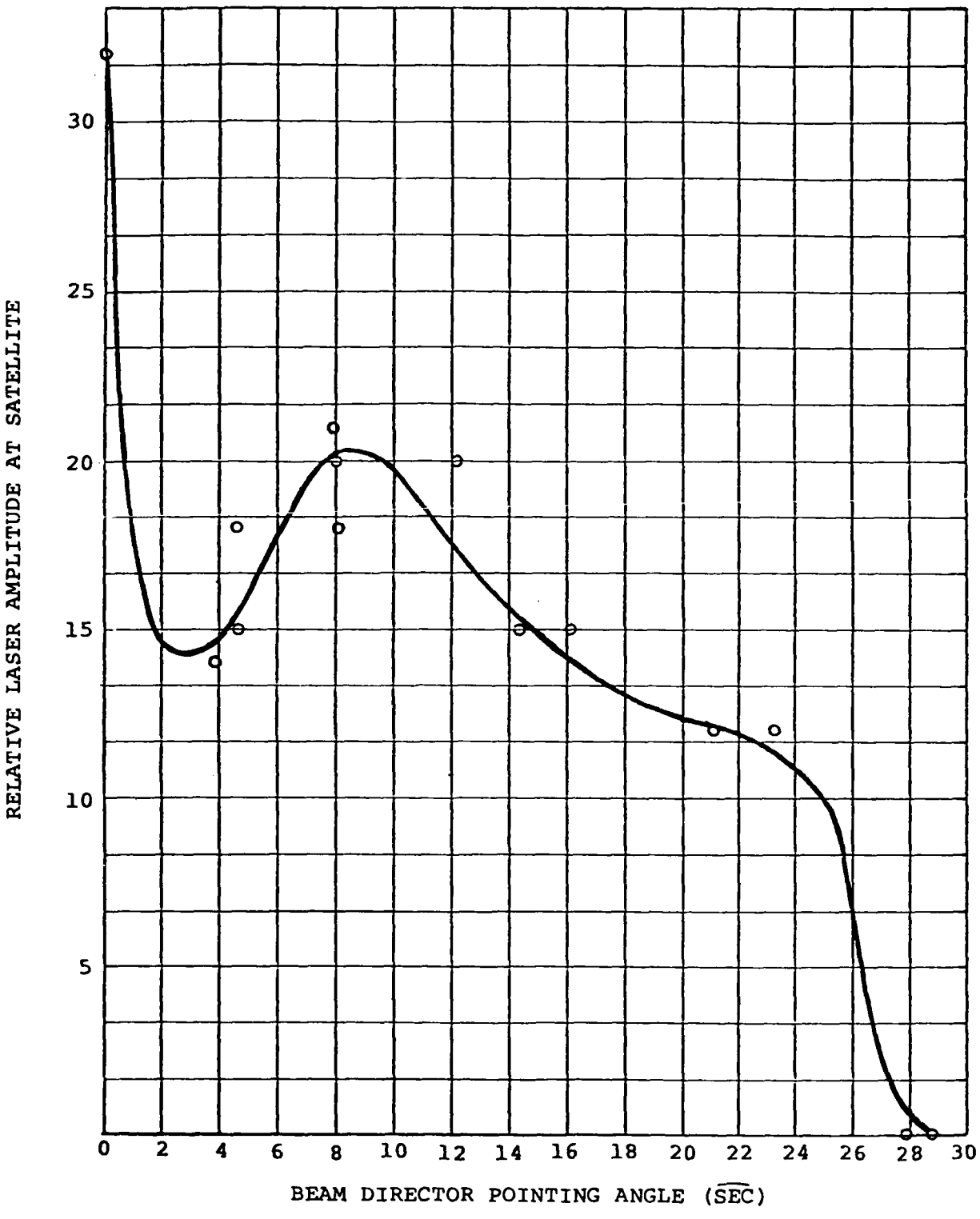

Fig. 20 Radial intensity profile of LBD as measured on 18 July 1978.

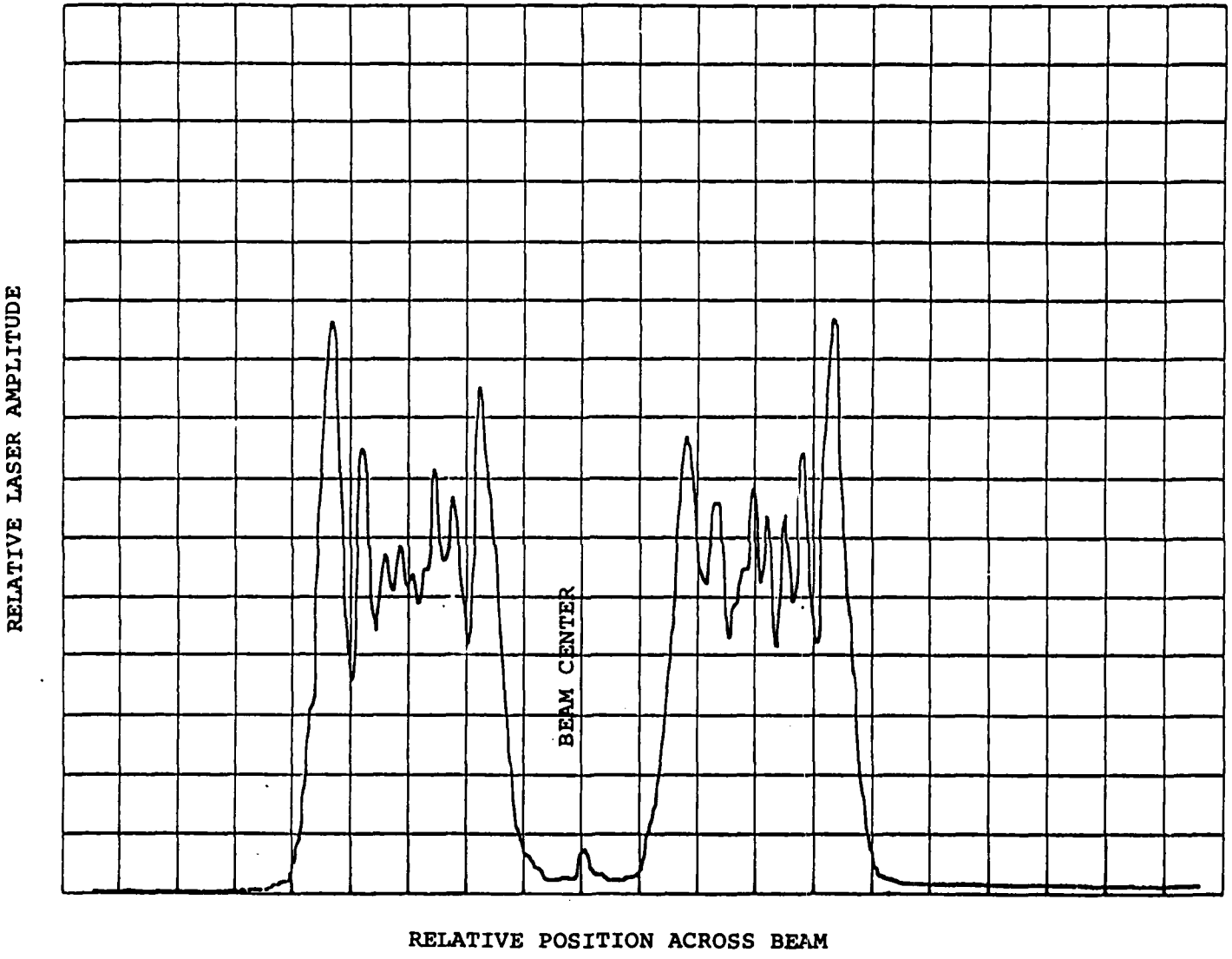

Fig. 21 Profile of far-field pattern using a simulation with a beam divergence of 25 arcseconds.

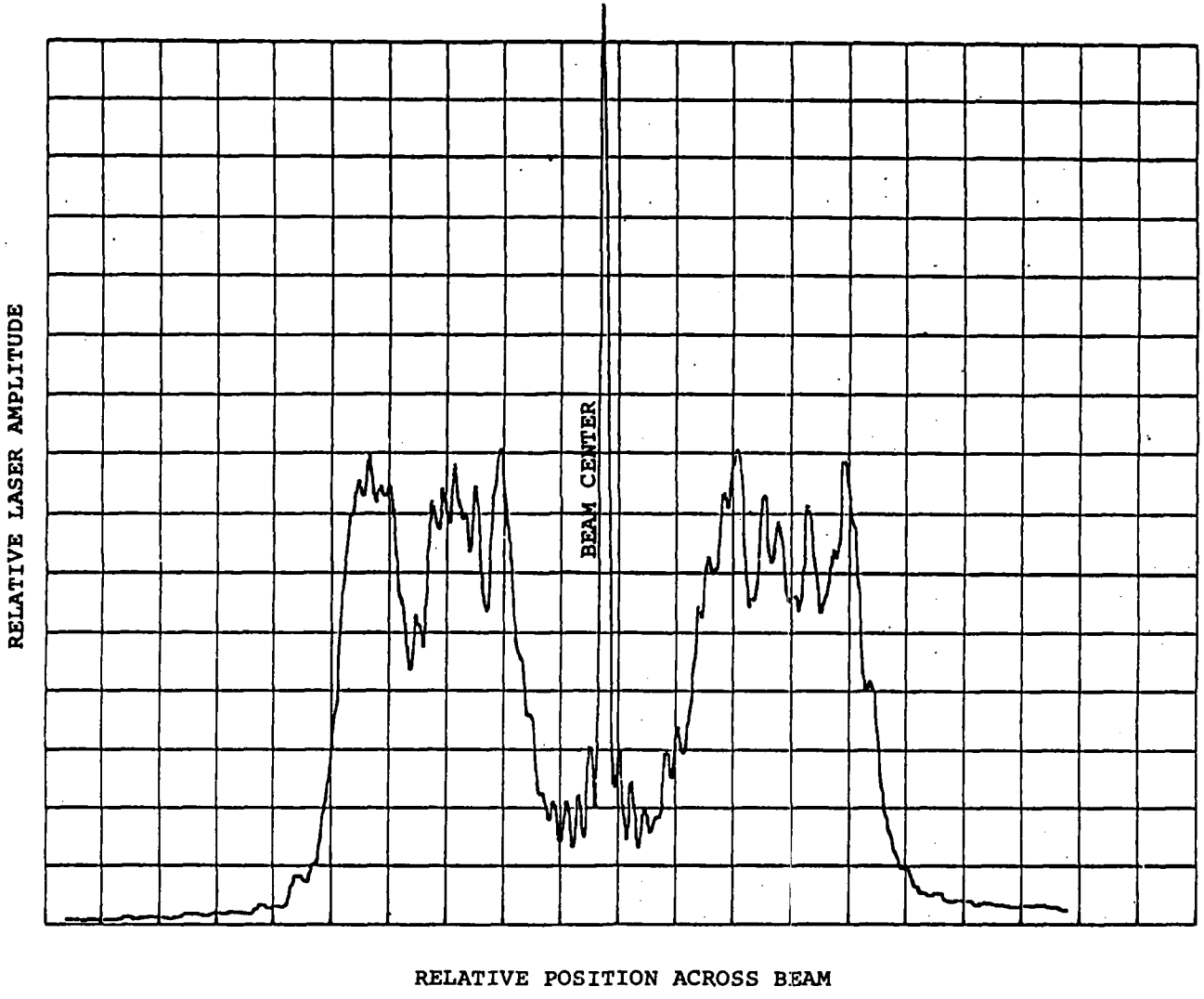

Fig. 22 Profile of far-field pattern using a simulation with a beam convergence of 25 arcseconds.

the 4-inch beam expanding optics to compensate for the focussing laser beam. The experiment did not require a perfectly collimated output.

Even though this data is only representative of the firing sequence from which it was taken, one can make the following conclusions.

1) During the AMOS/Sandia Experiment, the outgoing beam was highly convergent. This was most likely due to thermal focussing in the laser rod but the Beam Director optics may have contributed.
2) Focussing or defocussing the output beam of any beam director will cause substantial radial profile intensity variations due to Fresnel diffraction. The larger the aperture the more quickly one enters the Fresnel regime with a small optical power.
3) Using a cooperative target such as the Sandia satellite could provide valuable information on the far-field intensity profile. This would be extremely useful in predicting returns from non-cooperative targets and in tailoring the Beam Director optics to achieve the optimum beam size and shape for such targets.

4.3.2.2 ATMOSPHERIC CHARACTERIZATION EXPERIMENT

During the period 17 July to 11 August 1978, a visiting experiment was conducted in support of an existing atmospheric

characterization program. The experiment was designed to meet the following four objectives:

1) Obtain data to characterize the angular dependence of seeing;
2) Investigate the short-term statistics of seeing;
3) Characterize the noise in the AMOS Model II Star Sensor;
4) Process existing data previously collected with the Real-Time Atmospheric Monitor (RTAM).

Brief descriptions of each of these tasks, the measurements implemented and the results are given in the following four sections. A more complete discussion can be found in Turbulence Characterization and Control, Final Report for Contract F33602-76-C-0054 (Avco Everett Research Laboratory, December 1978).

Angular Dependence of Seeing

The conventional theory of propagation through turbulence predicts that the atmospheric correlation scale distance(r_o) varies with the (3/5) power of zenith angle. To investigate this effect, the following procedure was developed. A data run was defined as a series (6-8) of bright stars ($m_v < 4$) at various zenith angles. The star closest to zenith was designated as a reference. Data was collected with the AMOS Seeing Monitor/PDP-8 in a cyclic fashion. In all cases, measurements

on a specific star were bracketed with measurements on a reference star. This was done in order to evaluate temporal effects. PDP-8 processing was such that the averaging time was approximately one minute per star.

In total, nineteen such data runs were carried out on seven nights. In the subsequent processing, seven of these runs were eliminated because of excessive temporal nonstationarity. The remaining data clearly indicate that the experimental results are not consistent with the theoretical scaling. Furthermore, seeing does not appear to degrade with angle as rapidly as predicted.

In view of this conclusion, it is reasonable to try to develop a new model which is consistent with the data. One such physically-motivated model is characterized by an angular independent and dependent contribution. The general topology of Maui suggests that the former term is associated with low altitude turbulence whereas the latter term is associated with high altitude turbulence. While not entirely successful, it does appear that the limited amount of data tested does fit this model better than the conventional model.

Short-Term Statistics of Seeing

Seeing Monitor data taken with short averaging times was also collected during this period. The procedure used was to acquire a bright star ($m_v < 3$) near zenith and collect many cycles of averaged data over periods of 20 to 30 minutes. Averaging times of 72 seconds were used. In total, thirteen

such data runs were collected on seven nights. Reduced data gives values of r_o at a wavelength of 5000A ($\Delta\lambda$ = 1200A).

A variety of behavior is seen in the data, varying from rather smooth and relatively constant values of r_o to rapid and apparently random fluctuations.

Star Sensor Noise Characterization

To provide a direct estimate of the AMOS Model II Star Sensor noise characteristics, the following procedure was carried out. A low voltage light bulb, powered by a regulated dc power supply, was located such that it illuminated a portion of the diffuse interior surface of the dome. The Star Sensor telescope was pointed at the illuminated dome, the tracking motor was turned off and the mount was locked in position. The instrument was operated with photomultiplier voltages and outputs typical of the range of conditions seen during stellar operation. Data was collected on several occasions during a period of one week.

The data of primary interest were the log amplitude variances associated with the sum and difference signals. In both cases the results display a behavior characteristic of photoelectron fluctuations. Furthermore, the dependence on applied photomultiplier voltage is approximately exponential as observed previously. The absolute values of noise variances are somewhat smaller than the corresponding values for the AMOS Model I Star Sensor. Furthermore, an empirical model developed from this data is probably of sufficient accuracy to replace

the currently used calibration procedure.

RTAM Data Processing

Shortly after delivery of the Real-Time Atmospheric Monitor (RTAM) from Itek, a series of simultaneous operations with this device and the Seeing Monitor was conducted. While the Seeing Monitor data were processed in real-time, RTAM data were recorded on magnetic tape. In total, ten data runs, each approximately fifteen minutes in length, were obtained on two nights using the brightest stars available as objects.

During the period of these visting experiments, an attempt was made to process this previously obtained data. In order to obtain as direct a comparison with the Seeing Monitor results as possible, analog electronics were used to measure the half-MTF frequency of the RTAM signals. The output of these electronics was then processed by the PDP-8I system. In this fashion, the processed results from the two instruments yield essentially equivalent measures of atmospheric seeing.

Because of several problems, primarily low sensitivity of the RTAM, only a single data run was suitable for processing. Even for the single run, several problems relative to calibration, noise and instrumental artifacts were encountered. Taking all of the known uncertainties into account yielded an estimated RTAM value for r_o of from 10.8 cm to 14.3 cm with a nominal value of 12.6 cm. The Seeing Monitor result was 11.5 cm with a probable accuracy of $\pm$ 10%.

4.3.2.3 AFWL IR FLIR MEASUREMENT

As part of the AFWL IR Measurement program discussed in Section 4.3.1.2, a visiting experiment will be conducted at AMOS during the months of April and May 1979. A FLIR (Forward Looking Infrared) sensor and associated adaptive optics package will be installed on the 1.6 m Telescope. The package will be used to demonstrate the acquisition and tracking of satellites, particularly in the daytime, and to investigate the capabilities of an infrared adaptive optics system.

In preparation for this experiment, modifications are being made to the 1.6 m Telescope and to room 26 of the observatory which will house the system control electronics. Specifically a six inch diameter germanium lens will be installed in the optical system of the f/16 telescope to convert it to an afocal system as required by the FLIR. The requirements for the system control electronics which will be housed in room 26 are similar to the demands of the Itek Compensated Imaging System which will be installed in this same room in 1980. The modification schedule for room 26, which includes 10 tons of air conditioning and 20 kw of three phase primary power, is being accelerated for this visiting experiment.

Equipment Description

Figure 23 shows a sketch of the sensor package which will be mounted on the telescope. The primary components of the package are presently in existence at the AFWL and are being assembled for this experiment by FACC (Ford Aerospace &

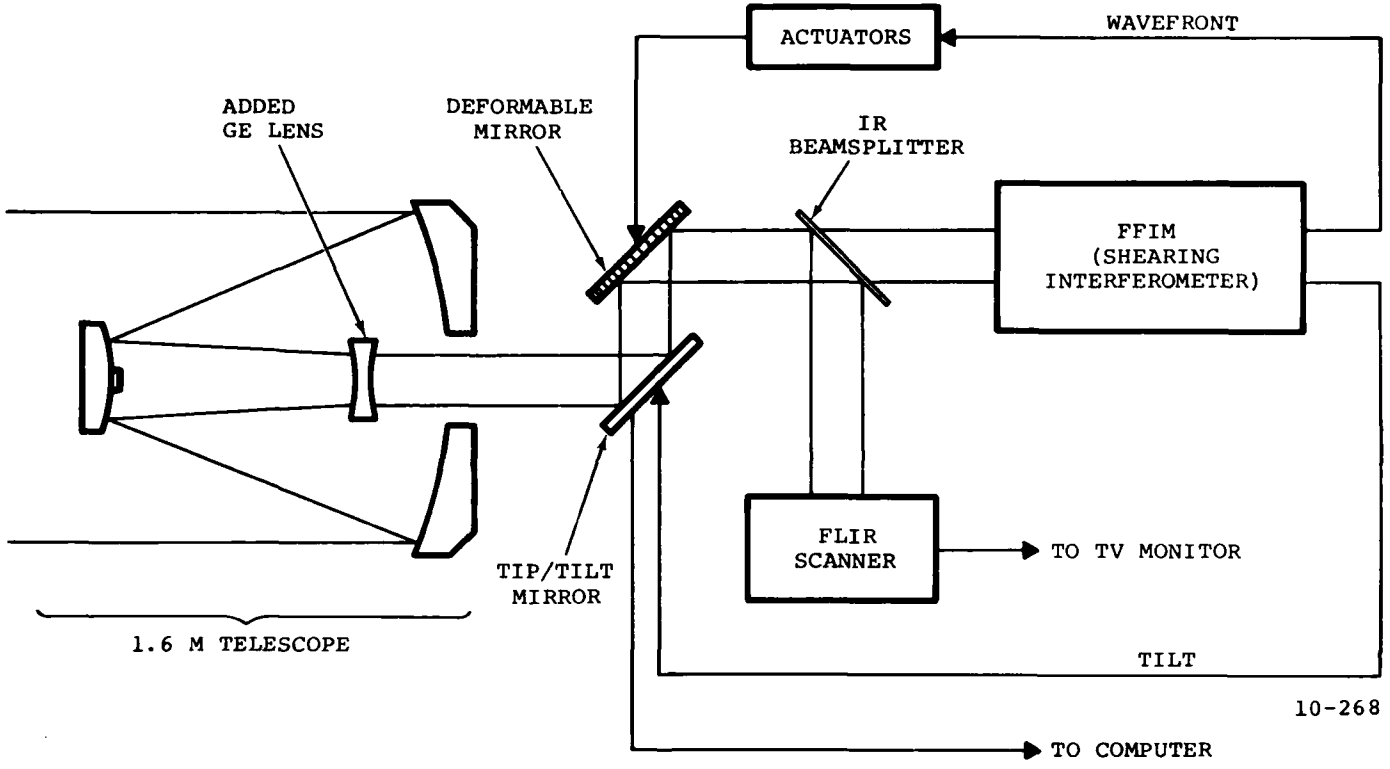

Fig. 23 Schematic of AFWL FLIR sensor package as mounted on the 1.6 meter telescope.

Communications Corporation). Components are included to correct the input beam for atmospheric induced aberrations before it is imaged in the FLIR. First order aberrations experienced in terms of wavefront tilt are corrected by a rapidly responding tip/tilt mirror. Higher order aberrations of wavefront distortion are corrected by a piezoelectric-driven deformable mirror. As in the Itek CIS, wavefront errors are detected by a shearing interferometer, known in the AFWL package as a FFIM (Far-Field Intensity Maximization) sensor.

The package requires a four inch diameter collimated input. To satisfy this requirement, a negative lens is being installed within the f/16 converging beam. The lens is being mounted on the tertiary mirror drive system which presently exists within the 1.6 m Telescope. It will be positioned such that, when the tertiary mirror is rotated into position, the lens is rotated out of the beam and vice versa. The side Blanchard surface of the telescope can then be used in a normal manner for other experiments.

Figure 24 shows a tentative layout for the control and processing electronics for the AFWL package. This equipment, which will be mounted in room 26, is similar to the corresponding electronics being developed for the CIS. The AFWL equipment, like the CIS electronics, is designed for three phase, 208 volt operation and the resulting heat loads will require a 10 ton air conditioner. Room 26 will additionally be supplied with overhead cable trays and an intercom system with provisions for

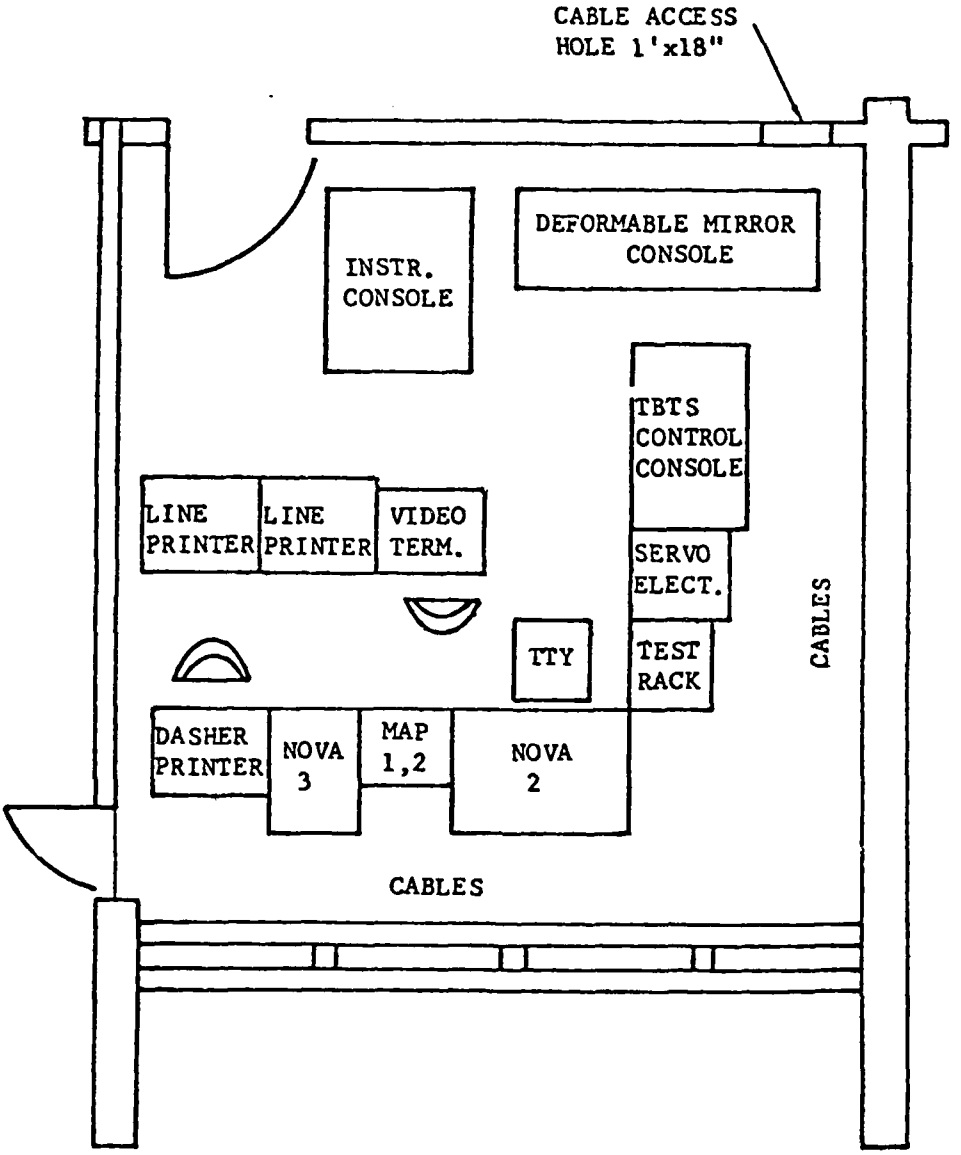

ROOM 26

Fig. 24 Tentative layout of the control electronics for the AFWL FLIR sensor package.

six headsets for tie-in to the remainder of the Observatory.

Preparation for the arrival of the AFWL package, including modification of room 26, is in progress. The equipment is scheduled to arrive 1 April and two weeks will be allotted for installation and check-out. Satellite tracking tests will then take place over the next six weeks, terminating 31 May 1979.

4.3.3 Large System Tests

In contrast to the type of program support discussed in Sections 4.3.1 and 4.3.2 which involves use of existing or slightly modified AMOS instrumentation (Measurement Programs) or temporary installation of special hardware (Visiting Experiments), certain major development activities are included in the Phase IV program. These activities are identified as Large System Tests and, in particular, include the DARPA Compensated Imaging System (CIS) program and various MOTIF system interface tasks.

4.3.3.1 MOTIF Interface

MOTIF Interface tasks include extensive modifications to the AMOS facility, which are discussed in detail in section 4.3.3.5, along with specific documentation and hardware upgrade efforts which are described in this section.

Documentation

This task consisted of upgrading the technical documentation on AMOS/MOTIF timing, facilities and common support equipment. The work was completed during January - March of 1978.

A Timing System Manual was prepared that contains system level technical information, two equipment manuals (one for the SC-17 Computer/Timing Interface and one for the Timing System Distribution Interface), supplements to existing vendor manuals and maintenance and operations procedures.

New documentation prepared for the AMOS/MOTIF Facilities includes detailed equipment manuals for the power distribution, computer room air conditioning and control room air conditioning systems. A less-detailed description of remaining facility systems is given in a new document, the "AMOS Facilities System Manual."

A system manual was also written that describes the Common Support Equipment used by AMOS/MOTIF.

The manuals were validated by AMOS quality assurance personnel and responsible technicians. As the periodic maintenance procedures contained in the manuals came due, they were performed as part of the validation effort.

Hardware

Hardware modifications implemented under the MOTIF interface task included design, fabrication, testing and documentation of; (1) a new mount control panel, (2) improvements to the dome consoles in the areas of maintainability and operator convenience, (3) rewiring of all hydraulic system control circuits, (4) modifications to the dome crane system and (5) replacement of the obsolete oil temperature controller with a new system.

One MOTIF Interface hardware task was not complete as of

31 December 1978. Contained in this task is the provision of a Low Light Level Television System (LLLTV) for the B37 Telescope. Although the basic system design and some of the fabrication was completed as early as the Fall of 1977, a special measurement program (SEP) required that an interim system be installed and used for operations. Although the interim system uses the basic LLLTV sensor (an ISIT) it does not have the light shroud, remote control units, filter wheels, and other features that the original design included.

During 1978, higher priority activities precluded completion of the LLLTV and the interim system on the B37 continued to support MOTIF measurements. Current schedules show the LLLTV system completed in the Spring of 1979.

4.3.3.2 Compensated Imaging System (CIS) Interface

Support for the DARPA CIS program constitutes a major effort in the AMOS Phase IV program.

As is the case for visiting experiments and certain measurement programs, AMOS has designated a CIS Interface Scientist for the Compensated Imaging activity. He is responsible for interaction with RADC, Itek, and Laboratory personnel and, in general, for assuring that the CIS is installed efficiently and on schedule at AMOS.

AMOS/CIS interface activities began early in Phase III and included participation in CIS design reviews, preparation of Interface Information Documents (IID's) and definition/implementation of special tests.

Interface activities and special testing related to the CIS have continued during Phase IV and are expected to increase in scope and intensity as the delivery date for CIS hardware draws near.

When the hardware arrives on-site, AERL will install the equipment on the 1.6 m Telescope and in the CIS control room and interface the system to the AMOS computer, timing and control systems. During the CIS evaluation period, AMOS will provide mission planning, operations, and technical support.

Significant Phase IV CIS activities during 1978 included the definition of major modifications to the AMOS facility for the CIS hardware, and the design and implementation of special tests on the 1.6 m Telescope to assure compatibility with the Itek equipment.

The facility modifications are discussed in section 4.3.3.5. Two of the most important special tests are described in detail in the next few paragraphs. Although other CIS testing was conducted during 1978, these two tests serve to demonstrate the scope and complexity of the efforts involved. The first test - 1.6 m Telescope vibration evaluation - was concerned with providing data to assist Itek in design of a baseplate structure, optical mounts, and other mechanical elements such that CIS performance specifications can indeed be achieved when operating in the AMOS environment. The second test was performed using weights mounted at various locations on the 1.6 m mount to simulate the Itek CIS hardware. This

test was performed to ensure that the mount hydraulic bearings can support the added weight and that the required velocity and acceleration performance can be achieved.

1.6 M Telescope Vibration Tests

A series of tests, designed to assess the effect of vibrational influences on the 1.6 m Telescope, was completed in September 1978. Vibration amplitudes at the instrument mounting surfaces and pointing stability were measured under maximum vibration conditions.

The first phase of this experiment was to identify all sources which might induce vibration in the telescope. Accelerometers were mounted on the end of the telescope tube, on the instrument mounting surfaces and on the telescope pedestal. The polar and declination axes were pressurized and the outputs of the accelerometers were monitored on an oscilloscope while various vibration sources were activated. Some of the sources monitored were the rotation of the telescope protective dome, the basement air compressor, footsteps, the telescope hydraulic pumps, and the 400 cycle generator located in the basement.

Rotating the dome at approximately 10°/sec produced g-forces in the telescope that were at least an order of magnitude greater than the sum of all other sources combined. Using this as a worst case condition, three accelerometers were mounted on the rear Blanchard surface and then on the south declination housing at a reinforced cross member. In both places the accelerometers were oriented so that one was

parallel to the line-of-sight, the second was parallel to the north-south coordinates and the third parallel to the east-west coordinates. With the telescope pointing at zenith in synchro mode and with polar and declination axes floating, the dome was rotated and the outputs of the accelerometers were recorded on a high speed chart recorder. Both surfaces showed similar accelerations of around 2.5×10^{-2} to 3×10^{-2} g.

Pointing stability was checked using the wander detectors of the atmospheric Seeing Monitor. The Seeing Monitor can detect pointing changes of approximately 0.1 arcsecond with a frequency response of approximately 200 Hz.

The first pointing stability test consisted of acquiring a star and then rotating the dome to note the effect. During this test a combination of wind buffeting and atmospheric conditions produced a short term (1 sec) image wander of 0.8 arcsecond. No noticeable difference was detected when the dome was rotated. The Seeing Monitor was then used to record actual pointing errors during a satellite pass. During this pass wind buffeting (30 mph) and atmospheric turbulence had increased to degrade pointing to several arcseconds in a 1 sec period. Again there was no noticeable effect on pointing when the dome was rotated.

It was concluded from these tests that the maximum expected operational acceleration at the rear instrument mounting surface or at the south declination surface will be about 3×10^{-2} g. Vibrationally-induced pointing errors will be less than a few tenths of an arcsecond.

1.6 M Telescope Inertia Tests

Inertia testing on the 1.6 m Telescope has been conducted on several occasions in support of the CIS program. The reason for this is that the telescope-mounted equipment has increased significantly in weight as Itek's detailed system design has progressed.

Table 3 summarizes the situation as of 30 September 1978 (reference Itek IID-A-0001-D) and shows the increase in inertia during 1978 alone.

AMOS conducted tests in November and December of 1978 using the weight distribution given in the referenced Itek IID plus additional weight to simulate a typical sensor package (e.g. AMTA, laser receiver) on the side Blanchard instrument mounting surface. Figure 25 shows two views of the 1.6 m Telescope with the weights installed.

The tests performed were similar to those conducted in March 1978 (float test, step response, simulated satellite pass) with the addition of an actual satellite pass and a pointing check.

The first step was to determine the amount and distribution of weight and how to mount it on the telescope. The existing adjustable polar counterweight assembly was determined to be structurally unsafe to carry the approximately 3600 pounds necessary to balance the telescope. To increase the safety factor, the diameter of the assembly's mounting bolts was increased from 3/8 to 3/4 inch, the mounting brackets were changed and much of

TABLE 3 CIS TELESCOPE-MOUNTED HARDWARE WEIGHT AND INERTIA DATA

	4/18/78	6/30/78	9/30/78
Total Weight (pounds) of ITEK CIS Hardware	3,202	3,376	3,618
Total Weight (pounds) added to 1.6M telescope*	5,945	6,438	7,761
Total Inertia (Slug-ft^2) about polar axis**	37,068	37,787	38,711

* Includes polar balance counterweight of 3,147 pounds for 9/30/78 configuration

** Original design specification by Century-Detroit was 32,500 slug-ft^2

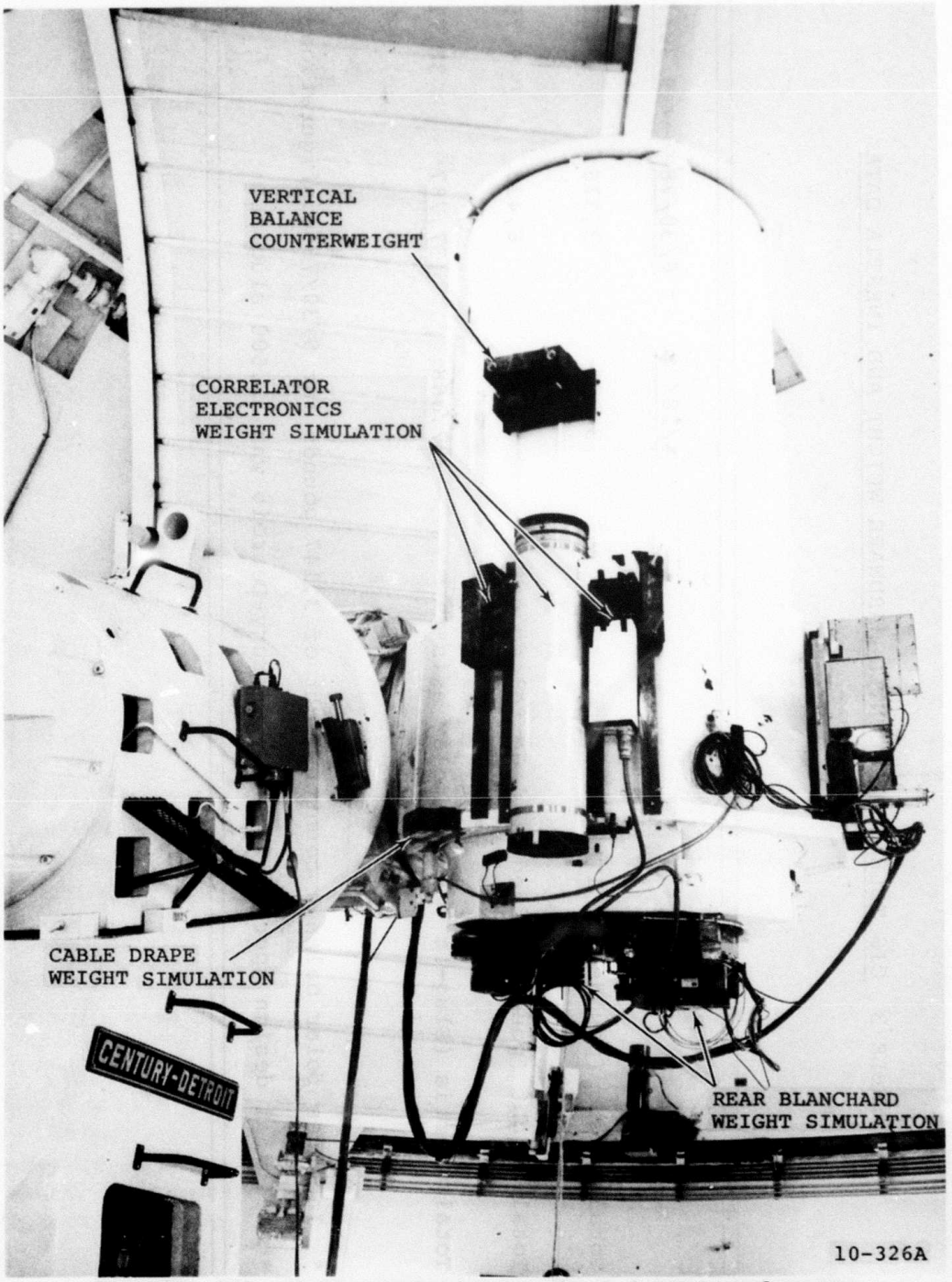

Fig. 25 CIS weight simulation on the 1.6 meter telescope (sheet 1 of 2).

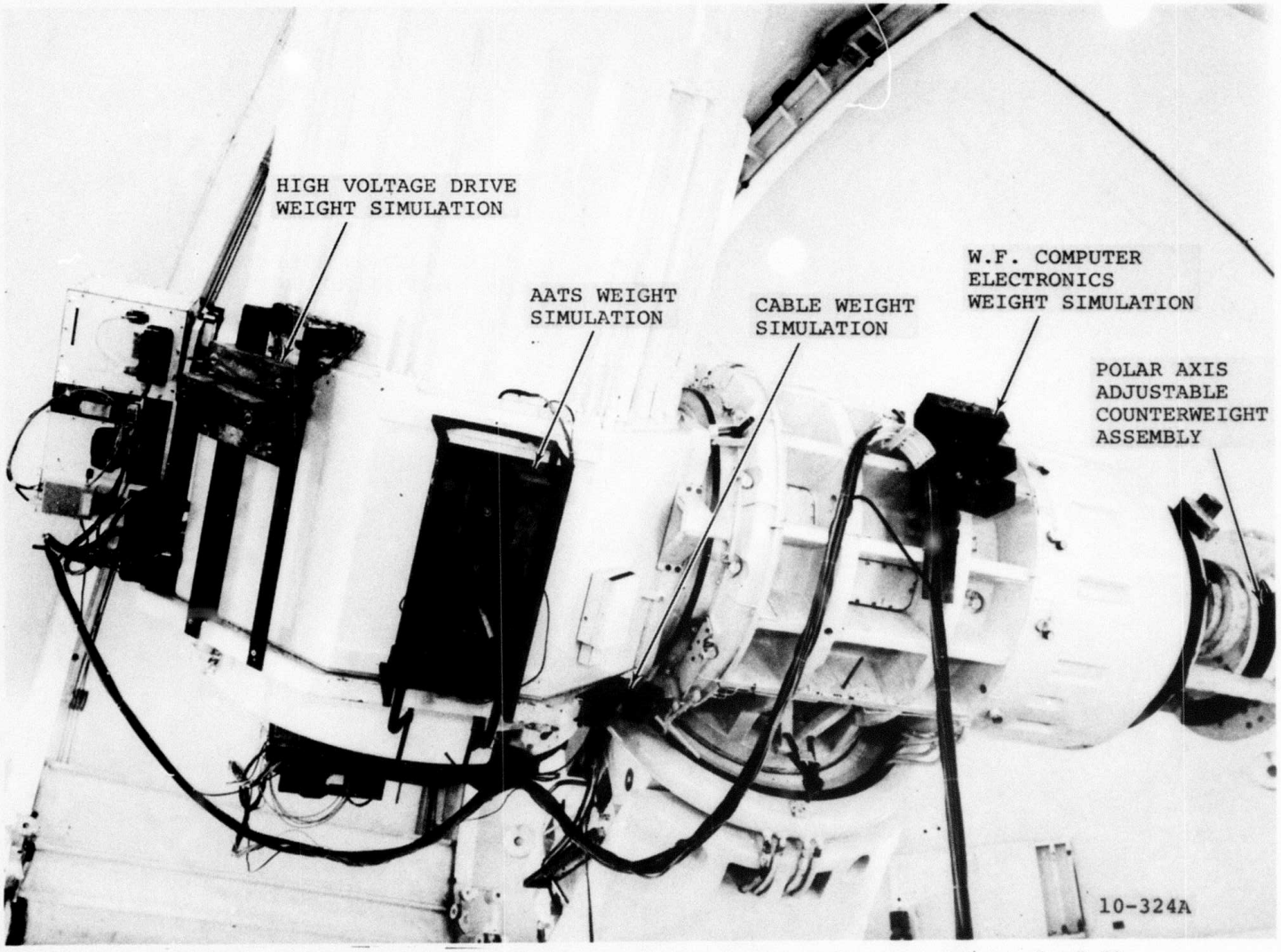

Fig. 25 CIS weight simulation on the 1.6 meter telescope (sheet 2 of 2).

the weight was mounted directly to the stationary counterweight to reduce loading on the adjustable counterweight structure. A modified polar counterweight system will be required prior to installation of the actual CIS hardware. After balancing the telescope, a test was performed to determine if the oil bearings were binding due to overloading. The polar and declination axes were independently computer-driven at 20 arcmin per minute through their normal operating angles. Strip chart recordings of the servo errors were made during the test. The declination axis showed only small servo error signals. The polar axis had large intermittent servo errors that always occurred at the same pointing angles. The polar bearing oil pressure was increased to maximum and the problem was lessened but not eliminated. The symptoms were indicative of bearing problems. The oil jets were then removed, inspected, cleaned, measured and reinstalled. A few jets were found to be plugged. The size and position of all jets in the polar axis were cataloged for future reference. When the float test was repeated, the results were similar. A careful inspection of the mount revealed that at least two of the declination oil return hoses were scraping on the horse collar that collects return oil. Evidently the additional weight reduced the oil bearing thickness such that contact was made. The return hoses were modified to increase their clearance and the test was repeated. Servo errors now remained acceptably small through the entire operational range.

The step response test involved recording the servo error while step commands were given to the telescope by the computer. Response time was found to be slowed by the additional weight but is considered to be satisfactory. No attempt was made to optimize response time by adjusting servo parameters.

Before the actual satellite pass, the telescope was run through the satellite track with the dome doors closed. Due to cable constraints, the telescope was positioned 180° from the computer-selected optimum azimuth setting. The simulated satellite pass produced low servo errors except through culmination where the declination axis was unable to achieve the acceleration necessary to keep the error signals at a low value. The computer-selected azimuth setting would have minimized declination axis acceleration and eliminated the large errors.

The actual satellite pass (a typical low orbit CIS target) was run with a strip chart recording of servo error and a video recording of the boresight camera. No indication of overloading of the telescope was evident. Tracking jitter was the order of $\pm$1 arcsecond rms even though wind gusts of up to 20 mph occurred during the pass.

The standard pointing check was the only test performed that indicated possible problems due to the increased weight. When the polar axis was driven in synchro mode to approximately zero degrees, and a nearby star was selected by the computer WIKISTAR program, the declination axis would not move. A visual inspection of the mount did not reveal any external interference.

The polar axis was returned to around 40 degrees and then the declination axis was free and able to drive. The polar axis was then returned to 5.3° and the declination could be driven in both directions. In other words, the problem did not repeat itself. One can only speculate as to why the mount did not move but the possibility of bearing seizure cannot be ruled out until more extensive testing is conducted.

Pointing repeatability is also of concern. When two stars, located less than 5 degrees apart, were pointed, the offsets were different by ~2 arcseconds. This difference is extremely large for angles so close together and may indicate some weight-induced hysteresis. Again, further testing is required.

The inertia testing was terminated in December for two reasons; (1) the 1.6 m Telescope was required to support MOTIF operations during the 1.2 m Telescope downtime for refurbishment, and (2) the Itek system weight estimates still had large uncertainties that needed to be eliminated before a major AMOS test program could be justified.

Both RADC and Itek were informed of the results of the November and December 1978 inertia testing. It was subsequently agreed that ITEK would provide firm values for the weights of the various telescope mounted components by April of 1979 and that AMOS would then perform further tests.

4.3.3.3 Classical Imaging Data Base

The classical imaging program being conducted during Phase IV has two basic goals.

1) Development of a classical imaging data base, augmented by atmospherics data (see section 4.3.3.4), to aid in the evaluation and optimization of the DARPA compensated imaging system when it arrives at AMOS in 1980;

2) SOI support for ADCOM and other DARPA approved users.

Three specific tasks were included in the 1978 effort in addition to the SOI support.

First, a standard AMOS Mission Instruction and Operation Plan (MIOP #025) was prepared and submitted to RADC for approval (CDRL 002). This document describes the hardware, operational procedures and data reduction required to support a classical imaging mission.

Second, a Classical Sensor Package (CSP) was designed, fabricated and tested by AERL. This effort, completed in 1978, is described in detail in the next section.

Third, accumulation of data for the CIS data base was initiated. Representative photographs are included below.

4.3.3.3.1 Classical Sensor Package

In January, design of the Classical Sensor Package (CSP) was begun. At that time the decision was made to incorporate the new hardware into the existing Laser Receiver package. This approach allowed achievement of two important goals: 1) the system was built at reduced cost by utilizing existing hardware, and 2) by making the new system compatible with the

laser receiver, neither system would have to compete for space or time on the telescope. Both the laser receiver and the imaging system can be used simultaneously for certain types of missions. The CSP was designed to operate on the side Blanchard mounting surface (folded-Cassegrain) of the 1.6 m Telescope. It contains three basic sensor systems:

1) a photometer (also used as the laser receiver);
2) a cine' film camera (16 mm);
3) a boresight TV camera (ISIT).

These sensors are located in three optical channels and it is possible to direct the beam from the telescope so that all of the light goes to any one of the sensors, or the beam can be split and shared by the sensors in various ways. The operator can select the desired beam-splitting combinations from the main control room. Figure 26 is a block diagram of the CSP which shows the relative location of the sensors and the optical components. Figure 27 shows the classical sensor package during fabrication. Table 4 lists the components which are used in the CSP in its current configuration. These components can be located by referring to Figure 26 which indicates approximately where they are positioned relative to the sensors.

The CSP was designed for an instrument working distance of 13 inches (close to the optimum working distance at the side mounting surface of the 1.6 m Telescope). When the secondary mirror has been properly adjusted, all three sensor systems will see a focussed image.

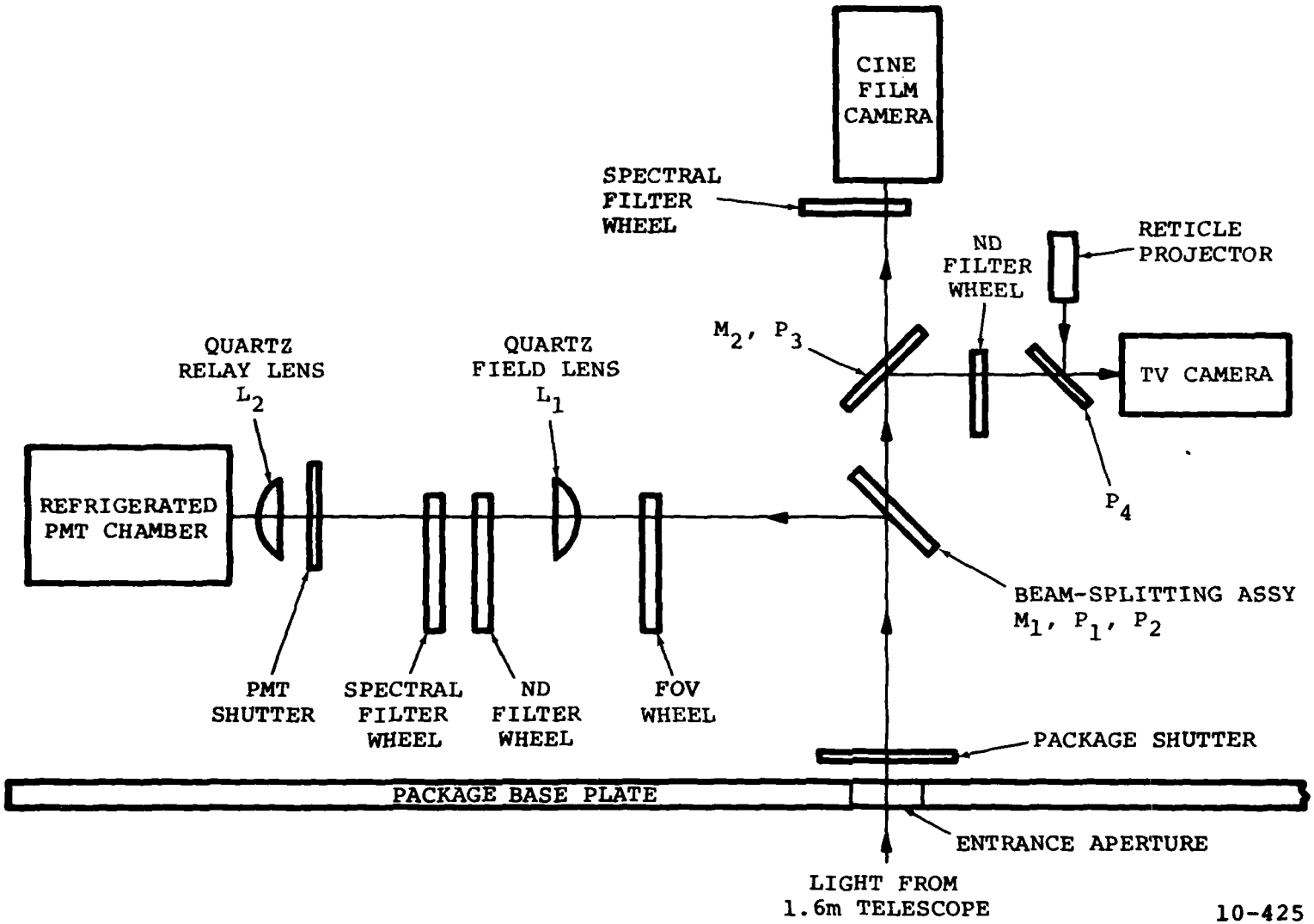

Fig. 26 Diagram of Classical Sensor Package.

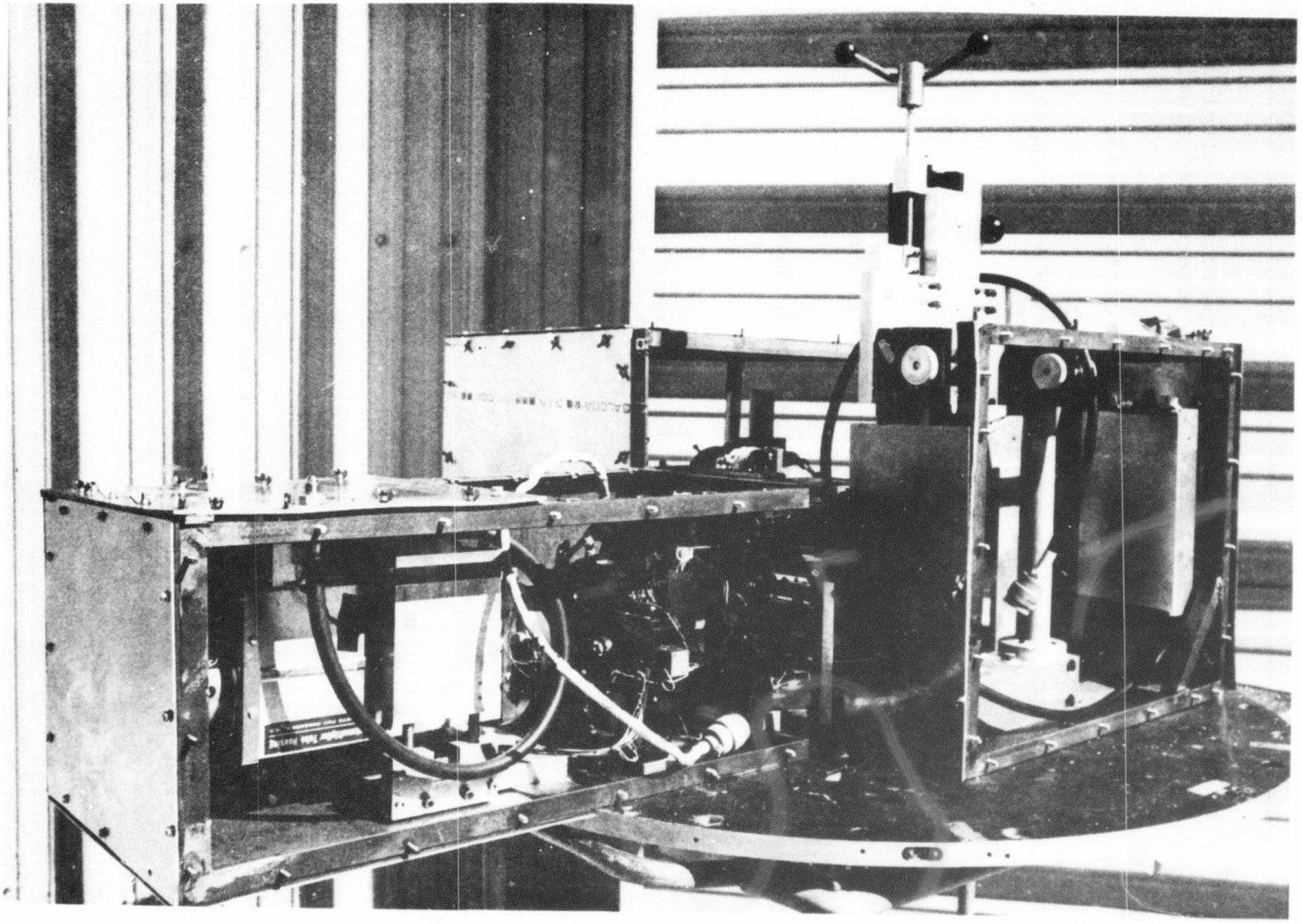

Fig. 27 Classical Sensor Package during fabrication.

TABLE 4. CLASSICAL SENSOR PACKAGE OPTICAL COMPONENT INVENTORY

MIRRORS

M_1: 75 mm diam., flat, front surface, overcoated aluminum

M_2: 3 inch square, flat, front surface, overcoated aluminum

PELLICLES

P_1: 3 inch diam., ST-LQ-NPX-40 "Even Split", coated, Reflects 40%, Transmits 40%

P_2: 3 inch diam., ST-LQ-Dichroic, coated, Reflects 90% @ 694.3 nm, Transmits 90% 400 nm to 550 nm

P_3: 3 inch diam., ST-LQ-UNC, uncoated, Reflects 8%, Transmits 92%

P_4: 2 inch diam., ST-LQ-UNC, uncoated, Reflects 8%, Transmits 92%

LENSES

L_1: 50 mm FL, 25 mm diam., Plano-Convex, Quartz, Broad-Band A-R coating

L_2 50 mm FL, 40 mm diam., Plano-Convex, Quartz, Broad-Band A-R coating

ND FILTERS

PHOTOMETER CHANNEL (1 inch diam., glass)

ND 1.0: Attenuates 2.5 Stellar Magnitudes
ND 2.0: Attenuates 5.0 Stellar Magnitudes
ND 2.5: Attenuates 6.25 Stellar Magnitudes
ND 4.0: Attenuates 10.0 Stellar Magnitudes

VIDEO CHANNEL (25 mm diam., glass)

ND 1.6: Attenuates 4.0 Stellar Magnitudes
ND 2.3: Attenuates 5.75 Stellar Magnitudes
ND 4.0 Attenuates 10.0 Stellar Magnitudes

SPECTRAL FILTERS

PHOTOMETER CHANNEL (1 inch diam., glass)

LASER 1: 694.3 nm, 5 nm passband
LASER 2: 694.3 nm, 1 nm passband

CINE CHANNEL (Wratten gelatin)

Wratten 21: Sharp cut-off at 540 nm, transmits longer wavelengths out to 900 nm.

PHOTOGRAPHIC SENSOR

Red Lake Labs, LOCAM Instrumentation Camera, 16 mm cine' film, pin registered, tri-mode shutter.

ELECTRO-OPTICAL SENSORS

PHOTOMULTIPLIER TUBE (PMT): EMI Type 9558
VIDEO CAMERA: RCA Type TC1040/HCX ISIT Camera, 16 mm Format ISIT tube

The telescope image is photographed directly by the LOCAM cine' camera using only a minimum of intermediate optics which might degrade the image. To ensure a good track, it is desirable to be able to view the target on a video display while the cine' camera is running. To provide this capability, a pellicle can be introduced into the beam to divert 8% of the energy to a boresight TV camera while transmitting 92% of the energy to the cine' camera. Used in transmission the pellicle has very little effect on the image quality.

During the CSP construction phase, electronic controls for the operation of the system were designed and constructed. Cabling from the 1.6 m Telescope to the main control room electronic racks was installed and all system control functions were checked out. Figure 28 shows the electronic control panels for the imaging section of the CSP.

Design, fabrication and installation of the CSP on the side Blanchard surface of the 1.6 m Telescope (Figure 29) was completed in April. During the next few weeks the system was aligned, boresighted, and tested for sensitivity. A complete new mount model was also obtained for the 1.6 m Telescope. With the exception of the auto-ranging software (see section 4.1.2), the system became operational in June.

4.3.3.3.2 Classical Imaging Measurements

During the design and fabrication period of the CSP, an interim film camera system was installed on the rear Blanchard surface of the 1.6 m Telescope. This system was used on several

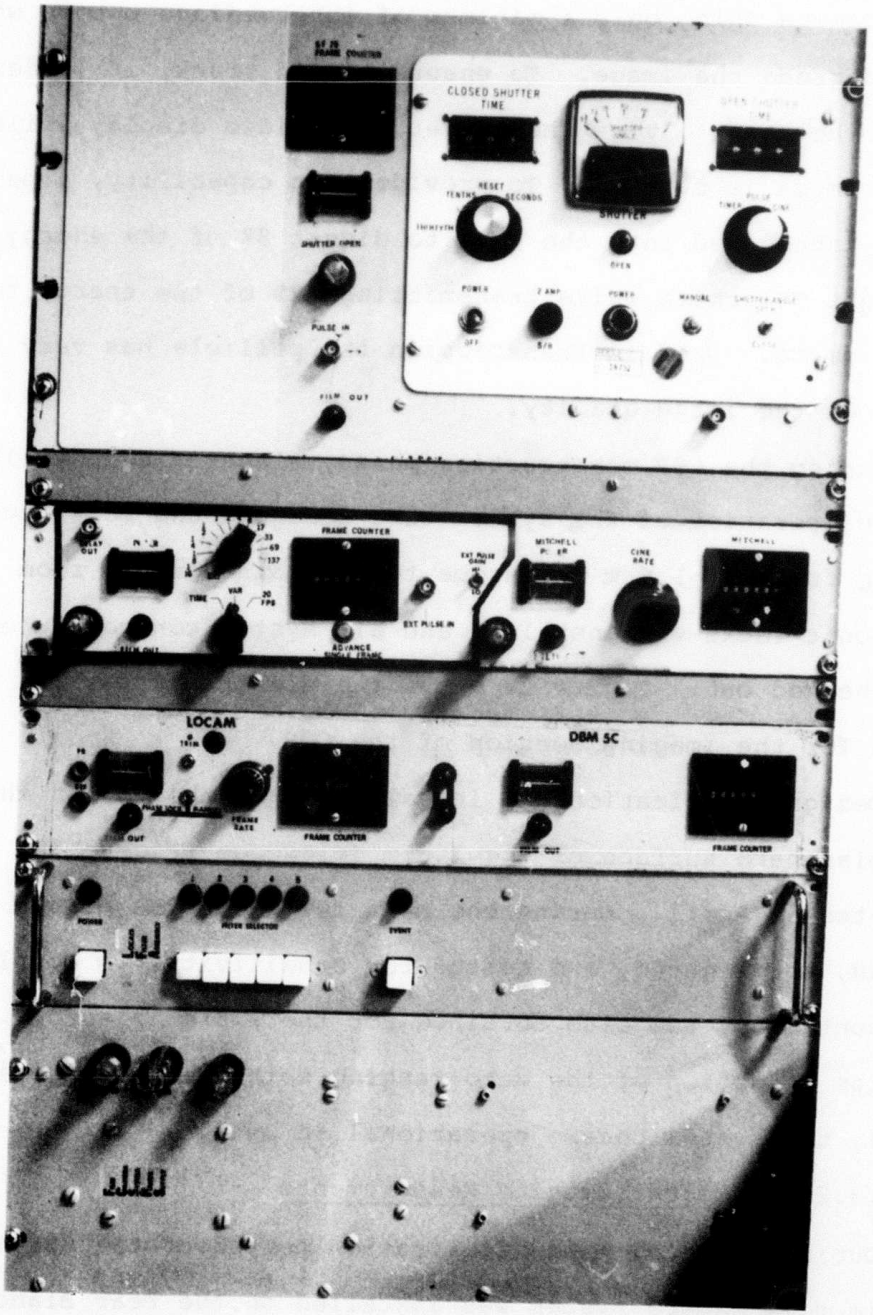

Fig. 28 Control panels for film camera and filter wheel of CSP.

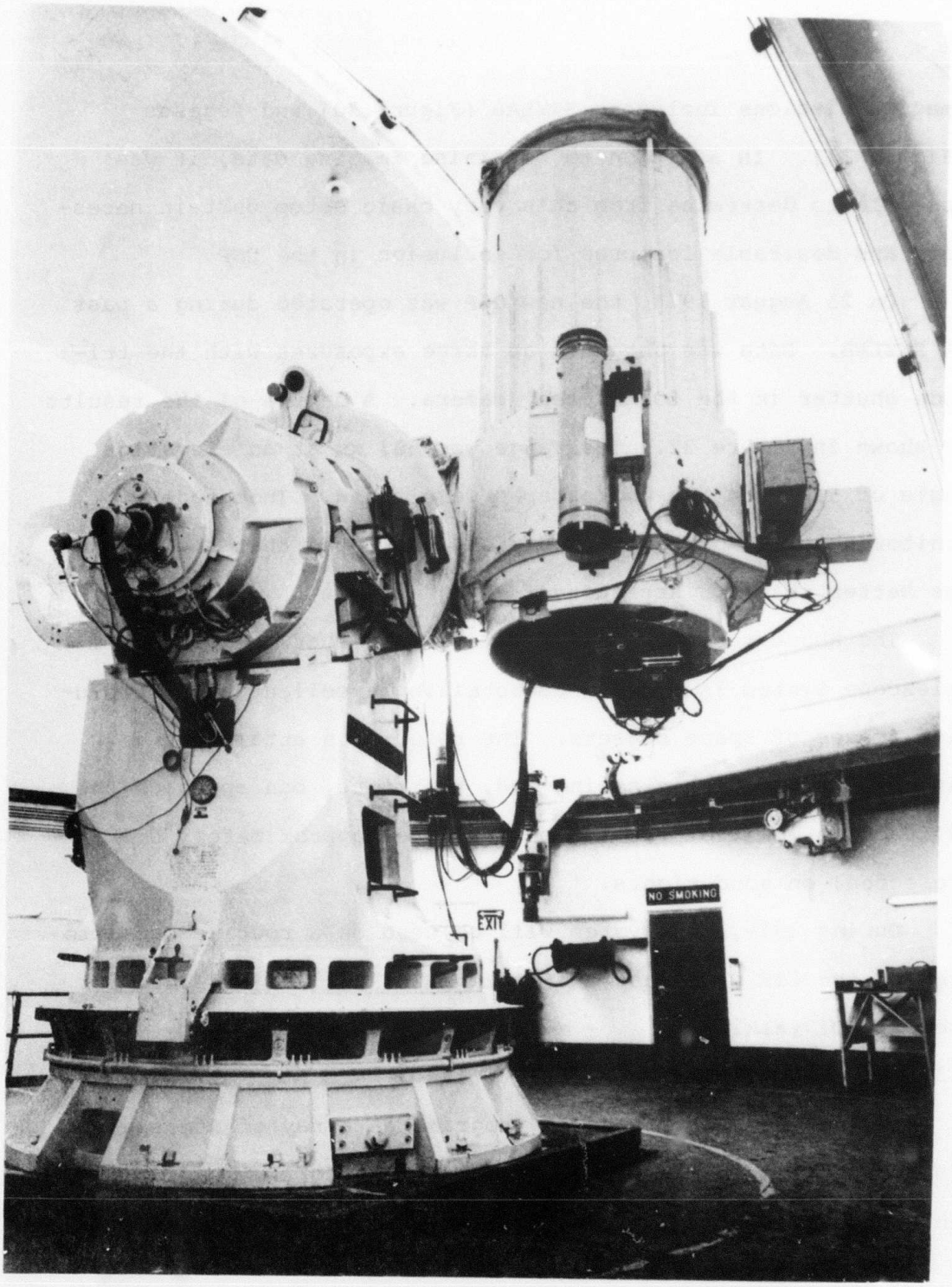

Fig. 29 Classical Sensor Package on side Blanchard of 1.6 m Telescope.

imaging missions including SKYLAB (Figure 30) and Pegasus (Figure 31). In addition to obtaining imaging data, it was possible to determine from this very basic setup certain necessary and desirable features for inclusion in the CSP.

On 23 August 1978, the new CSP was operated during a pass of SKYLAB. Data was obtained at three exposures with the tri-mode shutter in the LOCAM cine' camera. A sample of the results is shown in Figure 32. The range was 503 km at an elevation angle of 51° when the photographs were taken. Independent monitoring of atmospheric conditions indicated that the seeing was better than 0.5 arcsecond.

The above results clearly demonstrate that the CSP/1.6 m Telescope System is capable of obtaining excellent high resolution images of space objects. The resolution attainable is limited by atmospheric seeing and, therefore, can approach the diffraction limit of the 1.6 m Telescope (approximately 0.1 arcsecond) on good nights.

During 1979, the system will be used on a routine basis to provide the CIS data base and in addition will be utilized for special SOI tasking.

4.3.3.4 Atmospherics Data Base

During the AMOS Phase III program, an array of atmospheric instrumentation was installed at the Observatory. The implemented systems were:

Fig. 30 SKYLAB image taken with interim package.

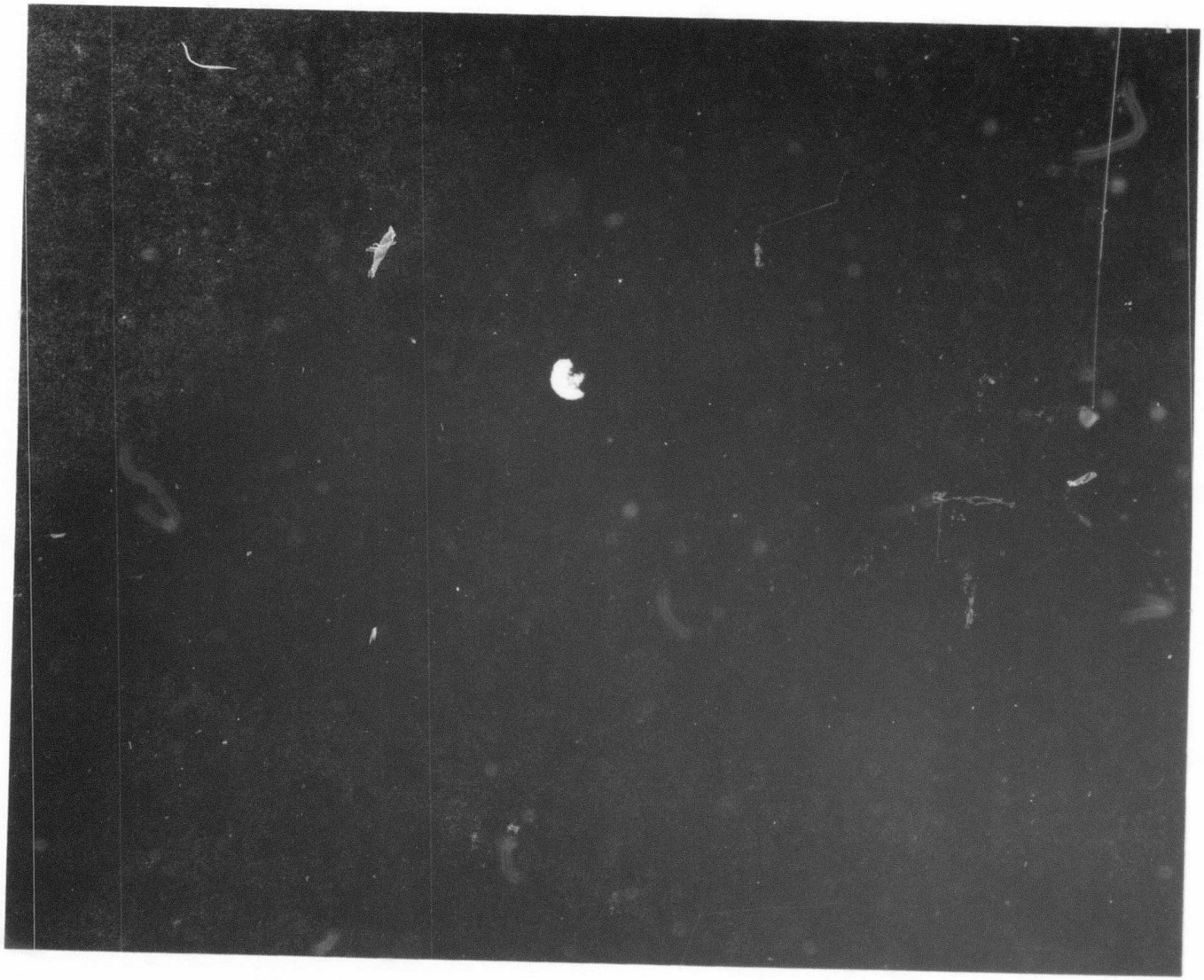

Fig. 31 Pegasus image taken with interim package.

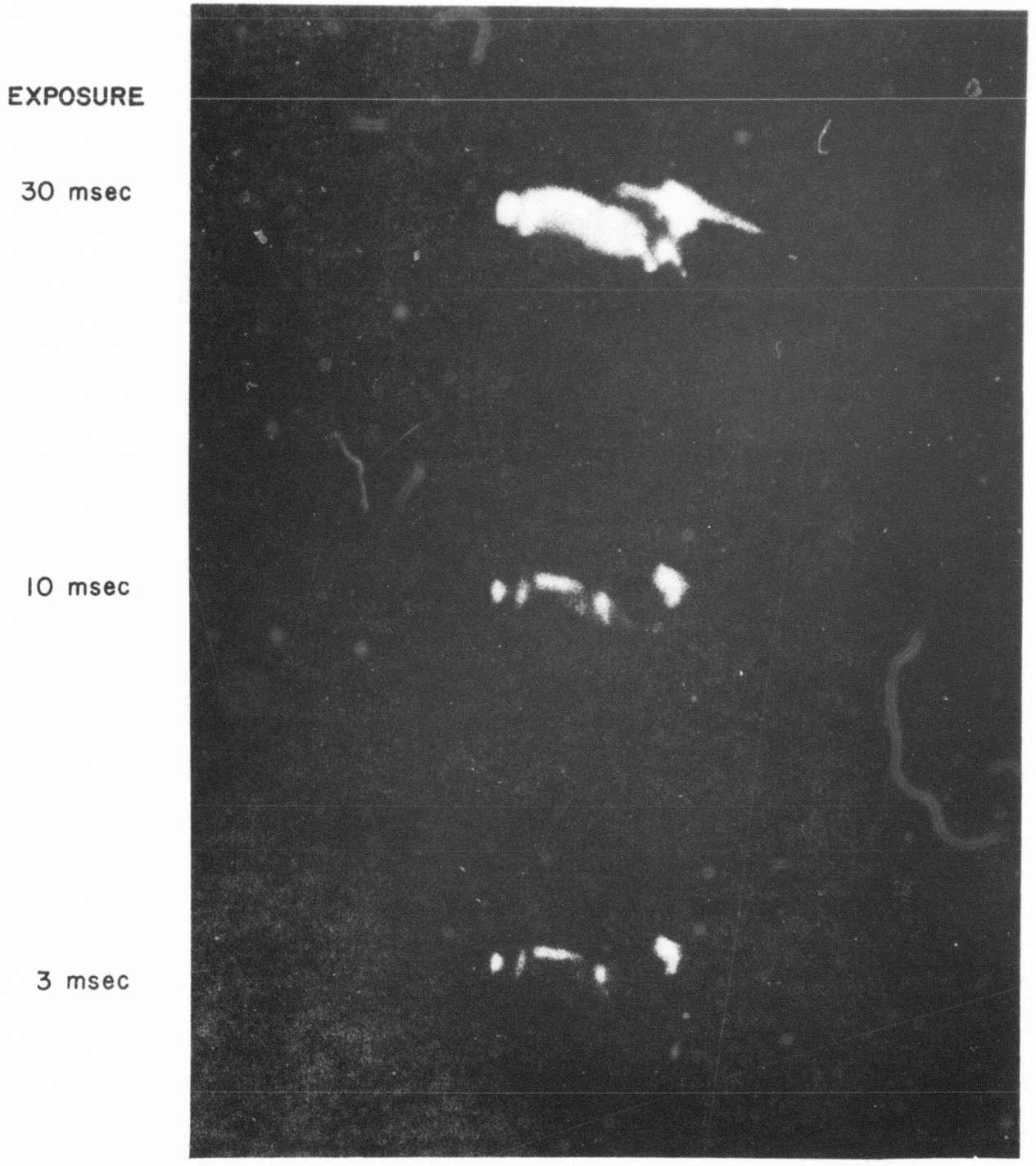

Fig. 32 SKYLAB image taken with Classical Sensor Package and tri-mode shutter - 23 August 1978.

Seeing Monitor - an instrument, located on the rear Blanchard surface of the 1.6 m Telescope, that measures r_o, the correlation scale length.

Star Sensor - an instrument, located in a separate dome at the northeast corner of the Observatory, that provides profiles of C_N^2.

Acoustic Sounder - an instrument that measures C_N^2 to 300 m altitude.

Microthermal Probes - two systems, consisting of three probes each, which measure C_N^2 at one level (18 m).

Routine Meteorological Sensors - instrumentation that measures wind speed, wind direction, temperature, dew point and barometric pressure.

All-Sky Camera - a camera that records cloud cover on a 24-hour schedule.

By the end of the Phase III program all of this instrumentation was functioning and had been used to obtain a preliminary atmospheric data base. One of the main purposes of this data was to aid in making critical design decisions for CIS hardware.

During the first few months of 1978, emphasis shifted towards making the hardware operational, accomplishing minor upgrades and fully documenting the systems.

By the fall of 1978, the atmospherics instrumentation was ready to be used for its primary goal - accumulation of an extensive data base, primarily in conjunction with classical

imaging data (see section 4.3.3.3), to be used for evaluation and optimization of CIS performance in 1980.

4.3.3.4.1 Atmospheric Operations Summmary

In addition to the work required to bring the five major atmospheric sensor systems to a routine operational readiness, several other operations activities were carried out during the year. These activities included data reduction, special measurements, tests and calibrations.

During the early part of the year, special emphasis was given to the Acoustic Sounder system due to the sensitive calibration technique required. Seven Acoustic Sounder runs were reduced in detail (20 atmospheric levels) using the Mark 5.0 reduction program. The AMOS SNDR PLOT program was then used to plot the data to allow graphic analysis. To complete the checkout of the Acoustic Sounder system a special test and compatibility tape was made for RADC. A special all-sensors data run was also conducted. Prior to this run a series of tests were performed to verify the optical alignment of the Star Sensor. The tests did verify that the Star Sensor was operating as designed.

In July, a series of data runs were conducted with the Seeing Monitor and the M&VI (means and variance, version one) program to collect data characterizing the azimuthal and elevation dependence of r_o. In addition, data runs were made to collect short term statistics on r_o. Five nights were devoted to these measurements. Three additional runs

were made in August to produce supplementary data. Also during this time period, three nights were devoted to noise characterization studies of the Star Sensor. At the conclusion of the Star Sensor studies, data reduction efforts on simultaneous RTAM and Seeing Monitor data began. These data had been collected previously and required special signal conditioning equipment which had been built in Everett. Three days were devoted to reduction of those data deemed to have sufficiently high S/N ratios to allow meaningful analysis.

In December, the Seeing Monitor was used along with an electronic correlator to study temporal variations in r_o. These studies ran two days and two nights. Additionally, the Seeing Monitor was operated in December in conjunction with the Classical Imaging program.

4.3.3.4.2 Atmospherics Instrumentation Status

Several upgrades and system improvements were made to the atmospheric sensors and their support systems in 1978. Systems affected were the 1) Microthermal Probes, 2) PDP-8I Computer, 3) Routine Meteorological sensors, 4) Star Sensor, 5) Dew Point sensor, 6) Acoustic Sounder and 7) VR-3700B Instrumentation Tape Recorder. These sensor upgrades and modifications will be discussed below along with other relevant, peripheral systems improvements.

Microthermal Probe Systems

The Microthermal Probe systems in use at the AMOS site have evolved over a period of three years from a fine-wire type to

a more rugged fat-wire type. Although these fat-wire probes proved to be more durable in regard to sensing element lifetime, they were still plagued by weather-related, corrosion-induced failures. A weather resistant version was fabricated at RADC and subsequently installed at AMOS. This new probe assembly replaces two non weather-proof Amphenol type connectors with a single weather-proof connector, thereby eliminating the electrical failures resulting from connector pin corrosion. All switching functions were incorporated into a single switch and unnecessary switches removed. Heavier gasketing was installed under the coverplates used to seal the electronics compartment. Perhaps the single most significant improvement was the incorporation of a plug-in sensor head. This interchangeability allows the quick replacement of a broken sensing wire by exchanging the sensor head, thereby eliminating the need to replace the entire probe system on the tower.

PDP-8I Computer Software

The PDP-8I Computing System was upgraded by the replacement of its teletype peripheral with a new unit. The controlling software that had been previously used to process microthermal probe, routine meteorological and seeing monitor data computed only the means, variances and covariances for the 15 channels involved. New software called the M&V2 program has now been installed and provides the added capability of some data reduction. For instance, microthermal data are averaged for the user-specified number of samples and then used to calculate

C_N^2 values for all three probe combinations on each tower. In addition, the wind speed and direction are averaged for both towers and tabulated with their respective variances. The mean temperature, dew point and barometric pressure are also tabulated. Seeing Monitor data are averaged and the data then used to compute values of r_o for the two Seeing Monitor channels. Figure 33 is an example of a typical 15-channel M&V2 printout.

Routine Meteorological Sensors

The data from the routine meteorological sensors had been previously collected only when the PDP-8I data processing system was operating. To provide continuous data collection, a Keithley System 70 Datalogger was installed. This system provides a printed record of each wind speed, wind direction, temperature, dew point and pressure sensor, hourly, seven days a week. These data are collected 24 hours a day, and require no other system to be operating. The data are tabulated on paper tape and annotated with date, time and channel number. The tapes are forwarded to RADC on a bimonthly basis. Film from the All Sky Camera is processed on a monthly basis, reduced and forwarded to RADC.

Star Sensor

In July 1977, the original Star Sensor system was replaced. Model II operated well until the Fall of 1978. A 15 volt power supply failed and during its repair another problem dealing with the Photomultiplier Circuit (PMC) outputs was identified

```
RECORD*          SAMPLE TOTAL
+    16.00            +  1000.00

DAY.MONTH.YEAR    HOURS
+     5.00            +    12.79

                CN SQUARED / 1*10 -18          M/S(M/S)↑2  DEG.(DEG.)↑2

 PROBES  (ONE & TWO)(ONE & THREE)(TWO & THREE)  (W/S)(W/SV)  (W/D)(W/DV)

 GRP*1  +   424.17   +  2581.71   +  2398.85   + 2.29+  .58+228.3+1638
 GRP*2  +  4988.52   + 54162.76   + 63937.00   + 2.83+  .89+281.0+318.6


AMBIENT TEMP(C) DEWP.TEMP(C)    PRESSURE
+     9.91   +      6.95   +   716.26
 RO +      .82             +      .82

RECORD*          SAMPLE TOTAL
+    17.00            +  1000.00

DAY.MONTH.YEAR    HOURS
+     5.00            +    12.99

                CN SQUARED / 1*10 -18          M/S(M/S)↑2  DEG.(DEG.)↑2

 PROBES  (ONE & TWO)(ONE & THREE)(TWO & THREE)  (W/S)(W/SV)  (W/D)(W/DV)

 GRP*1  +  4156.86   + 17746.13   +  6297.46   + 1.75+  .27+239.2+6148
 GRP*2  +  6009.24   +151299.60   +168421.20   + 2.54+  .61+270.2+991.5


AMBIENT TEMP(C) DEWP.TEMP(C)    PRESSURE
+    10.76   +      7.68   +   716.26
 RO +      .82             +      .82

RECORD*          SAMPLE TOTAL
+    18.00            +  1000.00

DAY.MONTH.YEAR    HOURS
+     5.00            +    13.19

                CN SQUARED / 1*10 -18          M/S(M/S)↑2  DEG.(DEG.)↑2

 PROBES  (ONE & TWO)(ONE & THREE)(TWO & THREE)  (W/S)(W/SV)  (W/D)(W/DV)

 GRP*1  +  1672.83   +  3505.81   +  2957.08   + 1.81+  .46+226.1+9802
 GRP*2  +  4425.37   + 37488.72   + 39241.83   + 3.14+  .70+252.3+341.4


AMBIENT TEMP(C) DEWP.TEMP(C)    PRESSURE
+    10.22   +      7.33   +   716.26
 RO +      .82             +      .82
```

Fig. 33 Example of 15-channel M&V2 printout.

and repaired. As a result of these repairs an internal inspection of the electro-optical-mechanical package was made and revealed excessive galling and wear on the cardioid scanning cam. Subsequently, the following repairs were made; 1) a new cam was fabricated from thicker stock, 2) the cam follower spring was replaced with one of smaller spring constant and 3) the cam follower roller bearing was replaced. These repairs, combined with an electronic alignment and wavelength calibration, have returned the Star Sensor System to operational status.

EG&G Model 110S-M Dew Point Sensor

Dew point data from the 110S-M has been extensively compared with psychrometrically determined data since August 1978. By use of a sling psychrometer and National Weather Service tables for the 711 mb level, dew points were determined coincidentally with those from the Model 110S-M set. A system bias was detected and removed. During the course of the investigations, several phenomena were observed; 1) During conditions of low humidity, the servo circuit that controls the mirror cooling module in the 110S-M tends to lose lock and over-cool the mirror, 2) the 110S-M system tracks the dew point better with the Auto Balance Circuit disabled and a manual balance performed once a week, 3) the system tracks the dew point more reliably if the condensate thickness is increased. The system is now operating accurately and continuously.

Acoustic Sounder

This system has been operating reliably since a new X-Y

multiplier chip was installed in the system's control unit. Early in 1978 the Acoustic Sounder's anechoic cuff was replaced with a newer improved version. This new cuff, hexagonal in shape, is approximately six feet high and uses a special sound absorbing material as a liner. A canvas cover and fasteners were designed and fabricated locally to provide weather protection to the antenna assembly. Figure 34 shows the new cuff assembly.

4.3.3.4.3 Atmospherics Sensors Support Systems

Several upgrades and general maintenance improvements were also made during 1978 to the systems that support the primary measurement systems. Principal support equipments upgraded were the VR-3700B tape recorder which is primary support for the Acoustic Sounder, and the NOVA 2/10 computing system which is primary support for the Star Sensor. General maintenance improvements were made to all tower-mounted equipment (routine meteorological sensors) and to certain ac power circuits in the atmospherics control room.

VR-3700B Instrumentation Recorder Reconditioning and Upgrade

The Bell & Howell VR-3700B recorder was given a depot level maintenance by Bell & Howell factory personnel in the Spring of 1978. Mechanical alignment, tracking, tape tension and extensive electronic adjustments and calibrations were performed. The system now has 13 FM reproduce amplifiers and one direct reproduce amplifier. The recording configuration now consists of two wide band group II, two wide-band group I and four

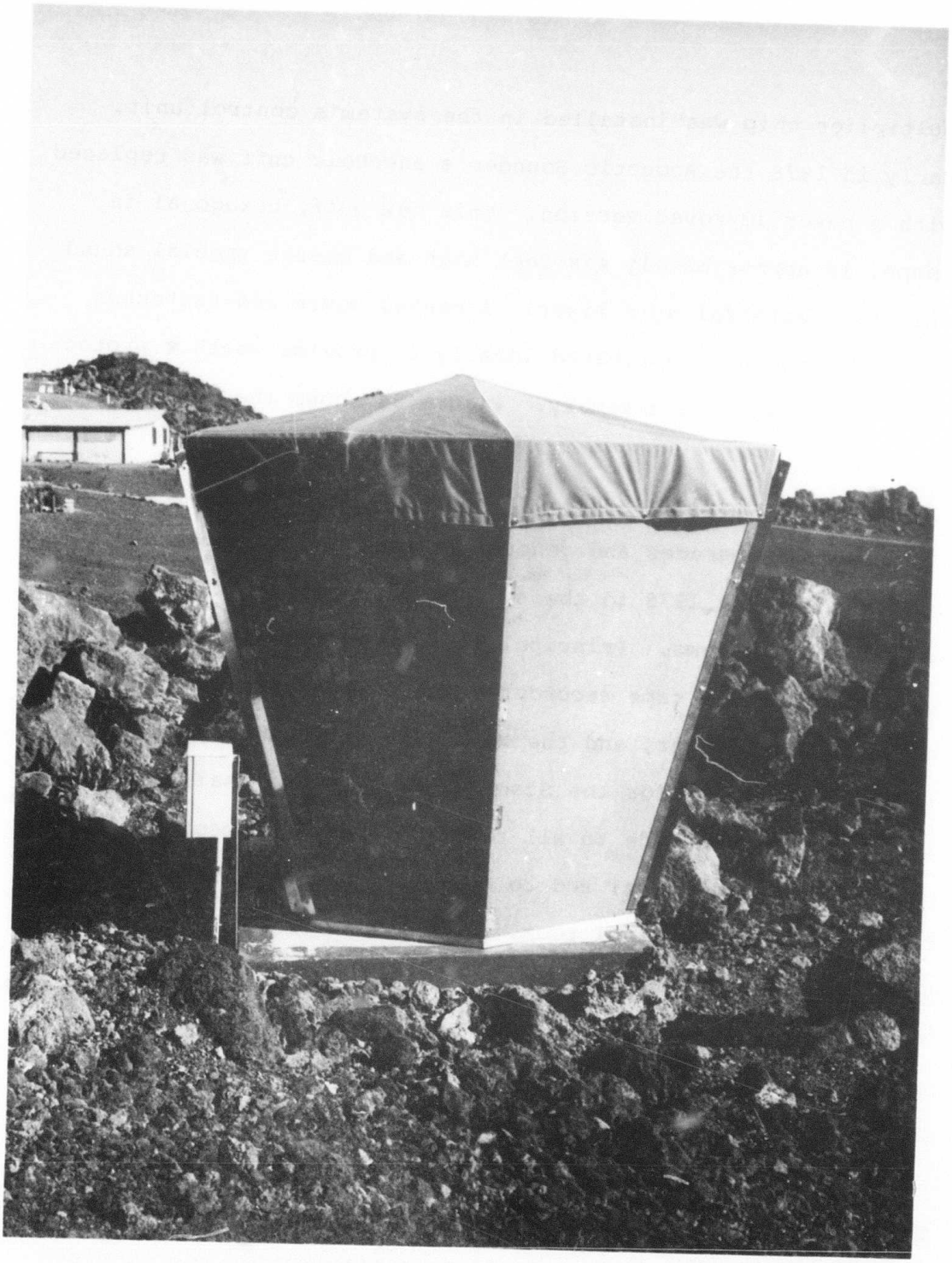

Fig. 34 New cuff assembly for acoustic sounder.

intermediate band FM record amplifiers. There is also one direct record amplifier. The system is shown in Figure 35.

NOVA 2/10 - Star Sensor Interface

Figure 36 shows the NOVA 2/10 computer and its peripherals as presently configured to support the Star Sensor, Model II. Several changes have been made to this equipment since its original installation, to improve the control and communications functions between the NOVA 2/10 computer and Star Sensor systems. Most important was the relocation of the CPU to its present position. Previously, it had been located below the high-speed tape reader and in this position was difficult to read and set. Additional physical protection for the switch register was also obtained by moving it to a higher position in the rack. When installed, the computer system had only a main power breaker-switch located in the panel above the CPU. To provide better communication and control, several other functions were added. The first switch added (to the right of the main power switch) provides remote power switching to the Star Sensor telescope package located in the Atmospherics Dome. This allows remote control of the scanning motor from the computer panel. Next to this switch is located a motor from the computer panel; then a 3-1/2 inch panel meter. This meter has associated with it four toggle switches. These switches allow the meter to read wavelength, whole aperture log-amplitude variance, filtered log-amplitude variance and whole aperture irradiance. These are the same signals normally available for

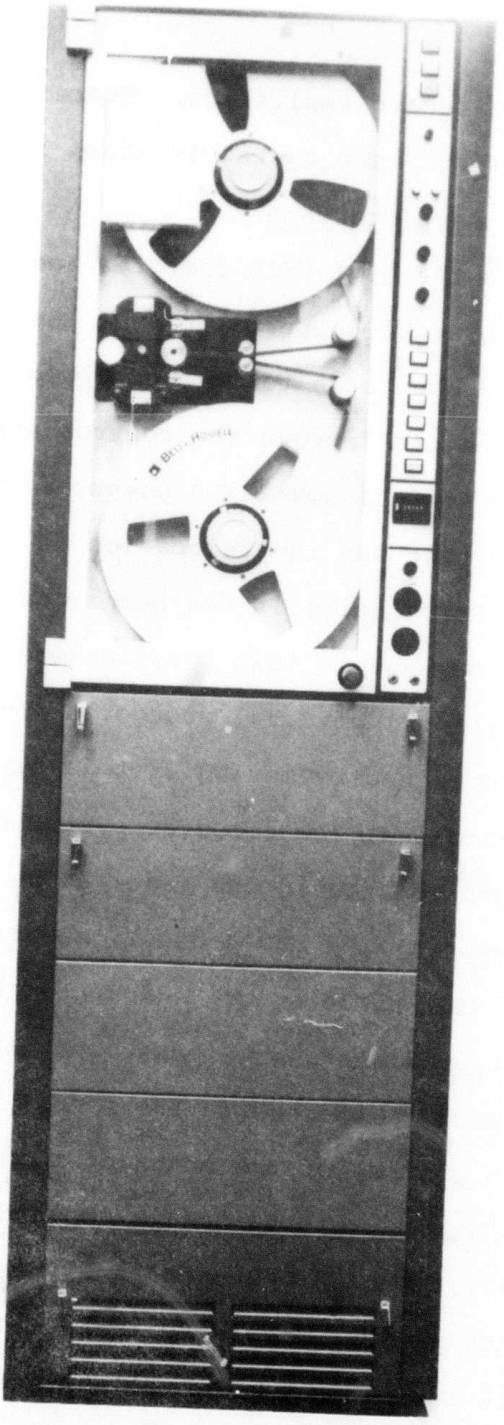

Fig. 35 Bell & Howell VR 3700B instrumentation recorder.

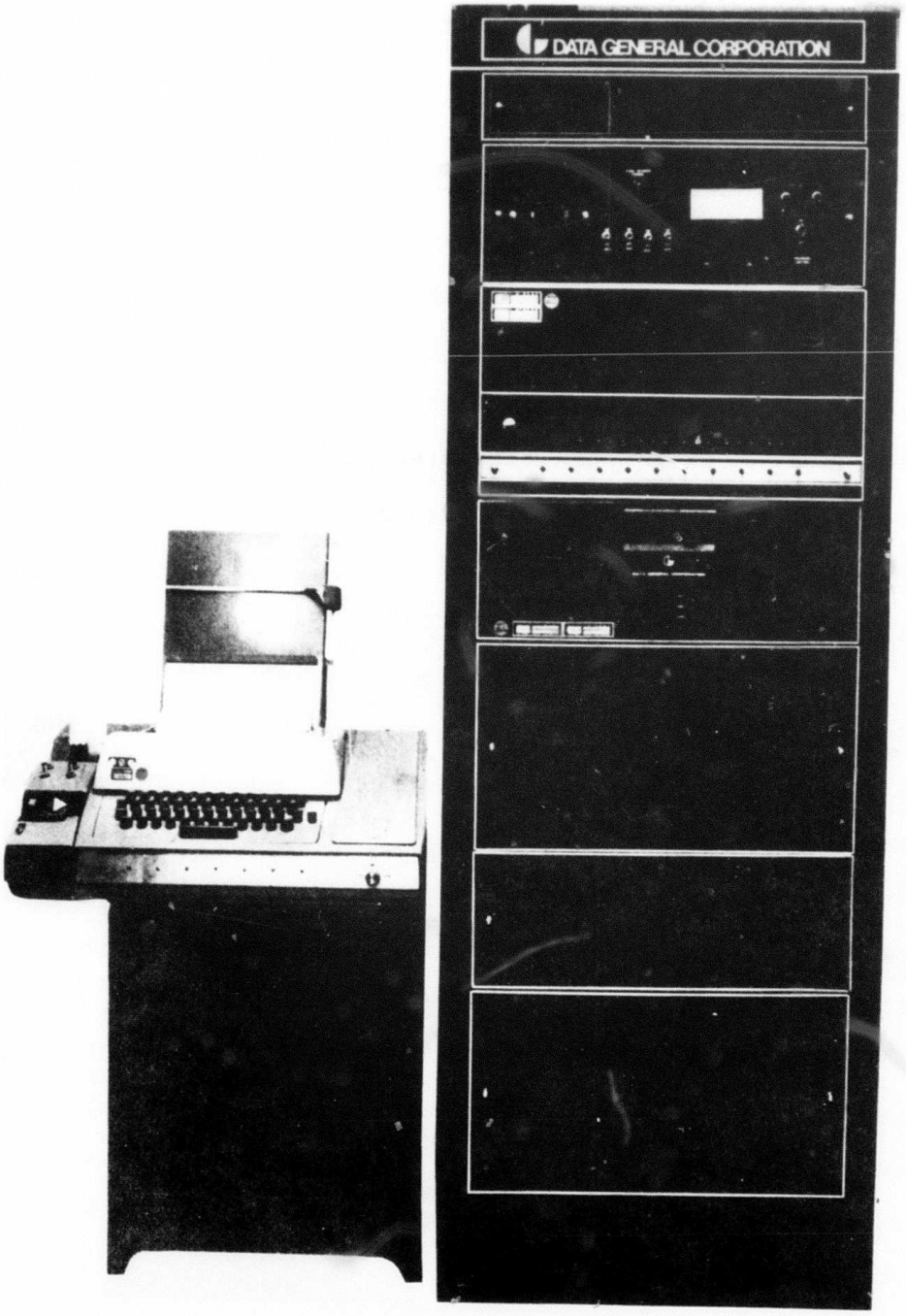

Fig. 36 NOVA 2/10 computer.

display at the telescope package. Just below the meter are installed two spring-loaded, center-off toggle switches that allow remote control of the telescope's declination and polar axes. These switches, when used in conjunction with the whole aperture irradiance switch and panel meter, allow accurate correction of telescope tracking error. The two-position toggle switch located to the right of the meter is a program control switch, which when activated, causes the software to perform the additional tasks of averaging and formatting the normal star sensor data.

Voltage Control and Noise Suppression

In order to minimize the effects of Maui Electric Company voltage fluctuations on sensitive equipments, certain line conditioning devices have been installed. These include a Sola saturable core-type transformer and a General Radio servo-controlled auto-transformer. The systems requiring this conditioned line voltage are the System 70 Datalogger, PDP-8I CPU and the DEC AD01-AN converter.

Sensors installed on the North tower (microthermal probes, wind speed, direction, dew point and ambient temperature) are subject to high levels of EMI. A systematic check of each instrument was made and appropriate bypass capacitors and ferrite chokes were installed.

4.3.3.4.4 Systems Documentation

As each of the primary measurement systems were brought to operational status, procedures manuals were prepared.

Operational procedures manuals have now been written for the following systems: 1) AMOS Microthermal Probe Systems and PDP-8I Data Processor, 2) AMOS Routine Meteorological and Datalogger Systems, 3) AMOS Star Sensor and NOVA 2/10 Data System, 4) AMOS Acoustic Sounder System, 5) AMOS Seeing Monitor System. These manuals contain step-by-step procedures for the start-up, operation and shutdown of the above five systems.

4.3.3.5 Facility Modifications

In order to meet the requirements of both the DARPA Compensated Imaging System and the MOTIF program, certain modifications and improvements must be made to the AMOS facility. Based upon a preliminary study (AMOS/MOTIF Space Allocation and System Interface Requirements Study, AERL, January, 1977) and a subsequent quote from a local construction firm, funding was included in the Phase IV contract to cover anticipated costs.

The Phase IV Program Plan scheduled the work to be accomplished during the period May-December 1978. This effort included a revision of the preliminary study, obtainment of necessary subcontractors' bids, awarding of subcontracts and implementation of the modifications along with certain tasks to be accomplished by AMOS personnel. The initial goal was to accomplish both the MOTIF and CIS tasks in parallel and complete the effort by 31 December 1978.

After the Phase IV contract was initiated on 1 January 1978, several facts became apparent.

1) Many specific requirements for CIS-related modifications were not firm. An AMOS/CIS Interface Meeting held in April produced twenty-seven (27) action items for resolution, many of which involved the implementation of facility modifications. AMOS staff members worked with RADC, Itek and AERL Everett personnel during the spring and summer of 1978 to complete the action items and come to agreement on specifics.
2) Since the CIS hardware is not scheduled to arrive on Maui until April 1980, no real need exists to have the AMOS facility ready for CIS until that time. (Decisions that impact Itek and/or AERL Everett designs must, of course, be addressed separately.)
3) MOTIF schedules require certain modifications to be completed by early 1979 in order to install and test the new DTS and CMS hardware.

Based upon the above, the task was reprogrammed in July.

1) MOTIF and CIS tasks were to be treated separately wherever possible.
2) MOTIF tasks were to be completed by 1 January 1979 if possible.
3) After necessary CIS modifications had been completely defined, a revised plan/specification would be issued which would be suitable for obtaining firm contractor's bids. The revised plan would also contain a schedule

to assure that the work was completed in a timely manner with respect to CIS requirements.

During July, interface meetings were held at Everett, Itek and RADC to discuss specific items of the Facility Modifications task in addition to the general approach described above. A reappraisal of MOTIF requirements was conducted. It was determined that the equipment could be installed in the existing computer and communications area with minimum interior construction. Included in this approach is the removal of the wall between rooms 41 and 42 and the addition of a door between rooms 41 and 47. The purpose of the changes was to accommodate the relocation of personnel and facilitate the addition of the MOTIF MODCOMP V computer. Electrical distribution changes in this area were also included. Several questions pertaining to CIS requirements were still pending; specifically, air conditioning requirements for room 22, door sizes, dome chiller location and CIS equipment handling requirements. A raised floor was added to room 25 and the air handling unit for the air conditioner was moved to that location. The raised floor will act as the air supply with room 26 serving as the return plenum. During the month of August 1978, it was determined that all MOTIF-related tasks could be completed by the first week in January 1979. Modifications to room 26 for CIS could be completed by mid-February 1979 to support the Air Force IR measurement program which requires basically the same facilities

as CIS. Remaining modifications would be completed as specific requirements were determined.

In September an engineering firm was engaged to prepare specifications for the MOTIF and CIS electrical modifications. Drawings and specifications for the CIS air conditioning system were sent to a Carrier Corporation engineer in Honolulu for review. At this time it was determined that Carrier could not supply a unit in time to support the IR measurements program. A substitute air conditioner was selected from Liebert Corporation in Columbus, Ohio and arrived on-site in December 1978. This unit had nearly identical capabilities and physical characteristics as the originally selected Carrier unit. At this time, a revised schedule was prepared to satisfy specific priorities.

During the month of October, all facility modification design work was completed. The AMOS/MOTIF Space Allocation and Interface Definition document was revised and submitted to RADC for approval. A bid package was prepared. When approval from RADC was received in November, competitive bids were sought. Proposal packages were sent to seven local contractors and an advertisement was placed in the Maui News. A bidders' conference was held on 22 November 1978. The deadline for receipt of bids was 8 December 1978 with work scheduled to commence on or about 8 January 1979.

Bids were received from two contracting firms. A review of the bid sheets revealed an obvious misunderstanding of what

materials were to be purchased by AERL. Both bids were higher than allocated subcontract funds. A meeting was held with both contractors and available subcontractors to clarify material requirements and to ask for a rebid on the original specifications. In addition, revised specifications were prepared eliminating particular items and relocating the CIS chiller and the room 26 air conditioning condensing unit to the north side of the Observatory. This relocation eliminates the trenching, steel and concrete work for the trench, and the enlargement of the existing air conditioning equipment enclosure.

Installation of these thermal sources on the north side of the building is undesirable from a technical standpoint because of the direction of the prevailing winds at AMOS. The ideal location is on the south side. Unfortunately, tentative plans for location of GEODSS facilities preclude use of this area at this time.

The door installation into room 5 is the only item eliminated from the specification which would not actually be accomplished. All other items will be implemented by AERL personnel, resulting in a savings of many thousands of dollars without sacrificing needed modifications. These items include: installation of the cable trays for rooms 25, 26, 39, 41, and 42; installation of partitions and cabinets; kitchen modifications and painting.

New bids were prepared by the contractors and submitted to AERL on 28 December 1978. The low bidder on both proposals

was Fuku Construction, Inc.

Current schedules now show all MOTIF-related modifications completed by 1 March with the remaining CIS work finished by early Summer.

The location of CIS and MOTIF equipments is shown in Figures 37, 38, 39, and 40.

4.4 AMOS Users Manual

The Phase IV Program includes a one-time revision of the AMOS Users Manual. The revision was originally scheduled to be accomplished in March of 1979. Since the intent of the task is to provide a document that accurately describes AMOS capabilities, it is advisable to delay the task for several months. This delay will allow the many hardware changes that are currently being implemented to be incorporated into the document. These changes include:

1) New acquisition telescopes (AATS),
2) Modifications to the laser ranging system,
3) Modifications to the B29 secondary,
4) Modifications to AMTA,
5) Facility modifications.

Based upon current schedules for the above modifications, a logical time to revise the AMOS Users Manual is October of 1979. The task has accordingly been rescheduled.

4.5 AMOS System Schedule

The AMOS System Schedule (CDRL 001) is published monthly. Its function is that of a management tool which provides current

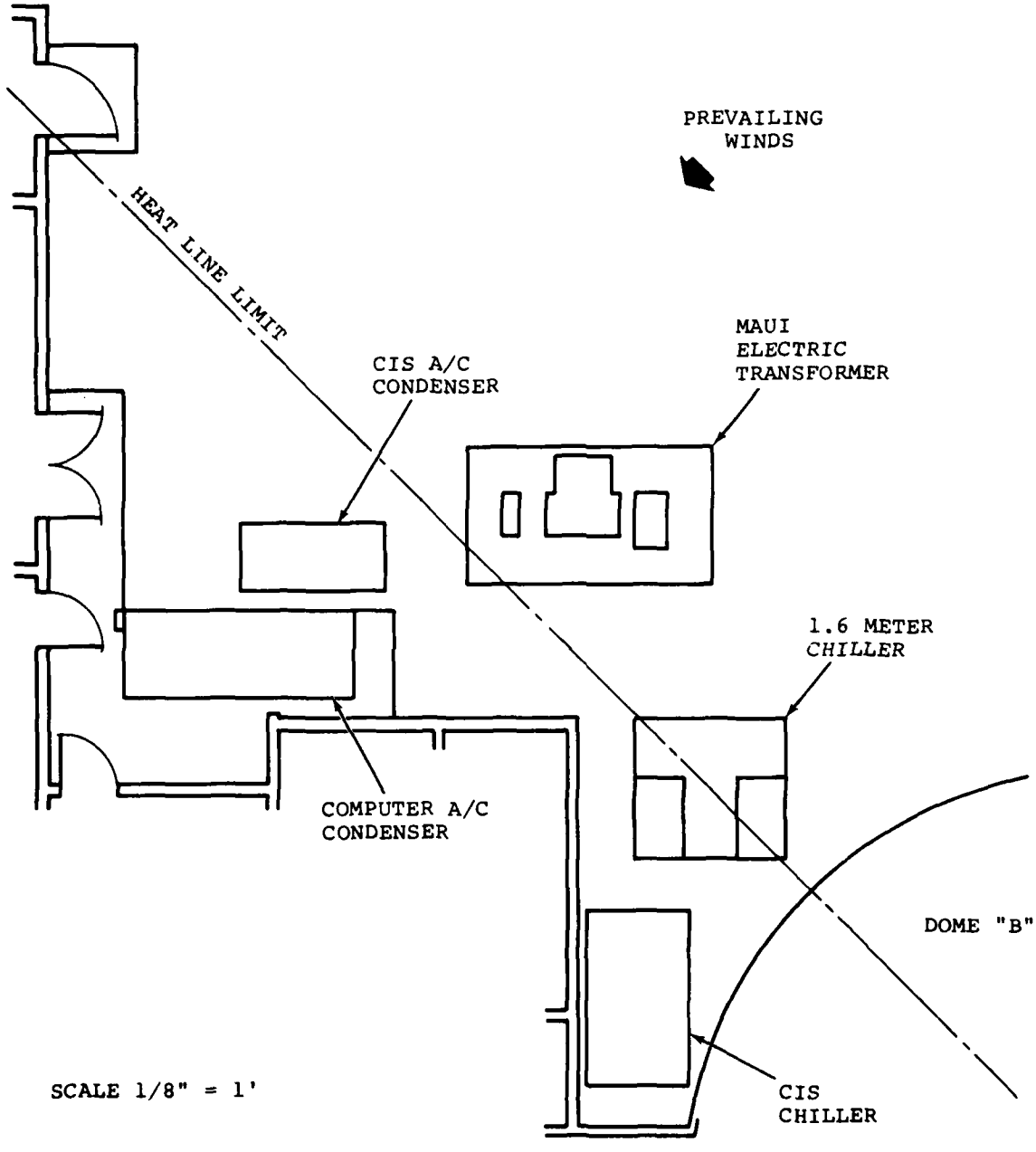

Fig. 37 CIS chiller and air conditioner location.

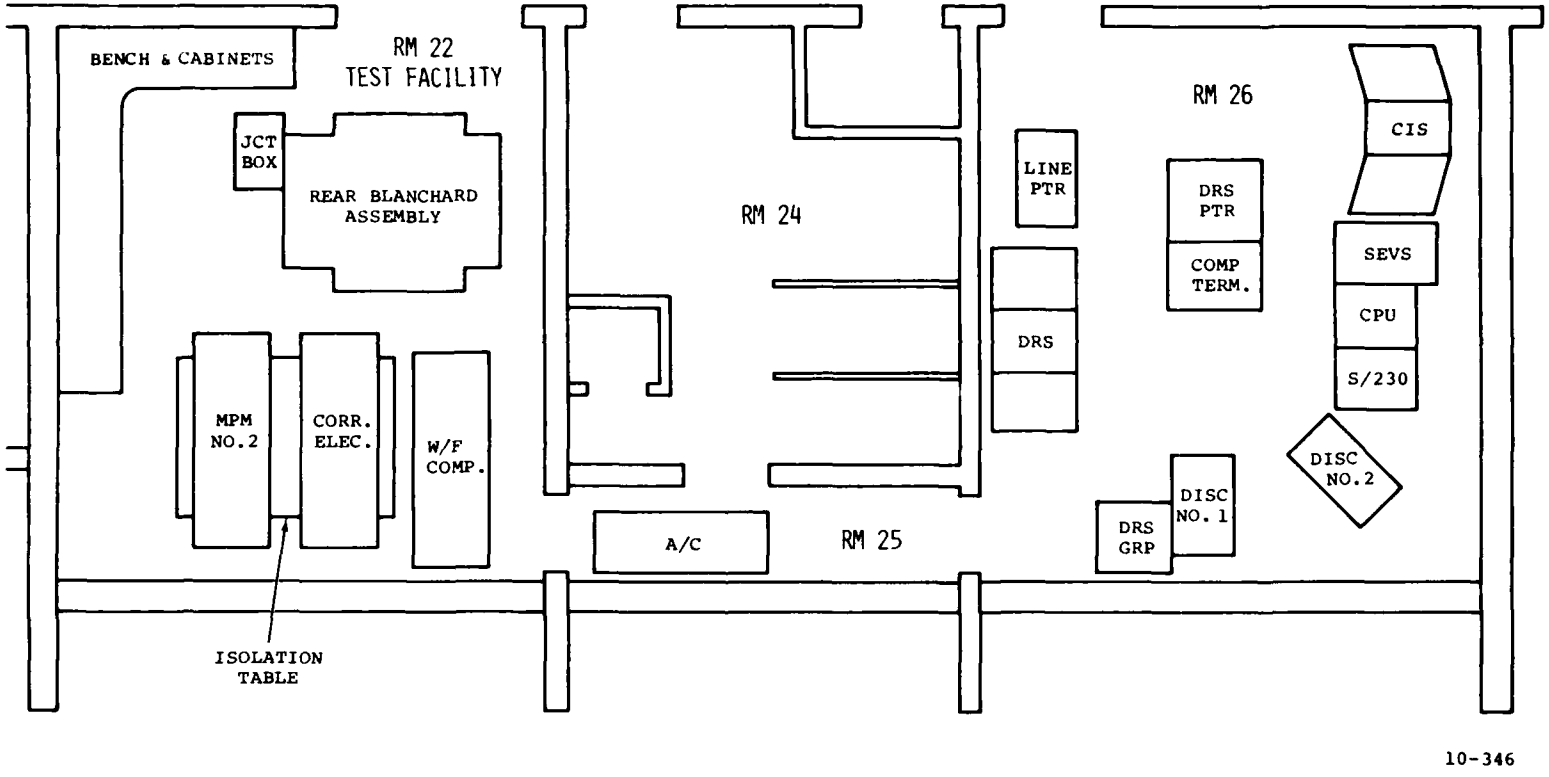

Fig. 38 CIS equipment location.

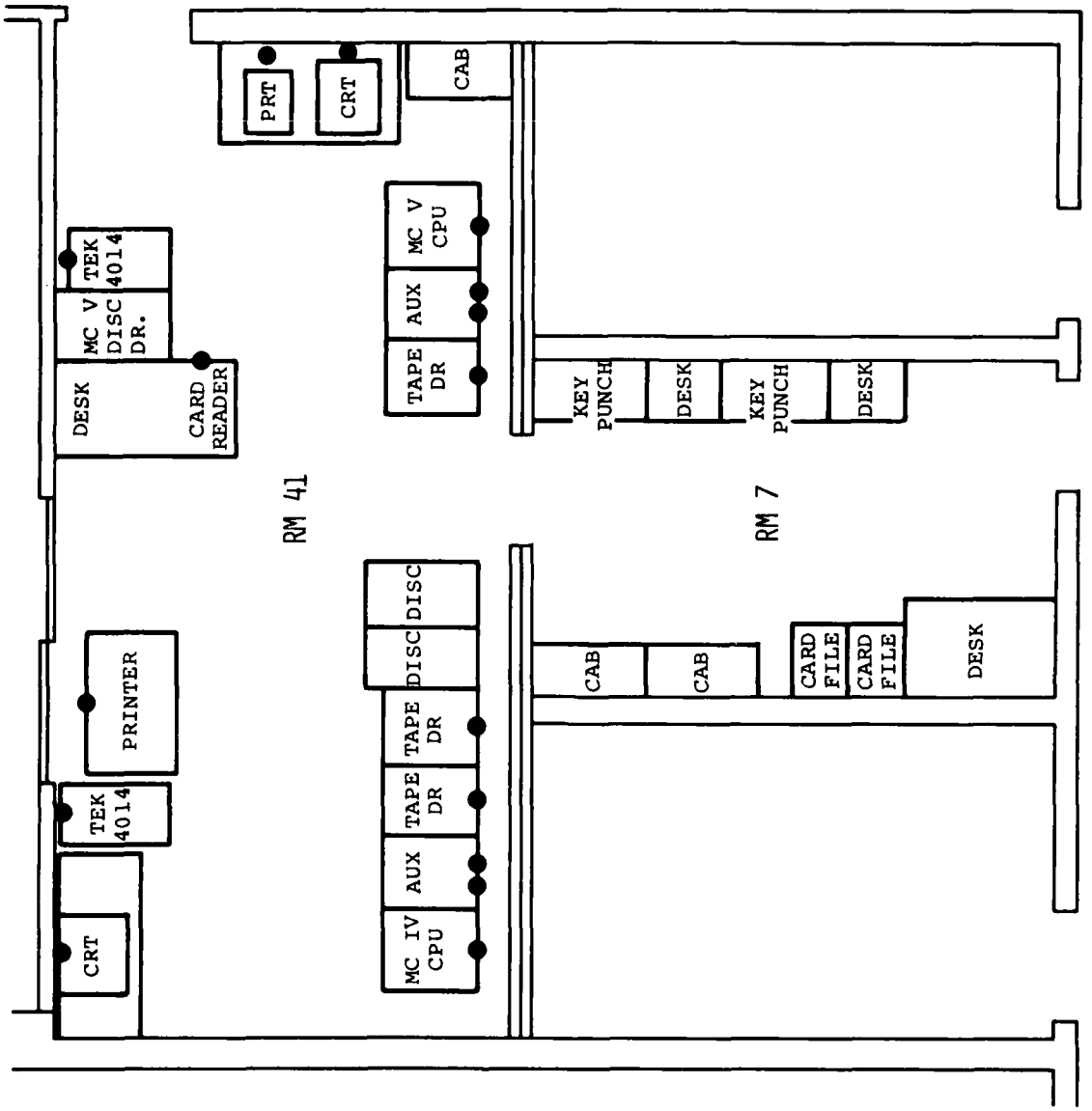

Fig. 39 MOTIF equipment location, rooms 7 and 41.

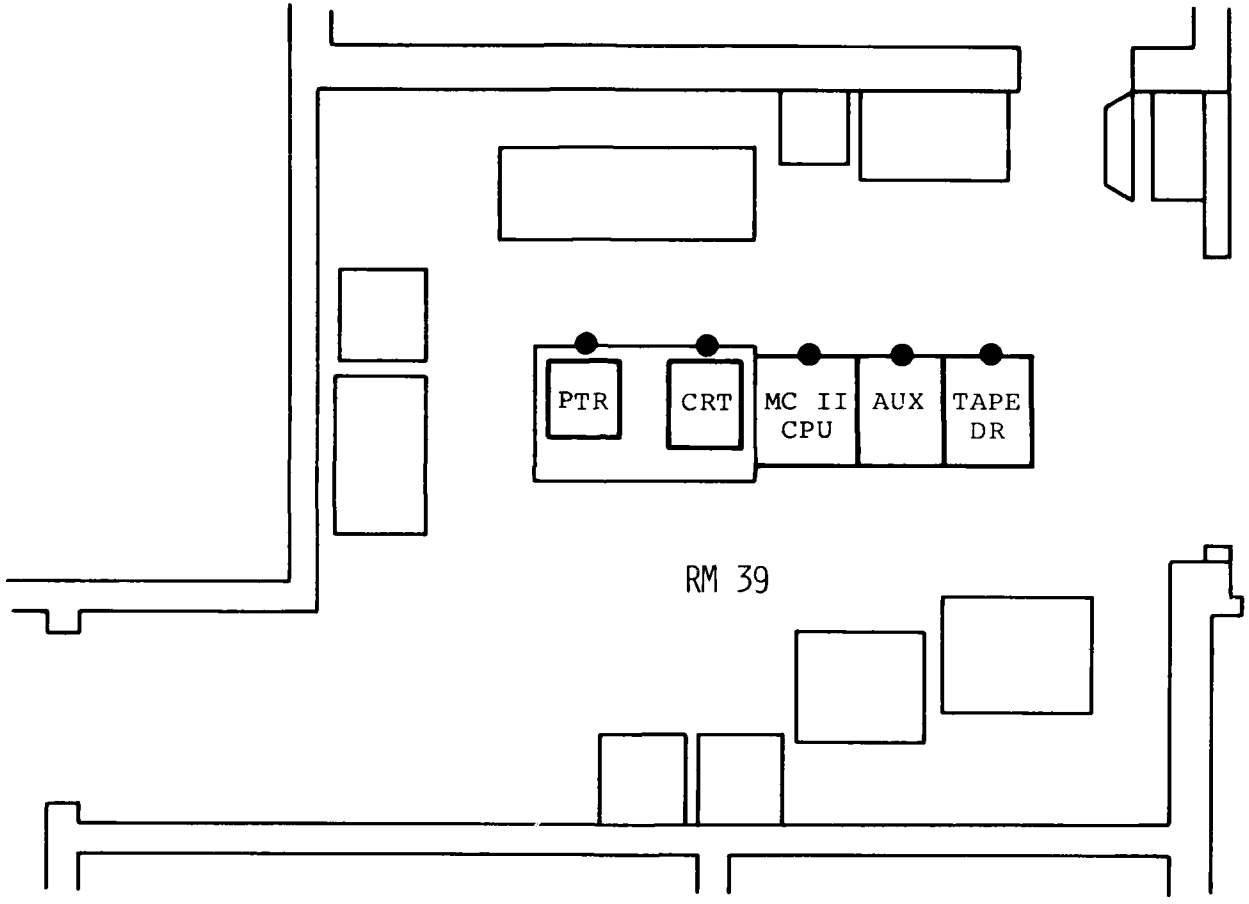

Fig. 40 MOTIF equipment location, room 39.

status and near term projection of AMOS activities. The schedule shows events each week for the month preceding and the three months following the report date. The schedule shows planned and actual events versus time, together with annotations referencing changes to original schedules.

Figure 41 shows a typical AMOS System Schedule.

4.6 System Maintenance

To accomplish preventive and corrective maintenance, configuration management and calibration necessary for operation of the AMOS system, AERL conducts a maintenance program in accordance with the AMOS Maintenance Procedure. (Existing subsystem procedures are revised as required).

The maintenance program consists of both periodic and corrective maintenance. All maintenance is performed in accordance with established AMOS quality assurance, safety and logistics procedures.

The maintenance program is conducted by engineering and technical personnel. Both in the periodic and corrective maintenance areas, engineering personnel ensure that the maintenance has been completed in such a manner that system operating characteristics are maintained or improved. Furthermore, corrective maintenance requires that cognizant systems or sensor engineering personnel be involved from initial diagnosis through the maintenance and subsequent test function in all but the most straightforward situations.

Periodic (preventive) maintenance in the form of inspection

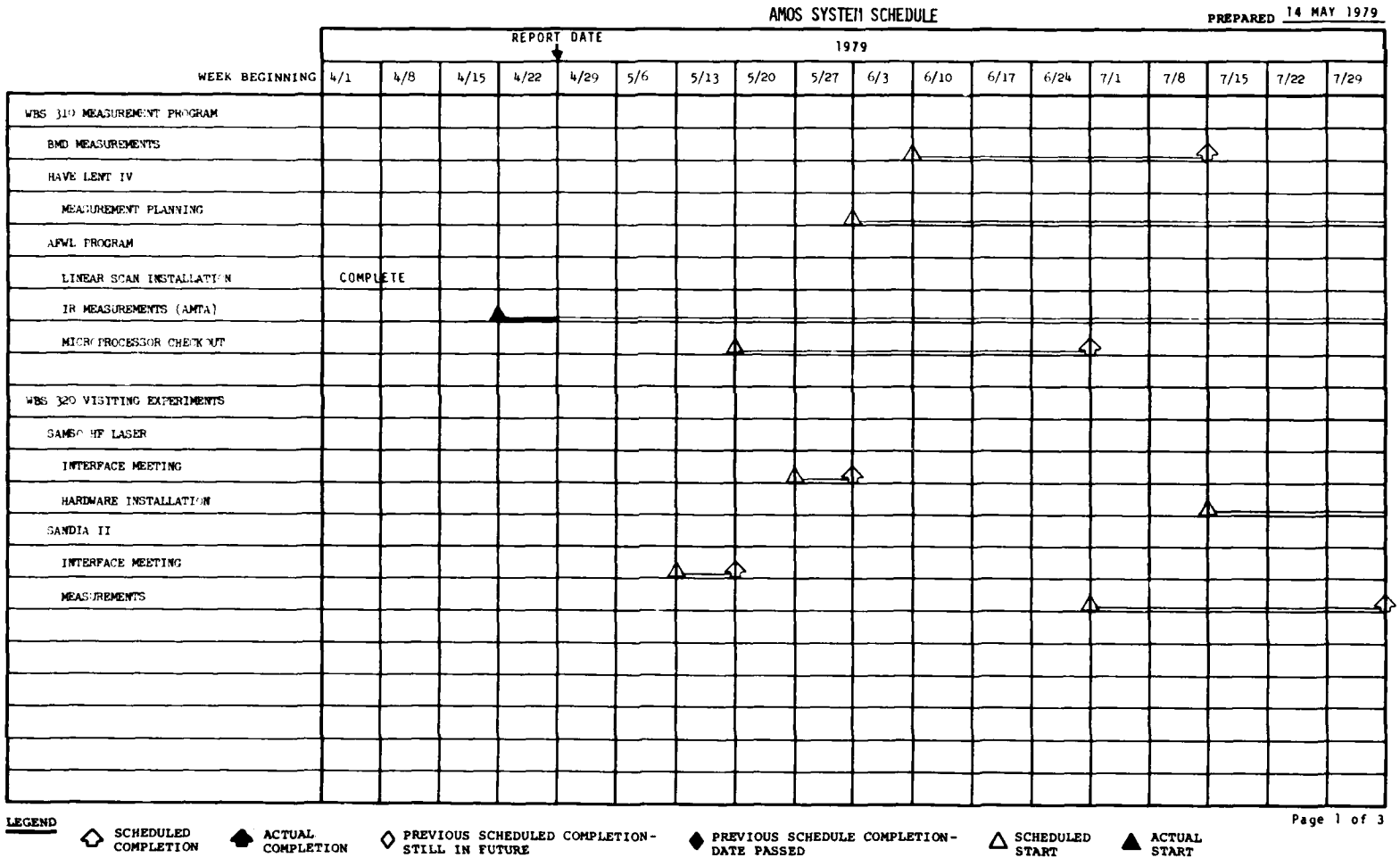

Fig. 41 Typical AMOS System Schedule (sheet 1 of 3).

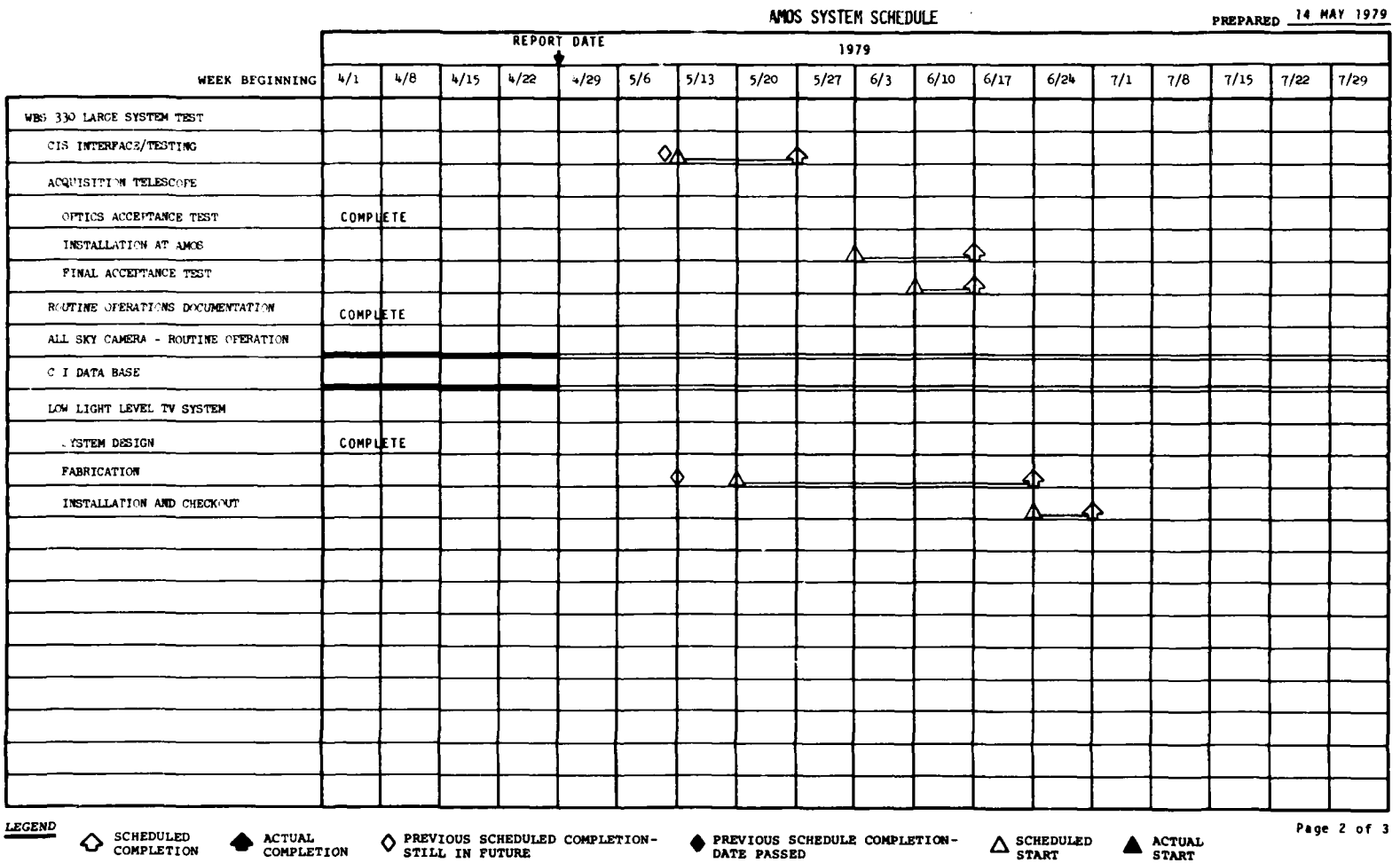

Fig. 41 Typical AMOS system schedule (sheet 2 of 3).

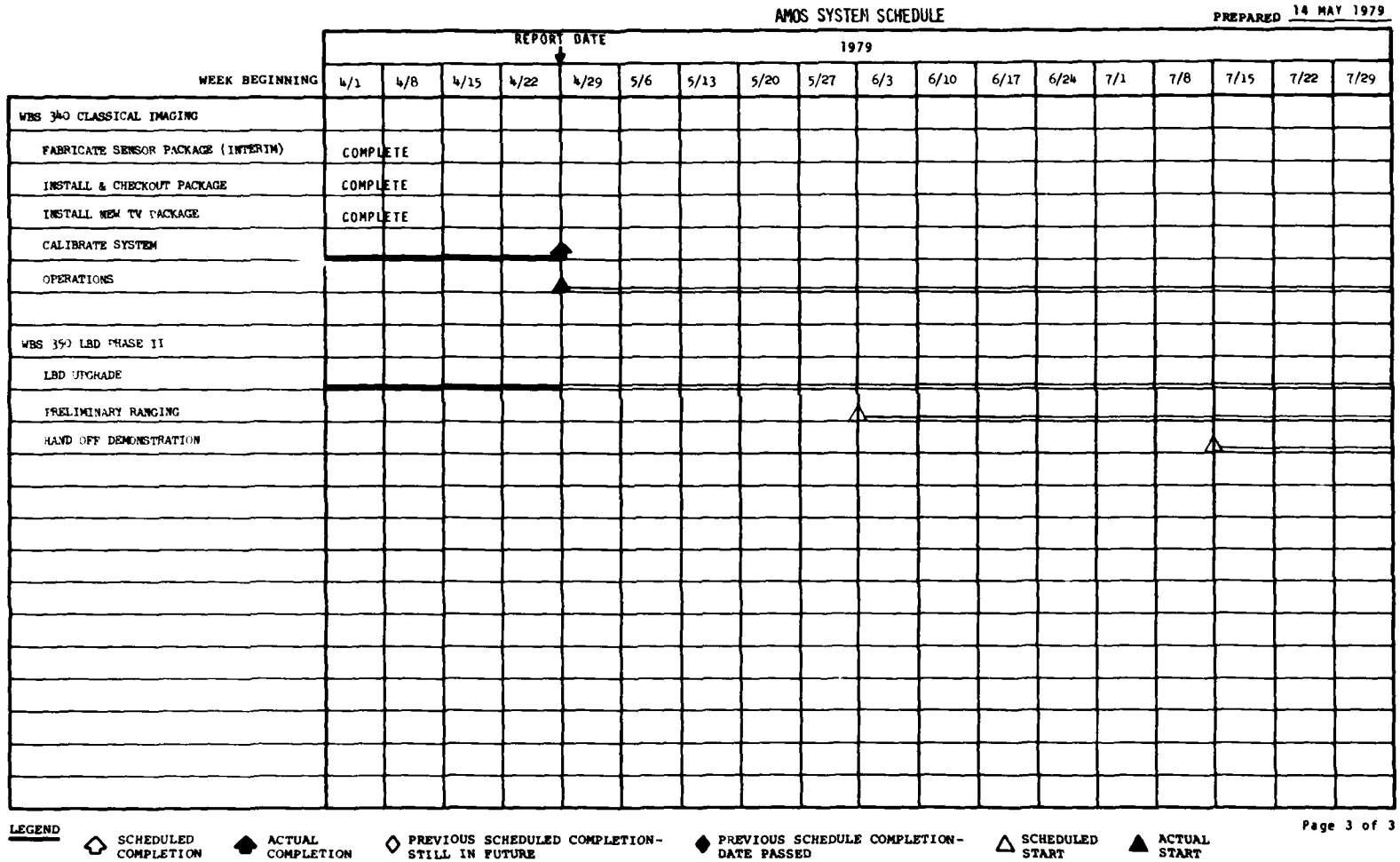

Fig. 41 Typical AMOS system schedule (sheet 3 of 3).

overhaul, lubrication, cleaning, alignment, adjustment and calibration is performed to assure satisfactory system operation. The objective is to reduce failures and to maximize operational availability. All preventive maintenance is performed in accordance with the master maintenance schedule. Maintenance activities are scheduled to increase efficiency and to minimize downtime. Major periodic maintenance activities that result in loss of operating time are included in the weekly observatory schedule. During 1978, over seven hundred (700) preventive maintenance inspections were performed.

A calibration laboratory, containing a select group of working standards, is maintained at AMOS. Working standards are calibrated at the USAF Precision Measurement Equipment Laboratory (PMEL) at Hickam AFB for periodic NBS traceability certification per established schedules. An additional schedule was generated to allow all test equipment within the facility to be periodically calibrated to AMOS working standards. This category of equipment is not sent to the USAF PMEL, except those equipments requiring repair or other service beyond the AMOS facility capability.

Corrective maintenance consists of troubleshooting and repair of malfunctioning hardware and software. Following corrective maintenance, performance verification and recalibrations are performed by AERL and, if required, subcontractor personnel under the direction of responsible engineering personnel. Corrective maintenance tasks that exceed the

capabilities of on-site personnel and/or support/test equipment utilize original equipment manufacturer field and factory maintenance services and AERL off-site engineering support.

The key element in maintenance reporting and record-keeping is the AMOS Maintenance Report. Each Maintenance Report represents an individual activity and contains: equipment name, date; a brief description of the requirement; corrective action; names of the initiator, implementor and validator; material use; and manhours expended. Selected information from these reports is entered into the AMOS Control Software (ACONS). Each month, ACONS processes this information and outputs a Discrepancy Report Status, Discrepancy Report History and Maintenance Accounting Information listings. Periodic maintenance performed is recorded on a Periodic Maintenance Card and is fed into the same ACONS data base. In accordance with the requirements of CDRL Item 001, the above information is used to generate the monthly Failure Summary Report. During 1978, one hundred eighty-three (183) Discrepancy Reports were opened and one hundred sixty-seven (167) of these were closed.

In accordance with the provisions of the AMOS Configuration Management Plan, AERL identifies and documents the functional and physical chartacteristics of system configuration items, controls changes to these characteristics and records and reports change processing and implementation.

AERL documents all changes made to AMOS hardware, technical documentation, computer software and maintenance and operating

procedures (CDRL 005). A file of this documentation is maintained at the Observatory and at the AERL office facility. A computerized index of operation and maintenance manuals, computer programs, specifications and drawings as well as an equipment inventory is maintained as part of ACONS.

Changes to released engineering drawings and specifications are processed, controlled and recorded in accordance with AERL's engineering change procedures.

4.7 Data Library

The AMOS Data Library consists of an area located in the Puunene office building which contains Operations Reports, annotated real-time and playback chart records, computer-generated plots and history reports, films, voice-time cassettes and other data items obtained in support of DARPA programs. It also includes areas at the AMOS Observatory reserved for storage of magnetic tapes. The Phase IV Data Library effort, which began in February and was completed on schedule in April of 1978, consisted of the following tasks:

1) Preparation of a Data Control and Access Plan,
2) Establishment of New Tape Recycling Procedures,
3) Generation of a Cross Reference File,
4) Evaluation of the level of accumulation of data for Phase IV,
5) Evaluation of the internal files for storage of memoranda and data and generation of recommendations for improvement.

4.7.1 Data Control and Access Plan

The Data Control and Access Plan (AERL Doc. #1010) was written to establish procedures for controlling the storage and access to data items obtained prior to or during the AMOS Phase IV Program. The plan defines responsibilities for the preparation, assembly and inventory of data package material. Figure 42 is a flow chart indicating normal data collection and handling procedures. Guidelines for access to AMOS data are defined for a number of different circumstances but basically place the library as a limited access area for AMOS personnel and as a no-access area for non-AMOS personnel (unless approval is obtained from RADC). Finally, the plan addresses the issue of data transmittal and Figure 43 is a flow chart depicting the normal sequence.

4.7.2 New Tape Recycling Procedures

The following history tape recycling guidelines were placed in effect:

1) History tapes obtained in support of Visiting Experiments and those obtained during DARPA sponsored Measurement Programs will not be recycled during Phase IV;
2) History tapes of routine missions (e.g. Classical Imaging) will be retained for a minimum period of six months;
3) The recycling interval for history tapes generated during special tasks will be determined for each

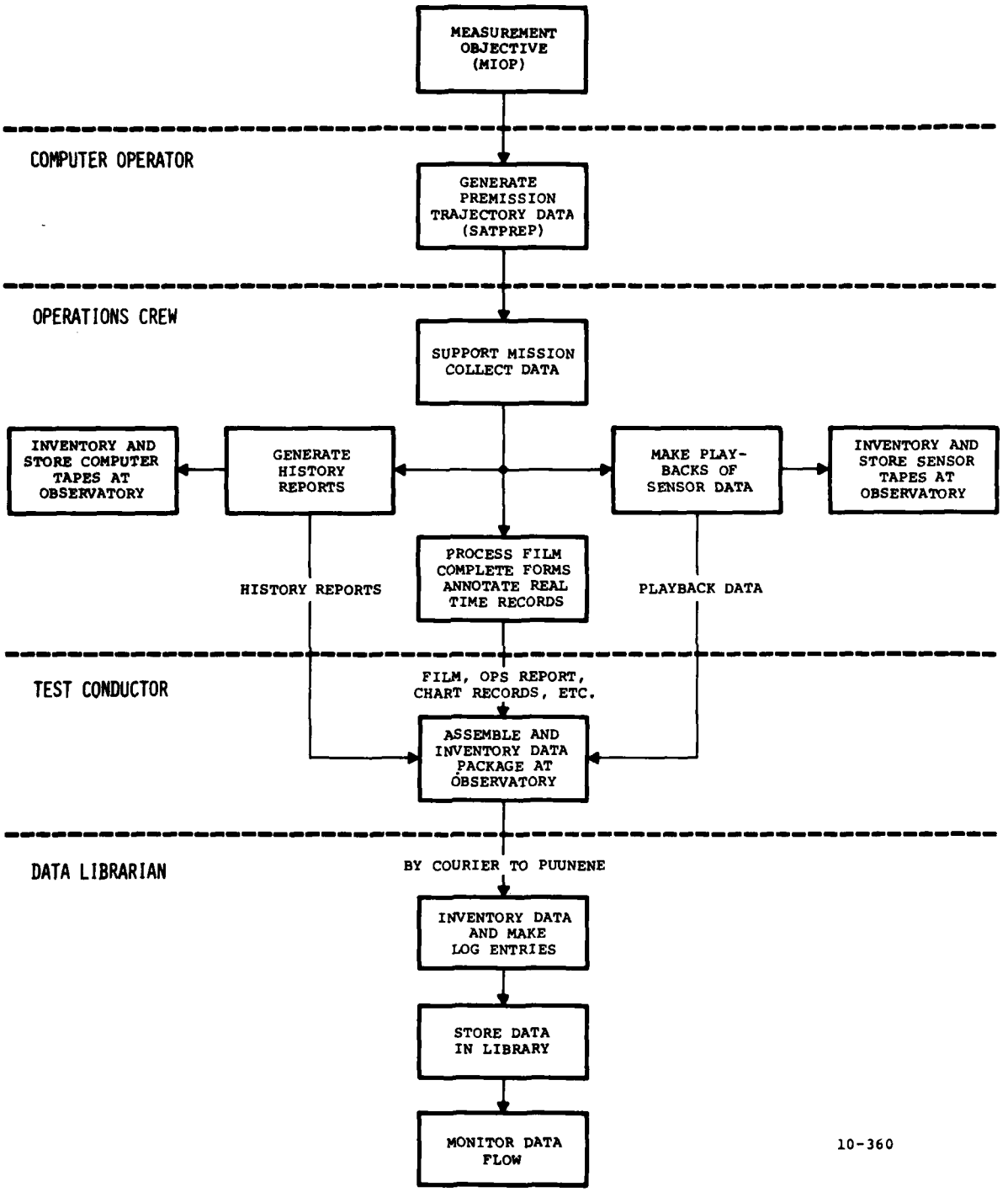

Fig. 42 Data collection & handling overview.

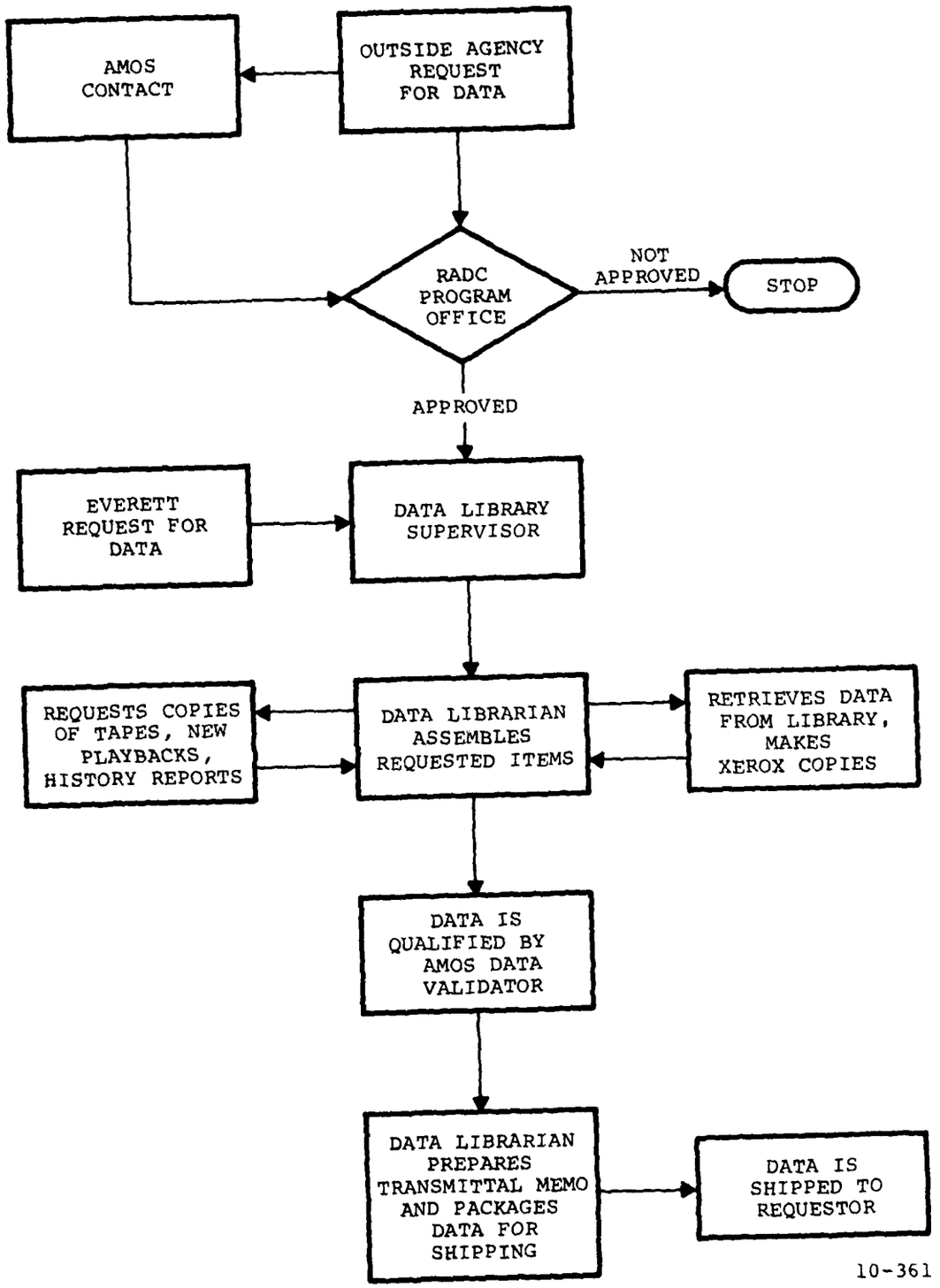

Fig. 43 Data transmittal flow chart.

task but will not be shorter than six months;

4) There will be no changes to the recycling guidelines for Phase III and earlier tapes.

4.7.3 Cross Reference File

A Cross Reference file was set up by the creation of an object number log which associates AMOS Test Numbers (ATN's) with object numbers. In this SECRET document, ATN's are listed under the object number as opposed to the ATN log which associates ATN and object number under a sequential ATN listing. The new log greatly facilitates data retrieval.

4.7.4 Data Accumulation Study

A data accumulation study was made to determine the storage capacity of the data library with respect to the storage needs of Phase IV. This study, based on the data accumulation rate of the last quarter of Phase III, suggested that some expansion would be required at Puunene and that tape recertification and degaussing needed to be implemented at the Observatory.

Since the data accumulation rate has been somewhat slower than anticipated by this study, expansion of storage space at Puunene has not yet been implemented. Recent indications are that tape storage space at the Observatory is approaching the saturation level. This applies to instrumentation tapes, video tapes and history tapes. If it becomes necessary, additional tape recycling guidelines may be required to alleviate the situation.

4.7.5 AIDS File - TM File Recommendations

The AMOS Internal Data Storage (AIDS) system is a subject-oriented file for the storage of informal data. Engineering notes, informal test results and handwritten descriptions of problems are but a few examples of the items made accessible to all AMOS employees by this file. The AIDS file was initiated to protect these kinds of data from being lost when personnel changes occur. The Technical Memoranda (TM) file contains the in-house memoranda that convey information among AMOS personnel and thereby provide continuity of operation of the site.

The AIDS file - TM file task led to recommendations for; 1) establishing a subject oriented TM file, 2) improving the AIDS file and 3) generating a subject-oriented computer index of TMs. The third item was not implemented due to non-availability of programmer time. Items 1 and 2 were combined into a single task by expanding the AIDS file to include technical memoranda.

4.8 Data Reduction

The Phase IV data reduction effort consists of two tasks. The first is the qualification and/or reduction of raw data obtained in support of DARPA-sponsored or approved programs. The nature and extent of this task varies with each mission and is dependent on the type of raw data, the level of qualification and/or reduction required to satisfy DARPA objectives, and the mission frequency. A major portion of this task is related to Compensated Imaging (CI) and, initially, to data

for the CI data base. With respect to the CI data base, the reduction/ qualification consists of the evaluation of photographs obtained with the Classical Sensor Package. It also includes correlation of imagery with atmospheric measurements obtained with the atmospheric characterization sensors at AMOS. In addition to the CI data base, data reduction/qualification is accomplished for photometric, metric and infrared missions. These missions utilize established validation techniques and reduction programs to yield signature and position data. Finally, the LBD Phase II program has resulted in an increase in the related qualification and reduction requirements for AMOS laser range data.

The second data reduction task is an ongoing evaluation of the existing AMOS data acquisition and reduction capabilities leading to improvements in these capabilities as they are needed in the Phase IV effort.

4.8.1 Classical Imaging

Support for this program included development of equations and sign conventions to facilitate the orientation of photographic images with respect to the horizon. This was specifically required to enable AMOS to provide SKYLAB orbital orientation data to NASA. The technique used is based on the parallactic angle calculation. The parallactic angle is the angle between the north pole and zenith (see Figure 44) and is determined for the frame of interest. The camera orientation in the instrument package defines the direction to the north pole of the telescope.

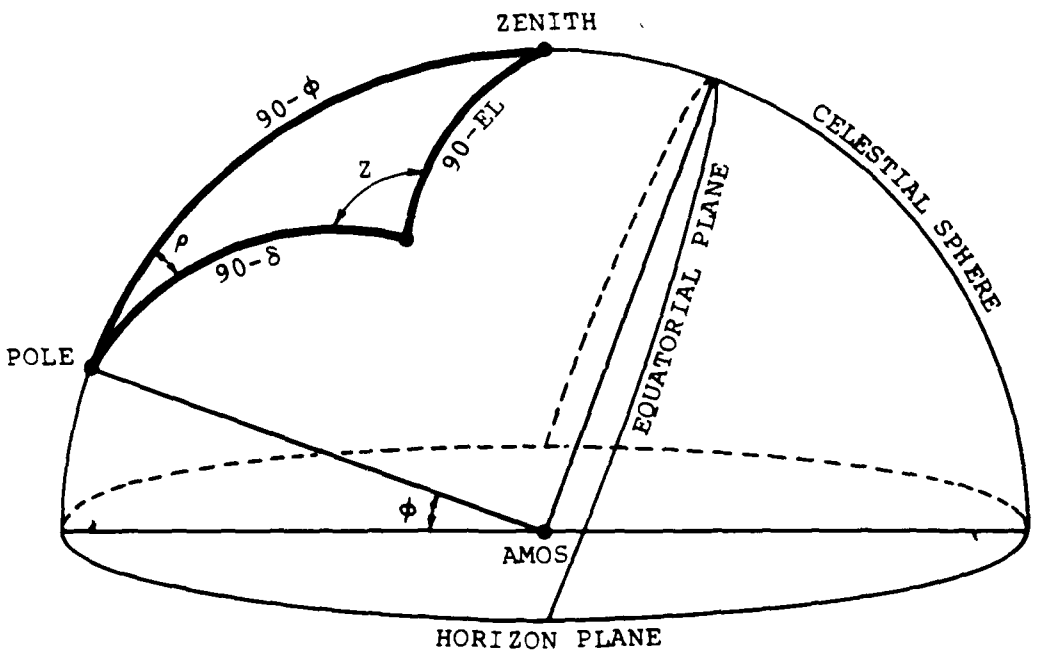

WHERE: ϕ = LATITUDE

ρ = POLAR ANGLE

δ = DECLINATION ANGLE

EL = ELEVATION

Z = PARALLACTIC ANGLE

$$\text{SIN (Z)} = \frac{\text{COS } (\phi) \text{ SIN } (\rho}{\text{COS (EL)}}$$

10-359

Fig. 44 Parallactic angle z.

Polar and declination velocity components of the track, optical inversion of the image in the telescope and film transport direction must all be considered in order to unravel the object orientation in the orbital plane.

Another routine developed for classical imaging was a satellite magnitude estimator. This routine is based on an article by D. E. Smith that appeared in the Proceedings of University of Miami Symposium on Optical Properties of Orbiting Satellites, May 1969. The AMOS routine allows the user to input the fraction of light specularly reflected and that diffusely reflected. The area of the target, range, phase angle and atmospheric extinction are then combined to yield an estimate of the magnitude. Various degrees of freedom are provided to allow refinement of the estimation on subsequent passes of the same target. Finally, a short routine was written to provide the expected angular subtense of a target and the image size at the focal plane of the AMOS telescopes. The routine has been used to compare measured to predicted image dimensions to determine the amount of image spread attributable to the photographic process.

The above routines were developed for use on an HP-67 programmable calculator. In this form, they are readily accessible to AMOS personnel without requiring premium computer time. Three additional HP-67 routines were obtained from the HP-67 User's [illegible] to check out dew point calculations of the atmospheric

sensors. These routines were coded and placed on HP-67 magnetic cards.

4.8.2 IR Signature Measurements

AMOS support for this program was basically to determine which missions warranted further reduction. The selected missions were then sent to Everett for final processing. A target identification problem occurred on one of these missions (ATN 5423) which led to a detailed examination of the data at AMOS. The result was to exercise playback and reduction techniques which had just recently been developed at AMOS. This served to demonstrate that AMOS now has an on-site capability for the reduction of IR signature data which duplicates the Everett reduction capability.

Increased requirements for on-site assessment and validation of digitally recorded AMTA (LWIR) data acquired during measurements such as SEP and the BMD tests were the prime impetus leading to the development of a computerized digital data processing system.

The system SEAD (Site Evaluation of AMTA Data), developed for the MODCOMP II computer, accomplishes two functions;

1) SEAD transfers data from nine-track magnetic tape, created by the AMTA LTI (Long Term Integration) system to disk file.
2) SEAD processes data stored on disk and provides a print-out of the mean and standard deviation of object or calibration voltages.

Although this system is designed primarily for use in data assessment and validation, it can readily be expanded to compute the object radiant intensity utilizing computed responsivities derived from calibration data and state vector input from which object range and elevation are computed. At present, object radiant intensity values are computed using a programmable TI-59 calculator.

The data evaluation program was used extensively to evaluate SEP and BMD data acquired during this reporting period. Options have also been provided in the system to process the dc data channels for retrieval of sky radiance data recorded during the AFWL program initiated during this period.

4.9 Data Analysis

AMOS participated in the SAMSO Evaluation Program during November 1977 and March 1978, with a total of five reducible data sets collected. These data were analyzed and reported in May and June respectively on a limited distribution basis.

A plan was prepared and presented at Lincoln Laboratories for satisfying certain BMDATC/MIT/LL needs for reentry vehicle signature information by using AMOS sensors. This effort included calculating necessary observational times, planning filter sequences and estimating measuring precision in terms of sensor performance, vehicle trajectories and atmospheric effects. The plan was eventually included in the mission support instructions. Later, additional effort was needed to instruct persons responsible for data reduction and to estimate

the validity of initial analysis results.

Estimates were made of the impact of atmospheric effects (radiant granularity and extinction uncertainty) upon space object thermal state observations (AMTA radiometric data). The utility of multicolor measurements and the best spectral options of those available for remote temperature sensing were investigated. This resulted in a change in filter recommendations for SOI mission support. The phenomenological study recommendations were eventually incorporated into mission instructions for the AFWL program.

In an effort to reduce the cavity or scan artifact signal which presently limits the sensitivity of AMTA for long integration missions, a quick fix method for nodding the B29 Telescope's secondary mirror was worked out and implemented. Although this arrangement proved to be mechanically unstable, it functioned long enough to definitely establish that scan artifact and slow baseline fluctuations could be greatly reduced by nodding the secondary instead of AMTA's internal scan mirror. The long-term stability improvement alone warranted a redesign of the secondary mirror mounting with integral drive motor for nodding. This work is now underway.

4.10 Laser Beam Director Program

Early in 1978, AERL completed the efforts described in Modification No. P00052 to Contract F04701-75-C-0047 entitled "Laser Ranging Experiments for Experimental System and Test

Program Definition, Phase I". The activity consisted of four principal tasks:

1) Reactivation and improvement of the ruby laser beam director system including bench calibration;
2) Measurements utilizing a retroreflector satellite to characterize range and angle errors;
3) Evaluation of measurement error and observation scenario effects on hand-off accuracy;
4) Definition of the elements of the next phase of the ongoing experimental program, based on the results of the preceding tasks.

Laser beam director reactivation encompassed transmitter component refurbishing, construction of a receiver instrument package for the 1.6 m Telescope, beam director pointing system repair and calibration, minor ranging system modifications, and associated software upgrades. Bench calibration and a preliminary satellite track verified overall ranging system performance at medium power output (4.5 J in 22 nsec) with 5 arcsecond beam divergence.

Passes of the retroreflector-equipped satellite, GEOS-C, were successfully tracked by AMOS in late Fall, 1977, yielding sets of range and angle observations for analysis at AERL. Comparison of these data with high-accuracy GEOS-C orbits provided by the Naval Surface Weapons Center (NSWC) showed range accuracy and precision to be the order of 2 meters and angle precision to be the order of 2 arcseconds. Unresolved

systematic errors limited the angle accuracy; this was the subject of a recommendation for Phase II.

A covariance analysis of hand-off accuracy at reentry was completed yielding several parametric plots which span AMOS capabilities. The parameters were measurement error, measurement rate, measurement interval, and distribution of intervals. The error analysis, together with the demonstrated AMOS performance, showed the feasibility of hand-off to downrange sensors.

Results of the Phase I efforts were documented in a final report "Laser Ranging Experiments for Experimental System and Test Program Definition - Phase I", April 1978.

Necessary modifications to the AMOS systems to provide real-time hand-off capability and to extend performance to permit measurements on targets without retroreflectors were identified. Recommended laser system modifications included dectector upgrade, multiple-return electronics and software, a more sensitive boresight television, multiple Q-switching, automatic range gate control and beam shaping. Suggested software modifications consisted of a refinement of the beam director pointing error model, addition of range measurement inputs to the real-time trajectory estimator, and an interface to the data communications hardware for transmitting handoff information. Two test periods, utilizing retroreflector satellites, were recommended to reevaluate performance of the upgraded systems (particularly angle measurement accuracy) prior to demonstration of hand-off.

These recommendations for Phase II were incorporated into

Modification No. P00002 to the AMOS Phase IV contract, with work commencing 1 September 1978. By the end of 1978, AERL had completed the first test missions and initiated laser systems and software modifications.

4.10.1 Important Results and Conclusions from Phase I

The first few months of the Phase I program consisted of reactivation and improvement of the existing AMOS laser ranging system (Figure 45).

A new receiver was designed and installed on the 1.6 m telescope (Figure 46). It includes a sensor system (various photomultipliers are available) along with appropriate relay optics. Neutral density and spectral filters (centered at λ = 694.3 nm and having 1.0 nm and 5.0 nm bandpasses) and fields-of-view of 8, 16, 32, 64 and 128 arcseconds are remotely selectable. An ISIT camera is used for acquisition and tracking of solar- and laser-illuminated targets.

A new system was designed and fabricated which allows absolute time-tagging of the laser firing to $\pm$ 10 microseconds. Since a typical target range rate is of the order of a few km per second or less, this assures that errors due to firing time uncertainties are less than about $\pm$ 0.05 meter.

Several software modifications related to acquisition and processing of laser range data were implemented. The real-time software was updated to account for changes to the laser/CDC 3500 interface (for example, the requirement to store time-tagged counter data). The ranging data analysis program was

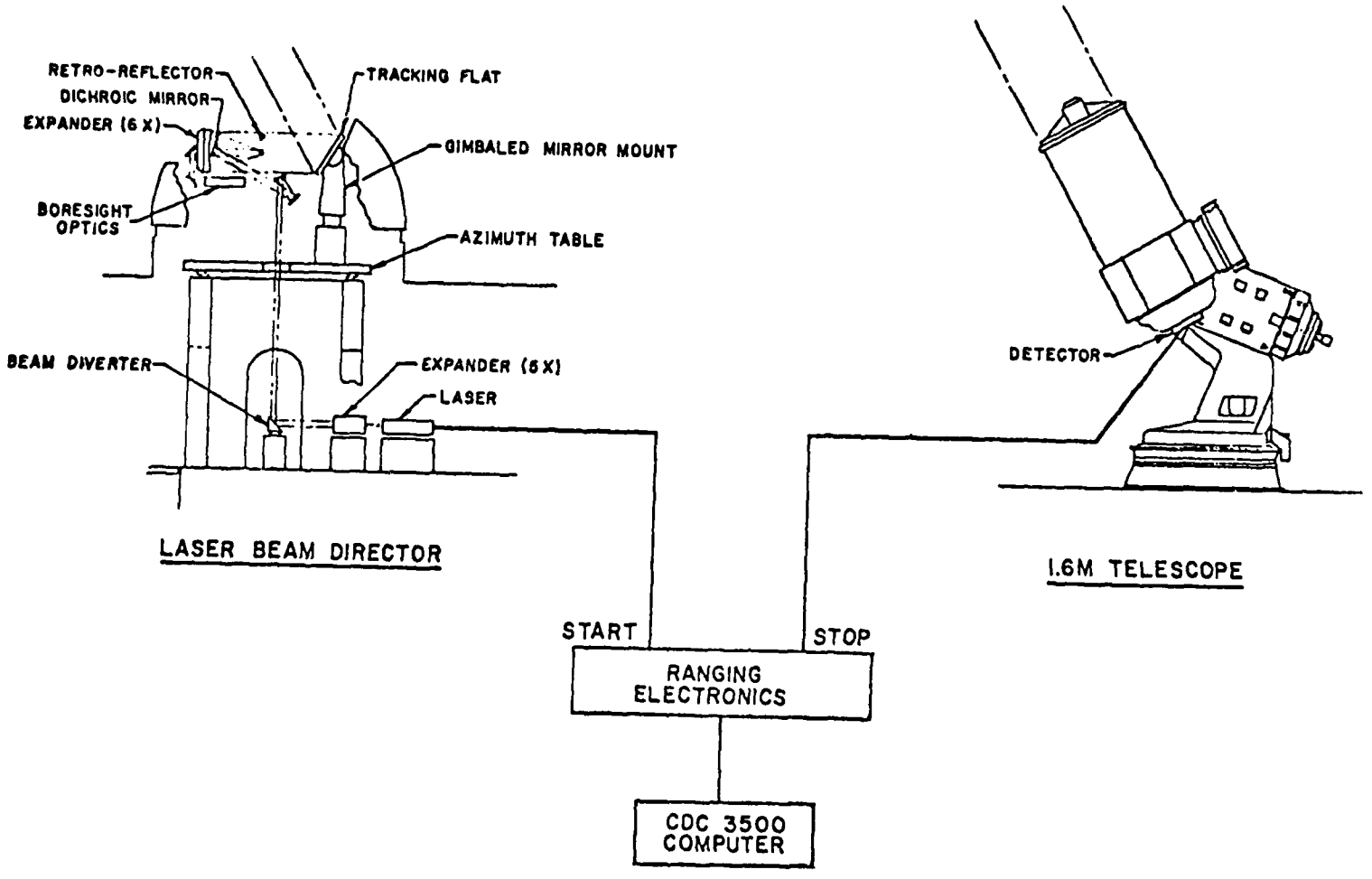

Fig. 45 AMOS laser ranging system.

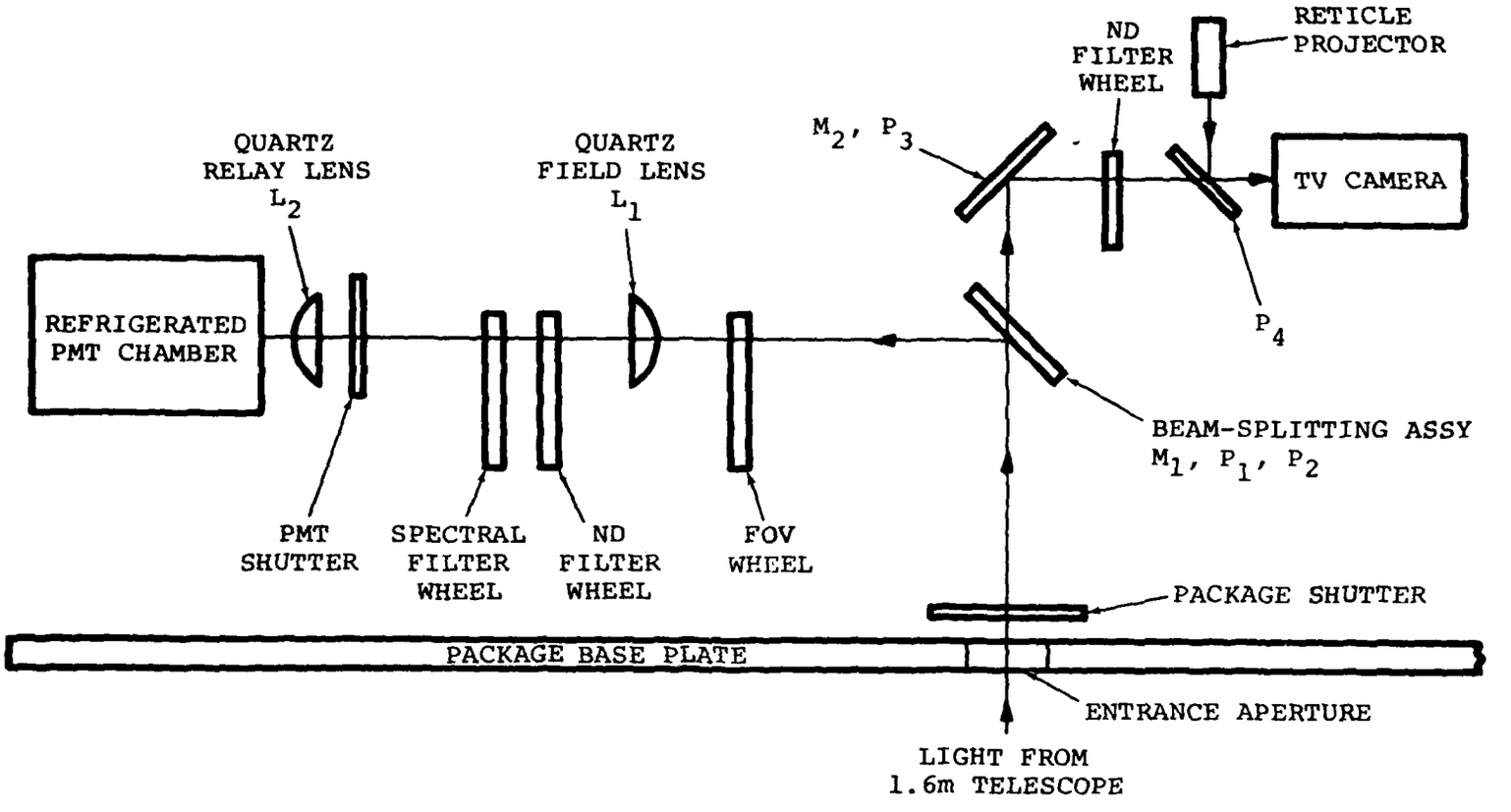

Fig. 46 Laser receiver.

revised to retrieve range observations from the history tape, edit the data, fit an n^{th} order (n = 1 to 20) polynomial through the residuals from a reference trajectory, and display the results. This program is a tool for on-site assessment of ranging system performance (e.g., hits/shots, number of false returns, range precision). In general, however, the program cannot evaluate range measurement accuracy, because the benchmark itself (reference trajectory) has significant errors. A second data reduction program retrieves both angles and range observations from the history tape, reformats and outputs this data on punched cards for final reduction and analysis.

After completion of the modifications described above, the entire laser transmitter was optimized and calibrated for medium power operation. The important system parameters were determined to be:

Pulse Energy	4.5 J
Pulse Width (FWHM)	22×10^{-9} sec
Beam Divergence (FWHM)	5 arcsec (from LBD)
Pulse Repetition Rate (PRR)	20 ppm

During November and December of 1977, the reactivated and improved laser ranging system obtained angles and range observations on passes of the GEOS-C satellite. These observations, together with ancillary information, were transmitted to Everett on cards for detailed analysis. The analysis procedure was to compute predicted values of the observations through an extensive

model of the measurement process, then study the statistics of the residuals (i.e., actual less predicted observations). Predicted data were derived from Naval Surface Weapons Center GEOS-C orbits.

The computer code ASTEP (AMOS Satellite Tracking Evaluation Program) evaluates AMOS range and angle measurements in terms of bias and variance for measurements on a target whose orbit is estimated from data gathered by a world-wide net of stations. A model calculates predicted measurements from the orbit through coordinate transformations and software analogs of the physical processes producing the measurements as discussed below.

First, a geometric position vector is calculated from the trajectory and site coordinates. This basic vector is then modified for atmospheric refraction, planetary aberration, diurnal aberration, eccentric positioning, and system delay. These corrections are small compared to the measurements, so the order of their application is immaterial.

Astronomical refraction is found from a curve fit through the refractivity profile, computed by a raytrace program, using the measured temperature, pressure, and relative humidity at AMOS linearly-faired into the 15° North Annual Atmosphere. Parallactic refraction is obtained using a formula derived by G. Veis. Predicted laser range is corrected for refraction effects using the model developed by Marini and Murray at NASA.

Planetary aberration is caused by target motion while light traverses the target/observer path. Angle predictions

are generated from the reference trajectory at time $t-\tau$, where t is the measurement time and τ is the light transit time. Range predictions use $t + \tau$, since t refers to the instant the laser beam leaves the transmitter. Diurnal aberration is an apparent angular shift toward the East in the line-of-sight caused by rotation of the Earth. This correction is made along with the refraction correction by adding directly to azimuth and elevation angles.

The observed angle is determined from the elapsed time between the laser pulse detection at the output photodiode and its detection at the photomultiplier located at the 1.6 m Telescope focal plane. The apex of the bistatic range triangle is defined by the retroreflector ring on the GEOS-C earth-directed face. Since this point is not at the vehicle center of gravity to which the reference ephemeris applies, an offset correction (depending on vehicle orientation and the site-relative aspect angle) should be made. Such a correction was not made in the analysis of the test missions. The CG/retroreflector distance is believed to be less than one meter.

Other offsets affect the transmitter and receiver locations relative to their surveyed positions as functions of local pointing angles. The transmitter offset is the distance from the intersection of the LBD optical axis and the innermost gimbal axis to the surveyed position at the center of the azimuth turntable; this offset is constant for a mission. The receiver offset is the distance from the intersection of the

declination and optical axes of the 1.6 m Telescope to the surveyed position, a point on the support pedestal, and depends on local pointing angles (polar and declination).

A fixed offset of 12.18 m exists betwen the laser output photodiode and the intersection of the LBD optical axis and the innermost gimbal axis, comprised primarily of several foldovers along the optical train. An additional delay of 135 nsec (40.47 m) is introduced by the cable from the photodiode output to the range counter input. The receiver system on the 1.6 m Telescope has a fixed optical path offset of 11.18 m, the distance from the photomultiplier to the intersection of the declination and optical axes. The cable delay between the the photomultiplier and the range counter stop inputs is 710 nsec (212.85 m).

Examples of ASTEP applied to a GEOS-C pass are shown in Figure 47 (3 sheets). The trend in range residuals is most likely caused by error in the location of the AMOS sensors on the NSWC ellipsoid and a possible systematic bias in the NSWC trajectory arising from the eccentric location of the Doppler antenna. Bias in the angular residuals was caused by an offset between the stellar calibration reference point and the laser receiver.

Results of the laser ranging measurements are shown in Table 5.

In summary, the analysis showed that range observation residuals with RMS values of 2 to 3 meters and angle observa-

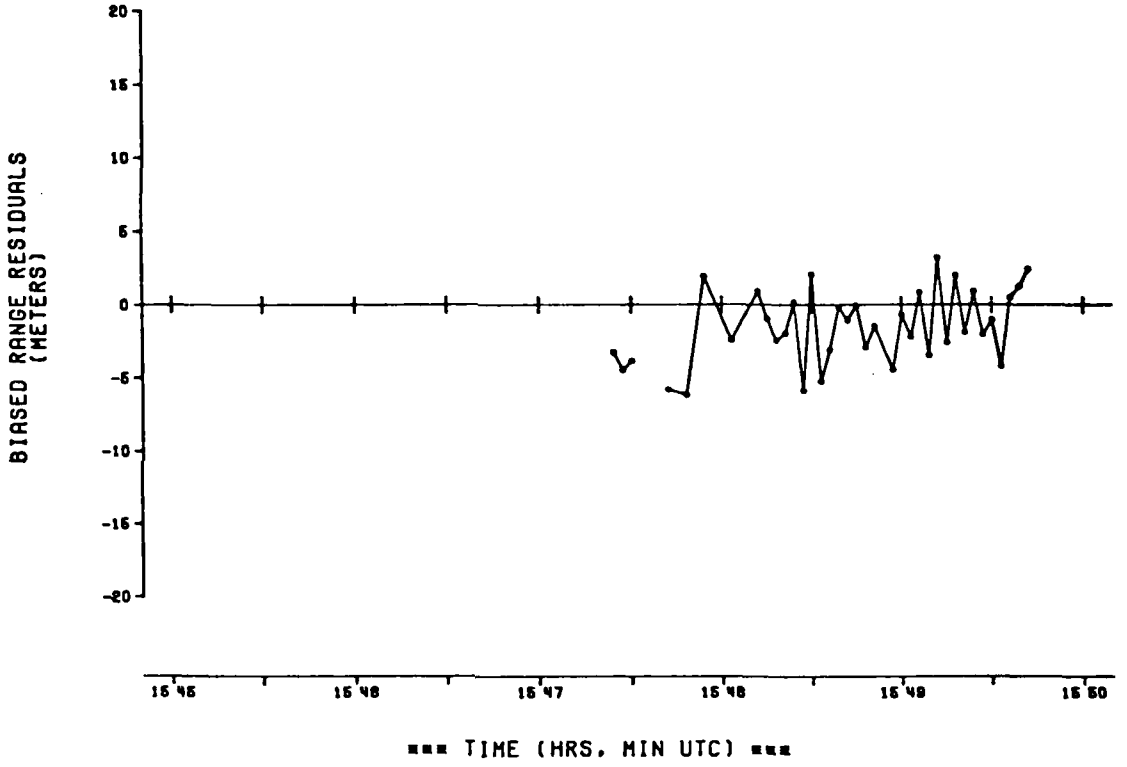

Fig. 47 GEOS-C tracking evaluation (sheet 1 of 3).

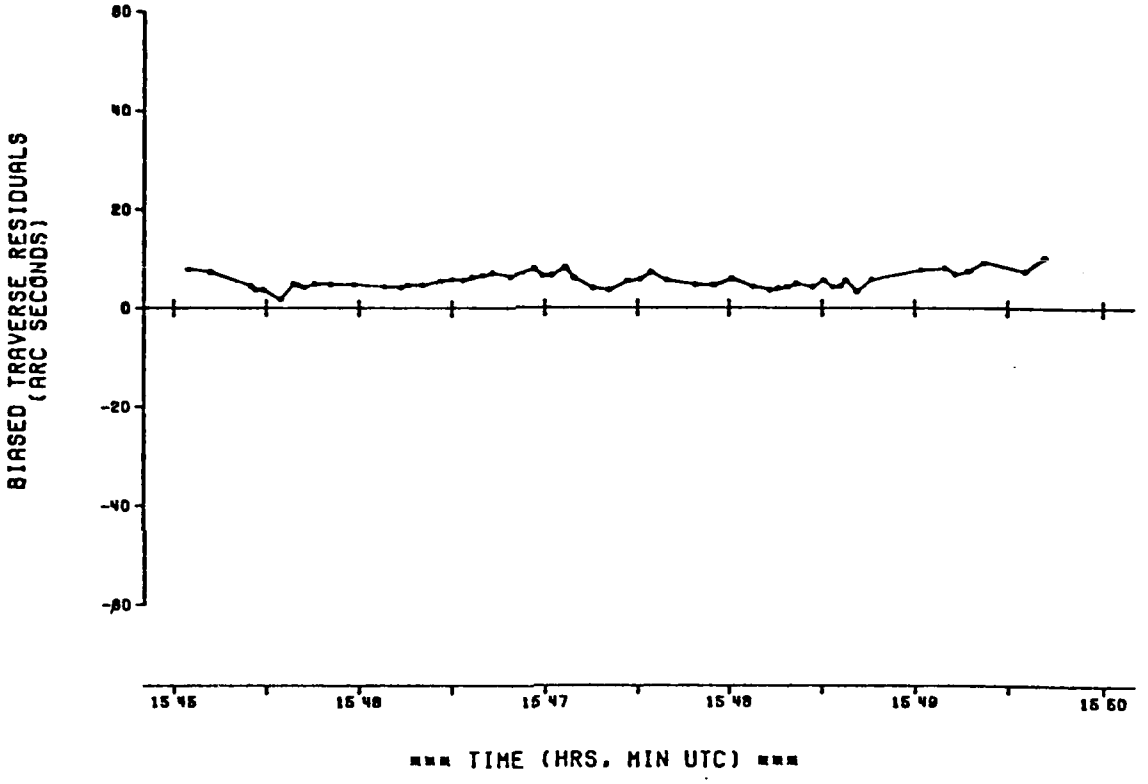

Fig. 47 GEOS-C tracking evaluation (sheet 2 of 3).

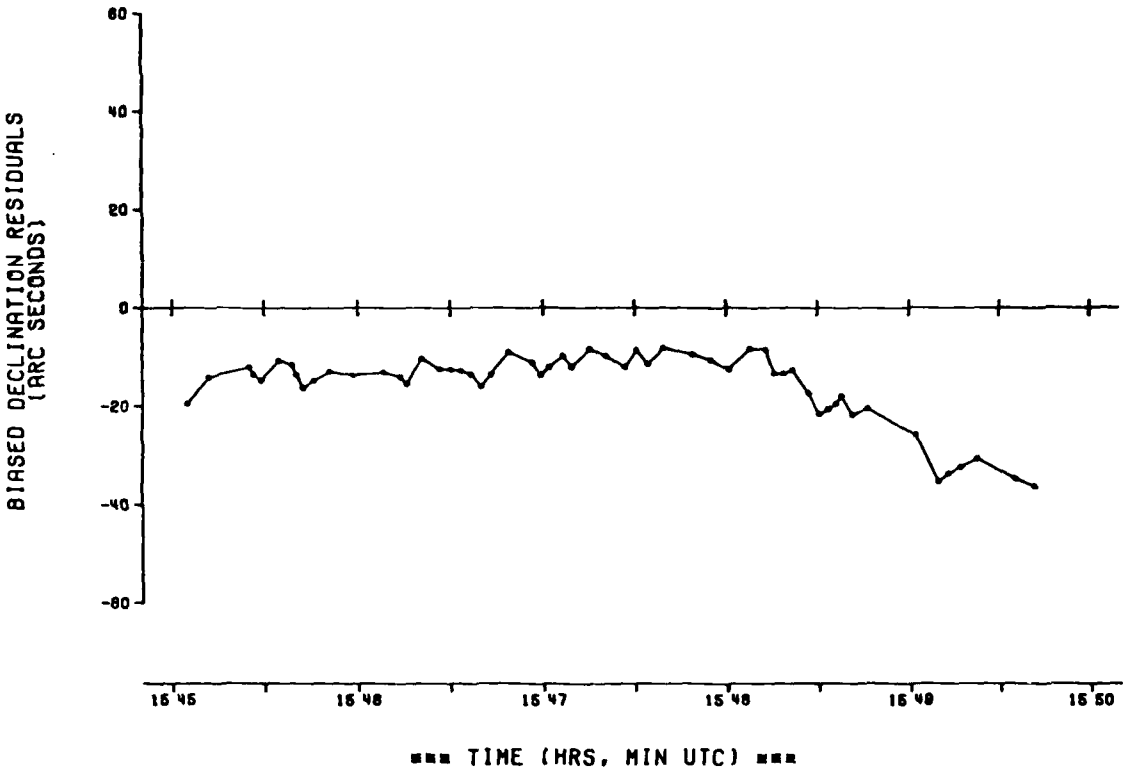

Fig. 47 GEOS-C tracking evaluation (sheet 3 of 3).

TABLE 5 LASER RANGING MEASUREMENTS ON GEOS-C

MAX ELEV	RETURNS/ SHOTS	X (M)	$R^{(M)}$	$P^{(sec)}$	$D^{(sec)}$
60^{o}	44/62	+ 0.5	2.0	1.8	2.6
43^{o}	37/48	- 1.6	2.3	1.3	2.0
53^{o}	77/77	- 1.5	2.8	1.6	1.6
85^{o}	91/96	- 1.0	2.6	3.1	2.0
	COMPOSITE	-1.0	2.4	2.1	2.1

tion residuals with RMS values of 2 to 3 arcseconds were achieved. These values represent the precision of the measurements. The analysis also showed that the average value of the range residuals was within the measurement resolution while, as stated above, the average value of the angle residuals showed unexplained biases and trends considerably larger than the angular measurement precision. Thus, the range measurement accuracy was shown to be the order of 2 meters while the angle measurements were shown to have important systematic errors. A specific task in the Phase II program is to identify the causes of and then eliminate these systematic errors.

The Phase I error analysis next addressed the question of the probable position error at reentry for a typical Vandenberg to Kwajalein trajectory when updated by range and angle observations from AMOS. The analysis method synthesized a state vector error covariance matrix by a standard least-squares estimation algorithm, then propagated the covariance to reentry. All error sources other than observation noise were neglected. The largest given value of the error covariance was used as a conservative measure of probable position error.

Figure 48 is a polar plot of a typical Kwajalein trajectory as seen from AMOS. Three observation intervals, or segments, are shown on the figure, labeled 1, 2 and 3. The first and third segments correspond to that segment of the arc just above 30° elevation, which is the limit of the AMOS laser controlled firing area. The second segment spans culmination. For

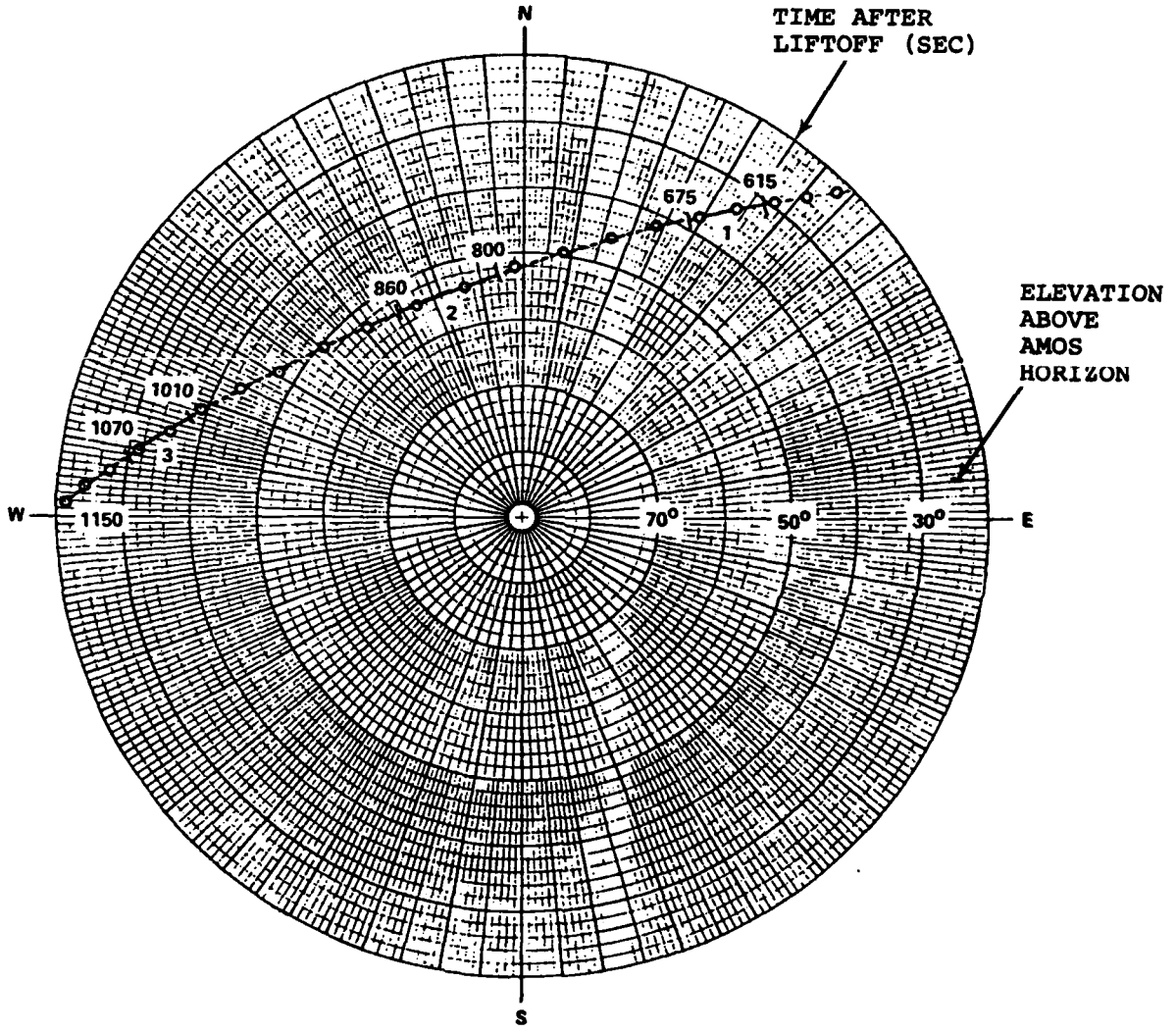

Fig. 48 Vandenburg-Kwajelein trajectory viewed from AMOS.

reference, the beginning and end of each segment are labeled with time after liftoff, in seconds. Reentry, defined as target altitude of 90 km (300 kft), occurs at 1584 seconds after liftoff, 16° below the AMOS horizon.

The parameters varied in the error analysis were:

1) combination of segments;

2) segment length;

3) observation rate;

4) observation uncertainty (measurement noise).

Each class of parameters was varied while holding the other three classes at a fixed operating point. The range of parameters used reflects the capability of the AMOS systems. Details of the results of the error analysis are given in the report "Laser Ranging Experiments for Experimental System and Test Program Definitions - Phase I", April 1978. An example of the results is shown in Figure 49. In this case, range and angle uncertainties were varied as shown on the figure while holding a fixed operating point (segments 1 and 3, segment length of 30 seconds, observation rate of 30 per minute). For angle uncertainties above 0.001°, there is not much advantage in improving range uncertainty beyond 30 m. For better angle uncertainty, and range uncertainty in the region of current AMOS performance, the error varies directly with angle uncertainty.

Values of the largest error ellipsoid axis throughout the studies varied from 1 to 100 m. Values below 10 are suspect due to neglected error sources. Nevertheless, these results

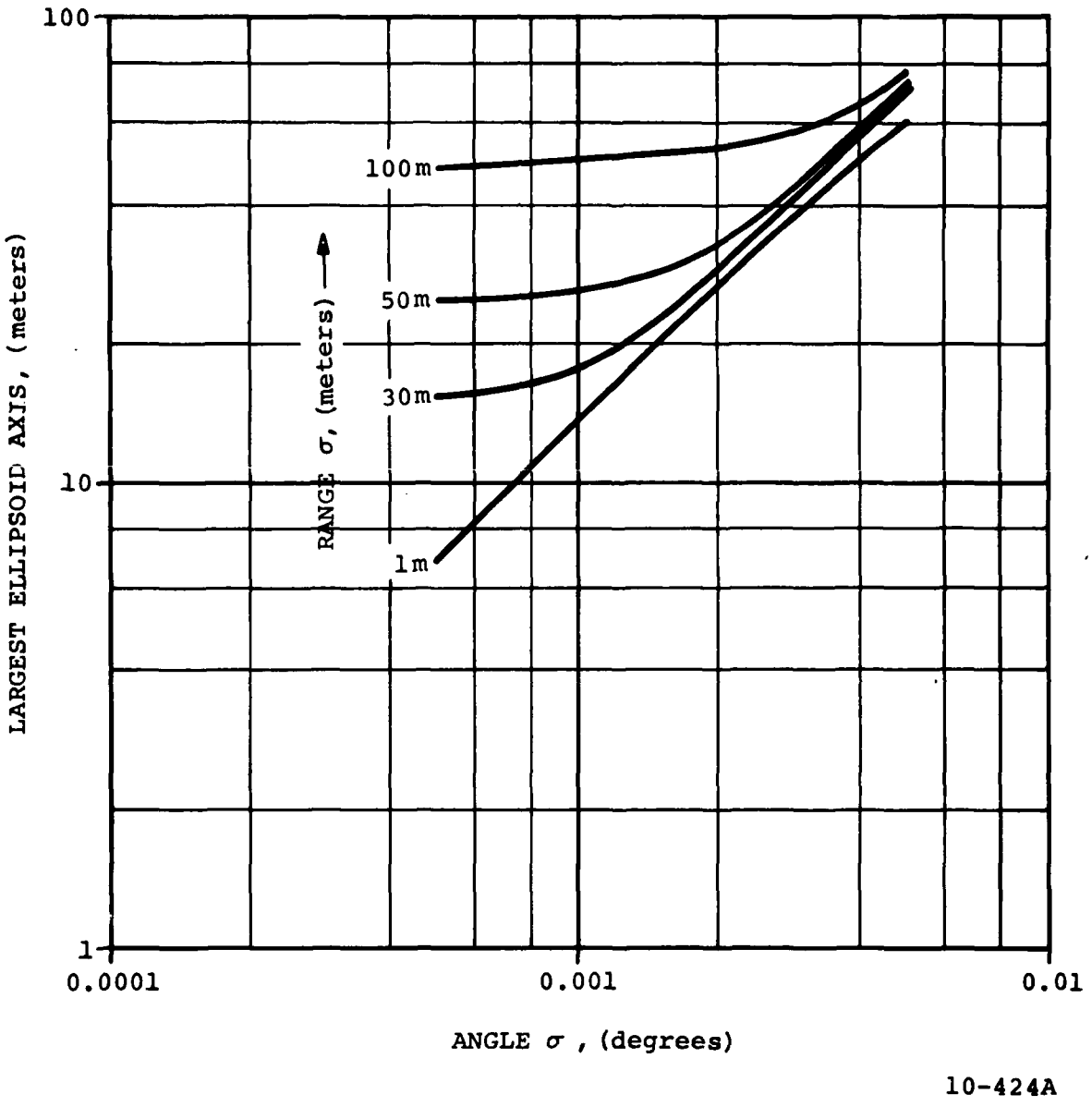

Fig. 49 Hand-off error at reentry vs observation uncertainty.

imply that the current AMOS system can generate a hand-off at reentry with the largest component of position error being less than 50 m. The greatest leverage for improving this result is in angle measurement uncertainty.

4.10.2 Laser Beam Director Program: Phase II

The primary goal of the Phase II Laser Beam Director Program at AMOS is to actually demonstrate the capabilities of a laser ranging system coupled with an angular measurement system to accomplish an accurate state vector hand-off of a ballistic target to a downrange sensor. The feasibility of achieving this goal was clearly established during Phase I of the program.

As stated in the introduction to this section, certain modifications to the AMOS systems to provide real-time hand-off capability and to extend performance to permit ranging measurements on targets not equipped with retroreflectors are required for Phase II. These modifications, along with progress on them during 1978, are discussed in the following paragraphs.

4.10.2.1 Laser Receiver Modifications

In order to allow ranging to non-cooperative (i.e., no retroreflector) targets with a reasonable signal-to-noise ratio per return, several modifications are being implemented in the laser receiver system.

The detector (EMI 9558 photomultiplier) used with the Phase I system has a quantum efficiency of about three percent at $\lambda = 6943$ Å. A new photomultiplier (RCA 31034) has been

procured which has a measured quantum efficiency of 23 percent at the same wavelength. Even when using this detector along with the basic AMOS laser system operating at the 7-10 Joule per pulse level, a mean return of only 5 or 6 photoelectrons will be produced by a Lambertian target at 1800 km range having a reflectivity/area product of 0.01 m^2.

Since the existing AMOS system uses threshold detection, the trigger level must be set at 2 or 3 photoelectrons to assure a high detection probability (>90 percent). A correspondingly high false alarm probability then occurs. The Phase I system, operating on extremely high level returns, allowed storage of only one return per laser firing. This is unacceptable for Phase II targets since the probability of triggering on noise is significant. To adapt the Phase I system to Phase II requirements, automatic range gate and multi-target ranging capabilities are being implemented. These new systems are discussed below.

Automatic Range Gate

The original laser receiver range gate used a manually-operated delay circuit. The delay was adjusted by observing a signal produced on an oscilloscope during real-time. Initial delays were adjusted to open the range gate a few hundred microseconds before a predicted return. (Nominal range predictions may differ by several kilometers from a target's actual range depending upon the age of the element set). This system suffered several obvious limitations. Most importantly, it did

not easily allow narrowing of the gate in response to improved knowledge of the actual range which was being obtained in real-time by the laser system. The new Automatic Range Gate (ARG) adjusts the start of the window in accordance with either nominal or real-time range data. Since uncertainties still exist, the window is started early by a predetermined amount. The ARG hardware uses a 16-bit, settable down-counter. It is loaded with predicted range data, once per second, under computer control. The Q-switched laser pulse generates a START signal which initiates the ARG counter. The ARG counter's resolution is 128 meters (it counts the range-counter clock pulses divided by 64).

The ARG Counter provides an output pulse at underflow (i.e. transition from 000... to 777...). This underflow pulse normally occurs about 55 microseconds prior to the expected range return. The underflow pulse is used to trigger a one-shot delay which can be used to reduce the preset early start time to as little as 5 microseconds.

The underflow pulse also triggers another one-shot delay which, in turn, generates a Z modulation pulse to enhance the brightness of an oscilloscope display at the time of the predicted return. An octal display is included on the ARG circuit card as an operator and troubleshooting aid. It displays the contents of the 16-bit down-counter.

A block diagram of the ARG is shown in Figure 50. A timing diagram is shown in Figure 51.

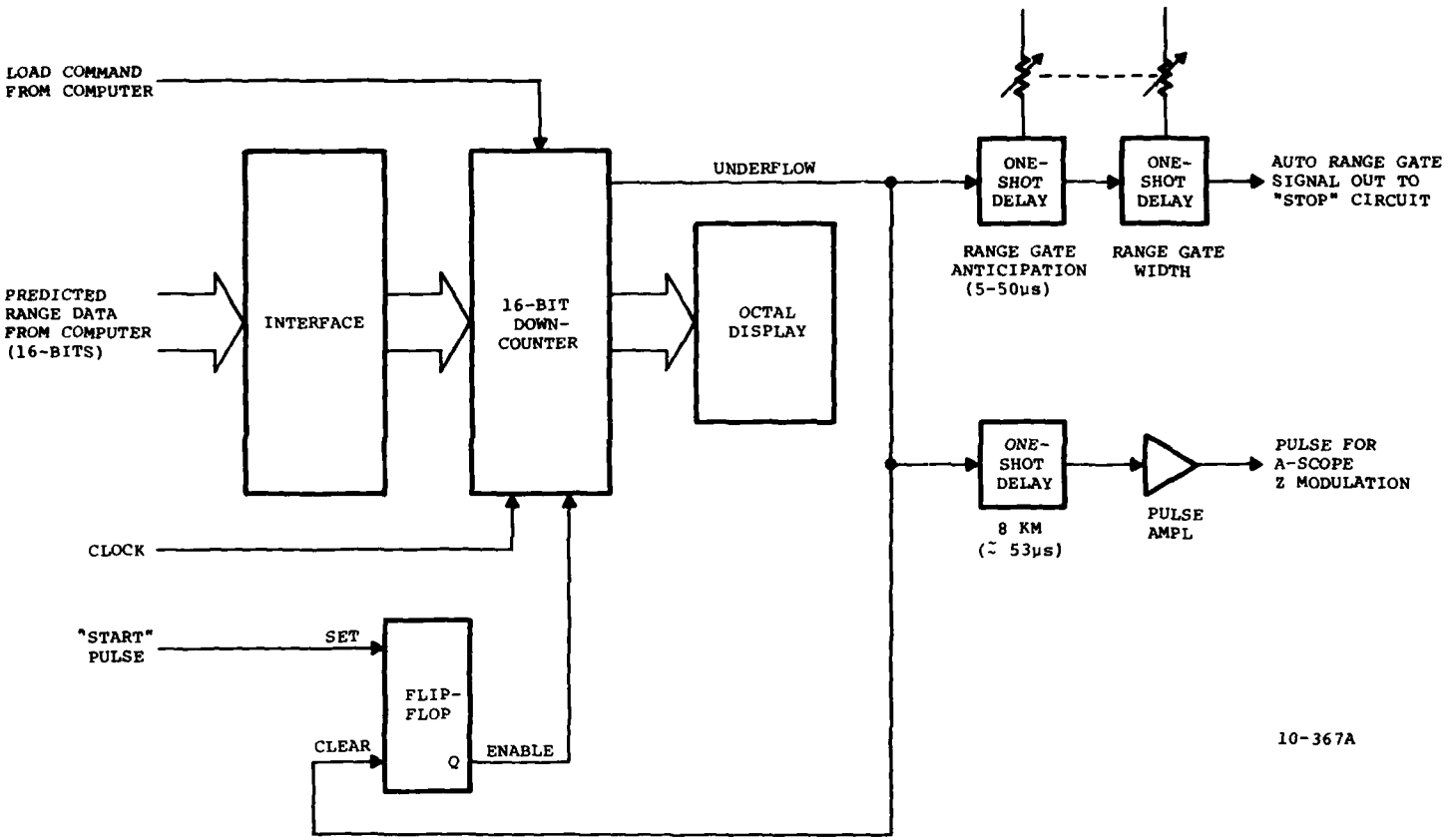

Fig. 50 Automatic Range Gate.

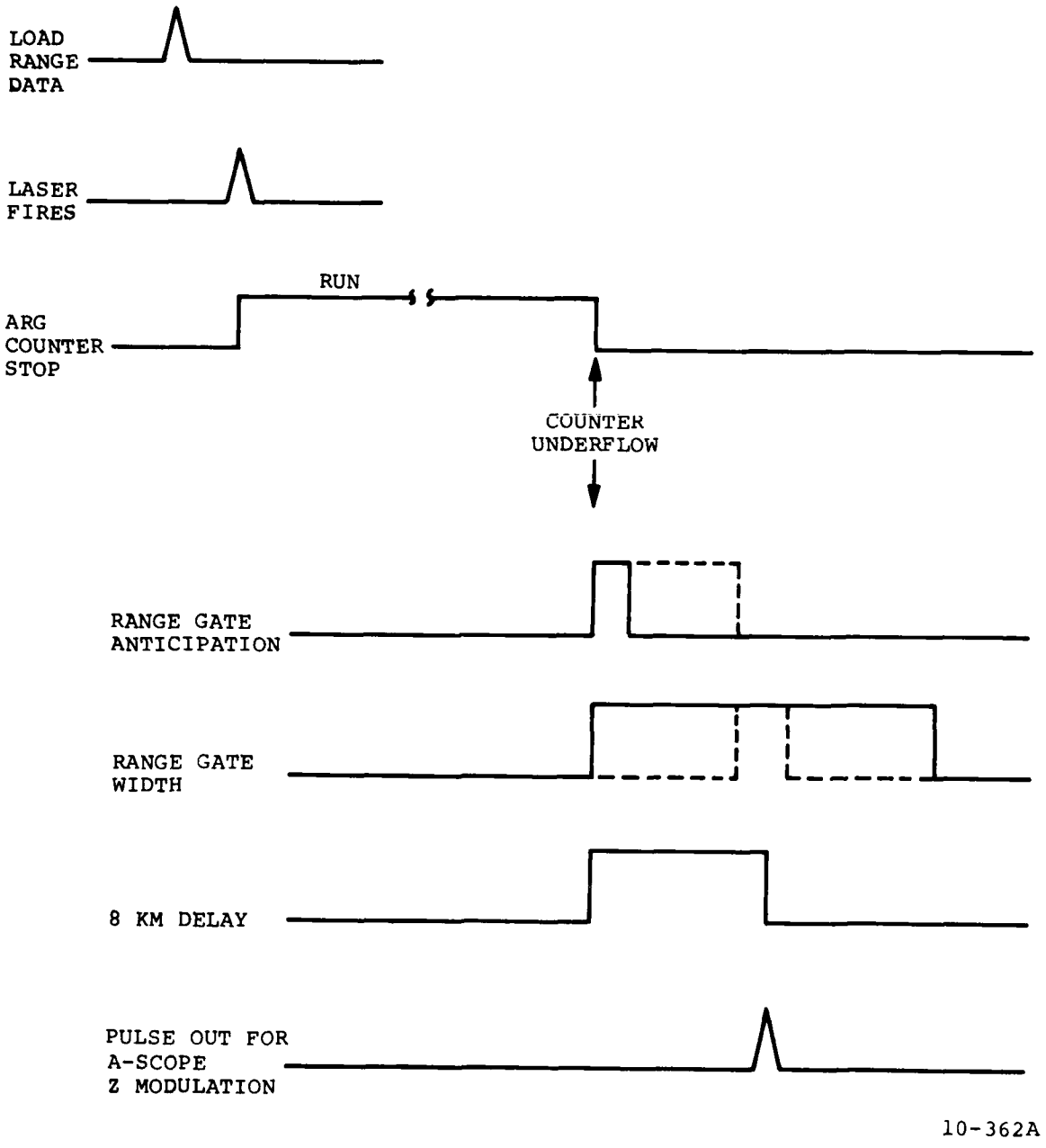

Fig. 51 ARG timing diagram.

By the end of 1978, the ARG hardware had been designed, fabricated and partially tested. Final testing will occur when the required software is completed in the Spring of 1979.

Multiple Return Counters

Multiple Return Counters (MRC) allow more than one range measurement per laser firing. Multiple range returns are generated by either multiplicity of targets (real or false) and/or by transmitting multiple Q-switch pulses.

The most important facet of a multiple return measuring system is that a false trigger (e.g. produced by EMI or dark current) occurring during the range gate, but preceding an actual range return, does not prevent acquisition of real range data. The false return stops the first counter, but the remaining counters are available to receive data.

After evaluation of several possible approaches to providing the required multiple return capability, it was decided that the most efficient and cost-effective method was to design and build the MRC at AMOS. A two-meter resolution ranging counter had successfully been designed and fabricated at AMOS for the Laser Phase I program. The MRC uses that experience as the foundation of the new system.

There are two basic methods of controlling multiple counters: (1) incremental start, or (2) simultaneous start. In the first case, only one counter at a time is running. When the laser fires, the first counter starts. Upon receipt of the first receiver STOP pulse, the first counter stops and the

second counter starts. The second STOP pulse stops the second counter and starts the third counter, etc. The capacity of the second and subsequent counters need not be as large as the primary counter which must be able to store ranges of up to about 2000 km. Disadvantages of the incremental counter approach include: (1) additional software is required to compute the range for each return; and (2) it is possible to drop a 75 MHz clock pulse during transitions if the returns (real or noise) are only separated by a few nanoseconds.

It was concluded that the best approach was to use simultaneous start counters in which all of the counters start when triggered by the laser transmitter firing pulse. Each return only causes successive counters to stop; no enabling of counters occurs in response to a STOP pulse. The basic system is shown in Figure 52.

A laser start-photodiode pulse, coincident and gated with the Pockels cell trigger pulse, sets all six outputs of a High Speed Shift Register (HSSR), thus enabling all six of the 14-bit binary counters simultaneously. Prior to laser firing, all outputs of the HSSR are cleared.

The J-K inputs of the first stage of the HSSR are connected such that the first STOP pulse clears that stage, thus disabling the first 14-bit counter. The Q and $\overline{Q}$ outputs of the first stage of the HSSR are connected to the J-K inputs of the second stage of the HSSR. Thus, the cleared state of the first HSSR stage enables the inputs of the second stage to be cleared by

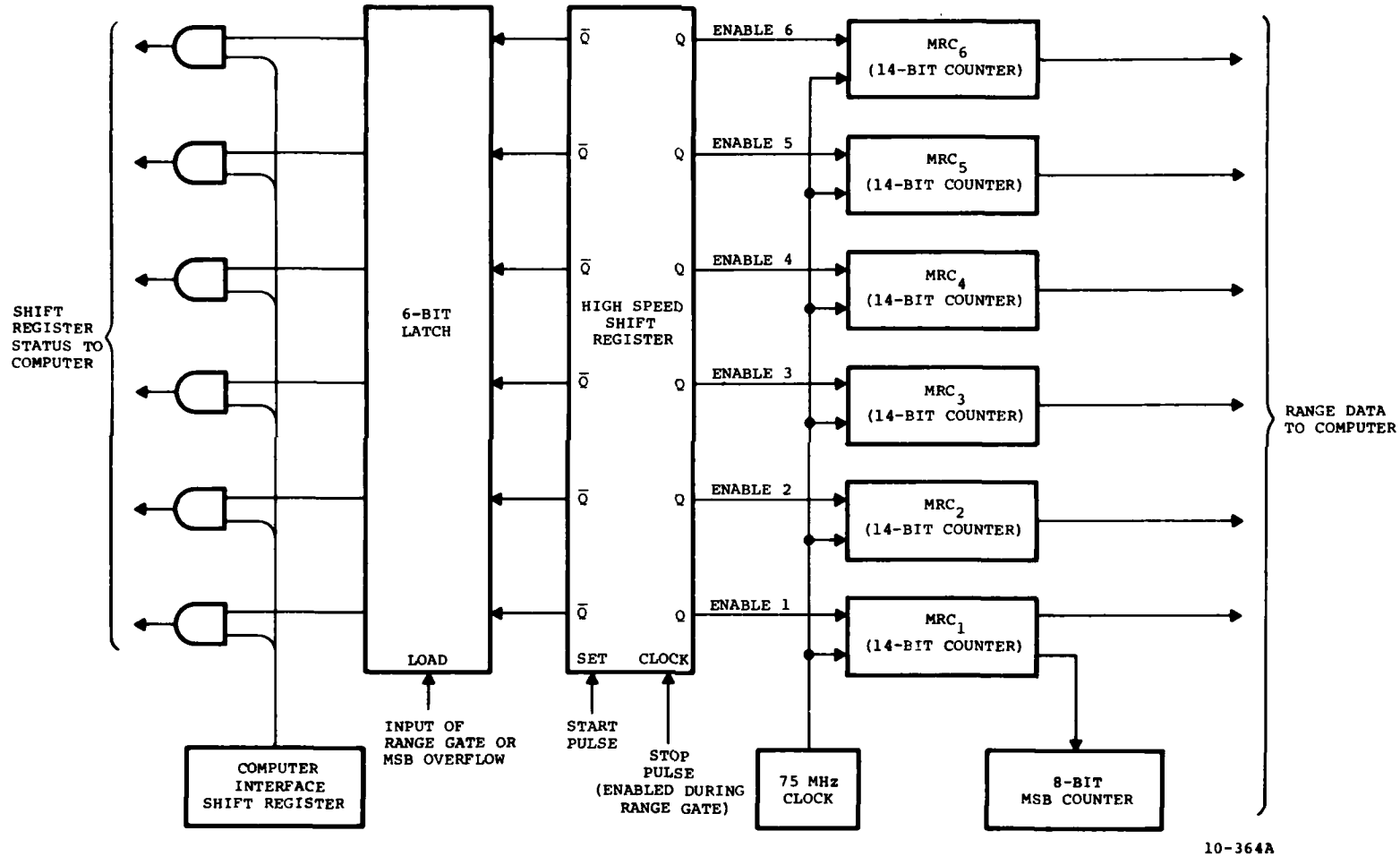

Fig. 52 Multiple Return Counter.

the second STOP pulse. This sequencing continues up to six STOP pulses. Each STOP pulse advances the progression of the enable/disable lines going from the HSSR to the enable inputs of the 14-bit counters.

If the Most Significant Bit (MSB) counter overflows when no STOP signals are seen by the receiver, that overflow condition causes all stages of the HSSR to be cleared and the contents of all 14-bit counters and the eight bits of the MSB counter to be set to zero.

The end of the range gate signal clears all stages of the HSSR. Just prior to this, however, the condition of the HSSR is read by a 6-bit latch to provide information to the computer as to how many numbers (actual or false returns) to process.

The 14-bit binary counter is based on one SN74S112N and three SN74197N (or SN74177N) IC's, connected in ripple-carry configuration. Power supply spiking is reduced by avoiding simultaneous transition or synchronous counters.

The outputs are displayed on HP 5082-7302 decoder/driver display modules. The outputs are also connected to an array of two-input NAND gates. These gates serve two purposes: (1) the gates are enabled to transmit the contents of an individual MRC card to the computer (to multiplex MRC data in sequence to the computer); and (2) when the gates are disabled, counter output transitions are not transmitted on the long lines between the ranging circuits and the computer inputs. (See Figure 53). During 1978, the MRC cards were designed and a vendor built

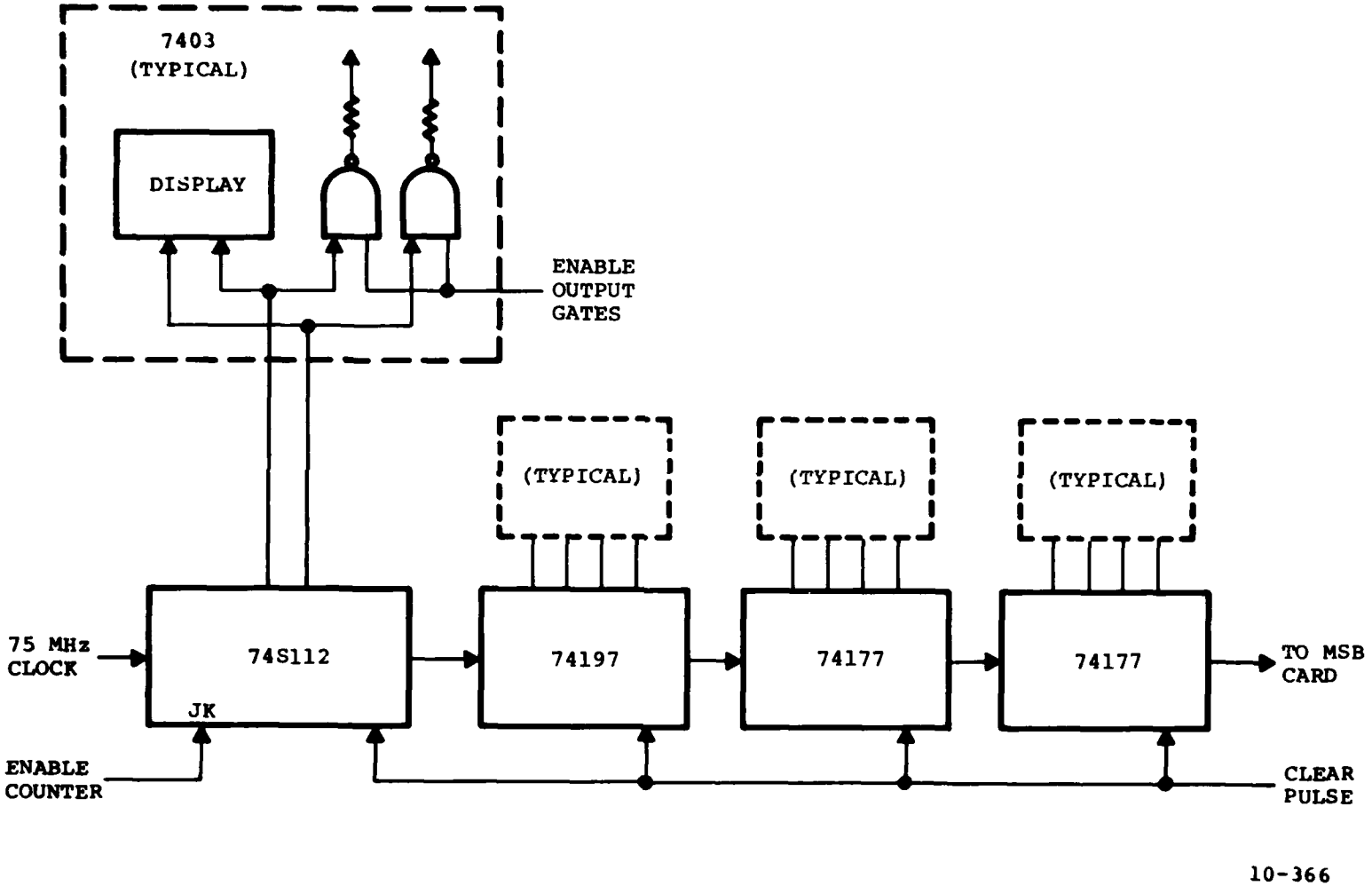

Fig. 53 14-bit binary counter.

the card layout to AMOS specifications. The drilled and etched cards were received and inspected. A prototype card was then fabricated to test the design and high frequency counting performance prior to proceeding with in-house manufacturing of the other six cards. The six other MRC cards have been fabricated including IC sockets, bypass and filtering capacitors and counter displays. Testing of the individual cards is now in progress.

A new laser ranging chassis has been designed. It includes two card cages. The circuit cards are held horizontally for the sake of readability of the on-card octal displays. Forced air cooling is used to maintain chassis temperatures in the correct range. The power supply is remote, connected to the chassis by a suitable cable. The crystal oscillator/oven is also located in the range chassis with additional thermal insulation provided to reduce oscillator frequency drift.

The front panel of the ranging chassis has the following controls:

1) Automatic/manual range gate select switch;
2) Manual range gate start delay potentiometer;
3) Manual range gate width control;
4) Automatic range gate potentiometer, ganged with the ARG width control;
5) Power on/off switch;
6) Test/operate switch;
7) Computer interrupt mode select switch.

The following numeric (octal) displays are also incorporated:

1) Each of the six MRC cards has a 5-bit octal display (14 binary bits, Least Significant Bit (LSB) is 2 meters);
2) The MSB counter card has a 3-bit octal display (8 binary bits, MSB is 2^{22} meters);
3) The ARG card has a six-octal-bit display (16-bit binary, MSB is also 2^{22} meters);
4) The time-tag counter card has a 4 bit octal display (12-bit binary, LSB is 10 microseconds).

4.10.2.2 Laser Transmitter Modifications

To optimize ranging performance, two modifications are being implemented in the laser transmitter.

Multiple Q-Switching

The existing ruby laser operates at a pulse repetition rate of 20 ppm thus providing a single range measurement every 3.0 seconds along the target trajectory. During the interval between successive measurements, target range can change in excess of a kilometer. The state vector is updated for each range realization. If a multiple Q-switching capability is added to the system, for example, a burst of 5 pulses can be produced for each firing with the pulse separation being about 150 microseconds. Target range change between pulses would be only a meter or less. It would be possible, therefore, to obtain multiple range realizations for each firing with a corresponding increase in the statistical confidence of the measurement.

The width and amplitude of the individual pulses is dependent upon the gain and length of the cavity and the stored energy in the rod. Maintaining the current (single pulse) pulse width of 20 nsec will require the system to be pumped somewhat harder and will incur some loss in the energy per pulse. Since, however, during normal Q-switch operation most of the stored energy in the rod is emitted as fluorescence, it is expected that the energy of each individual pulse in the train can be at least fifty percent of the giant pulse output. Therefore, a properly optimized system should provide about 5 pulses, each pulse having an energy of 4 or 5 Joules and a width of 20 nsec.

Since the individual pulses experience different thermal states of the ruby during the pumping cycle, the beam divergence of the pulses will also be different. This effect is not serious for high-return, retroreflector targets but could certainly be a problem for low-return targets. In principle, adaptive optics could be incorporated into the system to maintain a constant pulse beam divergence. Such are not included in the Phase II effort. Instead the system will be optimized for, say, the 3rd pulse with the first and last pulses suffering the greatest degradation. Very low cross section or extremely long range targets may, therefore, limit the number of usable pulses per firing.

During the Fall of 1978, AMOS defined the system requirements and ordered suitable hardware. Delivery is expected in

1979 at which time the new capability will be integrated into the existing hardware.

Beam Shaping

Basic goals of any laser ranging system are, of course, to maximize both the return from the target and the hit probability. This can usually be accomplished by (1) putting out more energy per pulse, (2) narrowing the beam divergence (though this places stringent requirements on pointing), and (3) optimizing the far-field beam pattern for a given energy and beam divergence.

The AMOS laser has sufficient gain to produce upwards of 20 Joules per Q-switched pulse. Hot spots currently limit the output to about 8-10 Joules due to damage thresholds for the rubies and optical components. These hot spots can be caused by two sources: (1) filamentary emission due to ruby characteristics; and (2) diffraction effects caused by sharp edged apertures in the laser system. The first is not easily eliminated and depends, essentially, on the state-of-the-art of ruby technology. The second can be solved by installing variable transmission apertures in the transmitter. Early in the Phase II program, the variable transmission aperture approach was evaluated. Based upon analysis and discussions with personnel at the Lawrence Livermore Radiation Laboratory, it was concluded that this technique would provide little, if any, improvement in AMOS system performance.

Dr. B. Johnson of Livermore suggested spatial filtering between the preamplifier and amplifier stages. Although

promising, this approach requires special optics, a diamond pinhole and an evacuated chamber to prevent air breakdown. Design and construction of such a spatial filter would, therefore, have been very costly and time consuming.

When the output pulse exits the 24-inch beam expander, its divergence can be adjusted to as little as 10^{-5} radians. Considering the normal atmospheric turbulence-induced limit of about $5x10^{-6}$ radians, a factor of at least four in irradiance could be gained, in principle, by narrowing the output beam divergence. Unfortunately, the only way to do this with the existing system would be to utilize a 48-inch beam expander which is not feasible within current funding limitations.

In summary, then, aperture shaping and narrowing of the output beam divergence do not appear viable with the present system - at least not during the Phase II program. This leaves the possibility of optimizing the far-field beam pattern.

Measurements made by AMOS personnel during the SANDIA visiting experiment (using the SANDIA laser) accentuated the need for an improved beam spoiler in the Laser Beam Director beam forming system. To minimize pointing requirements, the outgoing beam was diverged by introducing an optical plate into the expanding beam internal to the Tinsley 5X beam expander. Stepping the beam through small angles often resulted in large changes in energy on the target as determined by on-board sensors.

Shots that should have been hits were complete misses.

This can be quite bewildering to an operator if he is not aware of the effects of Fresnel diffraction on the far-field of a noncollimated beam.

Although no detailed attempt was made to map the intensity profile of the outgoing beam during the SANDIA experiment, incidental stepping of the beam to maximize hit intensity did provide useful information. Details of these and subsequent laboratory measurements are given in section 4.3.2.1 under the heading Beam Pattern Experiment.

As seen in Figure 54, part A, insertion of a thick lens, with radii of curvature equal to their distances from virtual focus of a negative lens, will have no effect on the diverging beam. If this same lens is then turned around (about its principal planes), the net power will still be zero but it will produce considerable spherical aberration in the expanding beam (Figure 54, part B). By selecting the proper parameters (distance from virtual focus, thickness and radii of curvature), a series of lenses has been designed which can be inserted in the 5x beam expander with sufficient spherical aberration to smooth out the far-field distribution. The lenses have been ordered and will be incorporated into the AMOS system in the Spring of 1979.

4.10.2.3 Laser-to-Computer Interface

Implementation of the receiver and transmitter modifications described in previous paragraphs requires a completely new laser/computer interface for the ranging system.

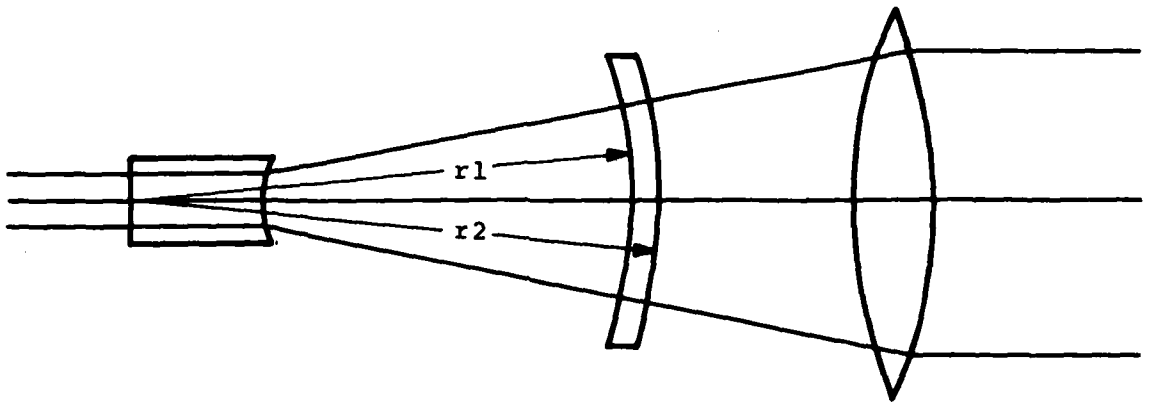

A. NON-ABERRATING

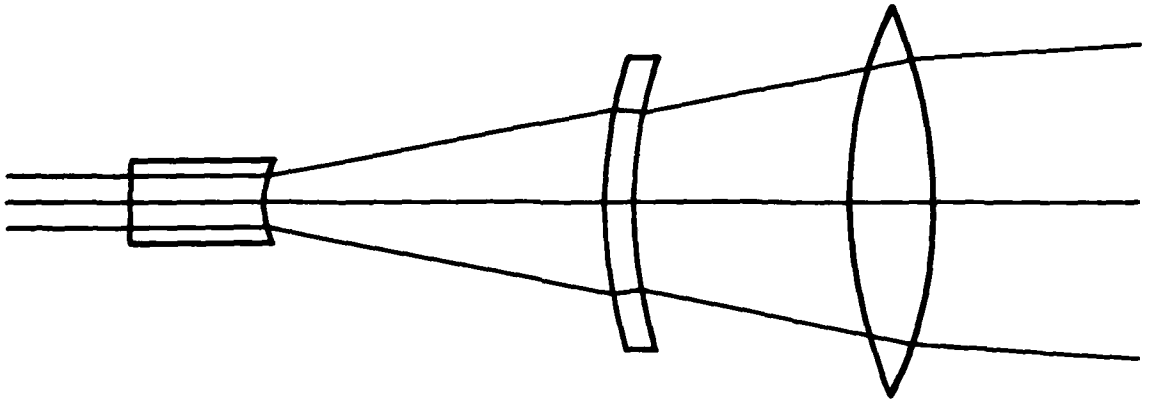

B. ABERRATING

10-363

Fig. 54 Beam shaping techique for the LBD.

Data from the Multiple Return Counters and the Most Significant Bit counter along with the contents of the Time-Tag Counter (TTC) are multiplexed to the CDC 3500 computer. As discussed previously, the outputs of the various counters are gated. The output gates are selectively enabled to connect the desired data to the lines going to the computer. Data is synchronously input to the computer as follows:

WORD 1 : TTC, 12-bits

WORD 2 : MSB counter, 8-bits

WORDS 3-8: MRC 1-6, 14-bits, 1 valid data bit.

A block diagram of the laser/computer interface is shown in Figure 55. The outgoing laser pulse generates a START pulse which then triggers a 0.17 second delay. At the end of that delay, the data transmission cycle is initiated. The delay ensures that all range returns are in and that all counters have settled.

A shift-register is used to sequentially enable the output gates in synchronization with the interrupt request signals going to the computer and the COMPLETE signals from the computer. The end of the 0.17 second delay causes a ONE to be shifted into the first stage of the shift register. Simultaneously, the Interrupt Request flip-flop is set, thus sending an interrupt request signal to the computer.

The first stage output of the shift-register is used to enable the output gates of the TTC. The TTC's data is now connected to the lines going to the computer simultaneously

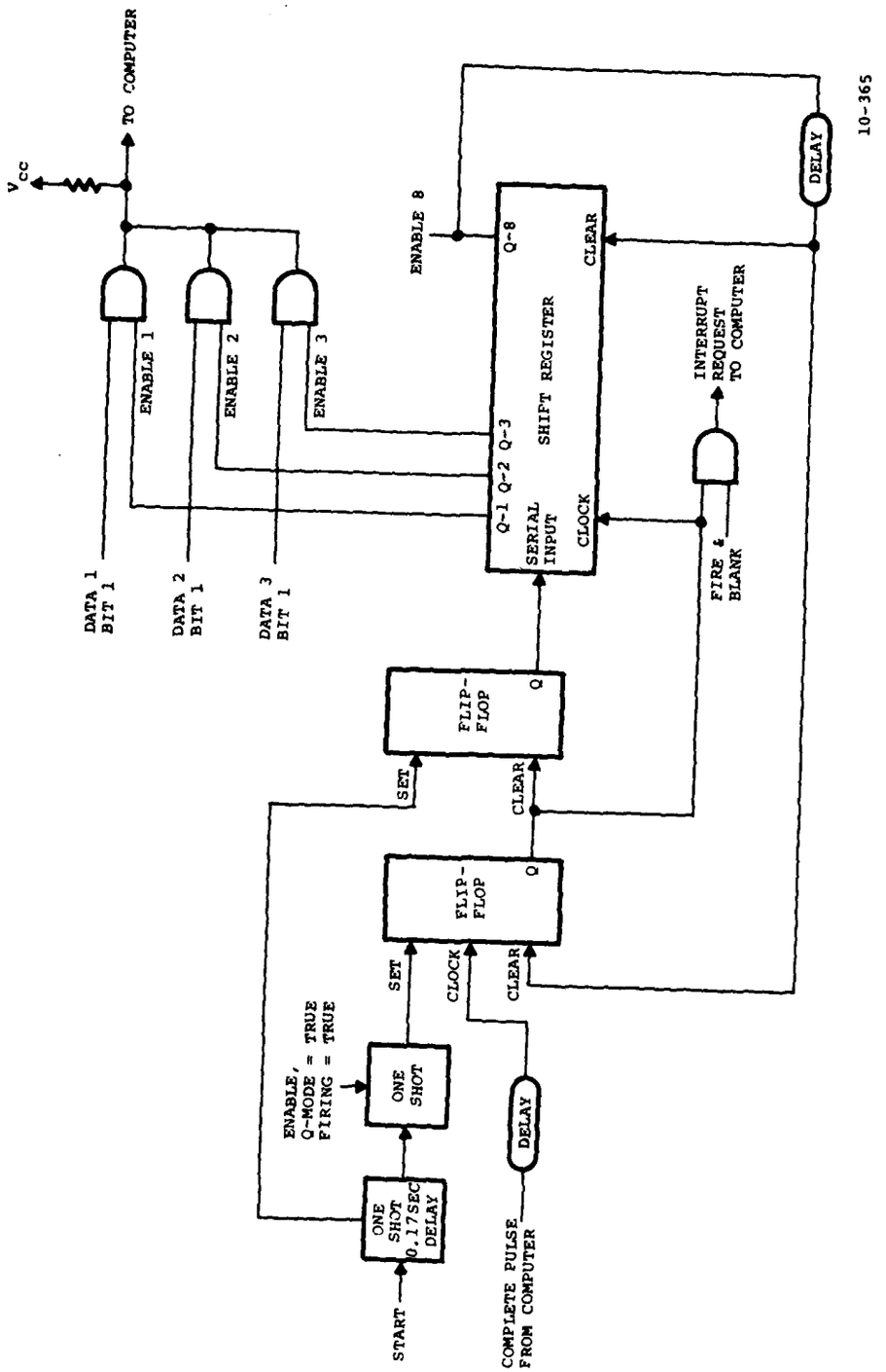

Fig. 55 Laser/computer interface.

with the interrupt request signal. As soon as the computer has acknowledged the interrupt request and read the TTC word, it transmits a COMPLETE pulse to the ranging chassis. The COMPLETE pulse clears the interrupt-request flip-flop and also clocks the ONE state of the shift-register from its first stage to its second stage.

The end of the COMPLETE pulse (via a one-shot delay) then resets the interrupt-request flip-flop and the second word is transmitted to the computer. This process is repeated until all eight words have been transmitted to the computer, at which time the shift-register is cleared. The interrupt-request line to the computer is gated with the laser's (0.2 second) FIRE & BLANK pulse. The pulse used to set the interrupt-request flip-flop is gated with the Q-switch mode and firing state of the laser. Therefore, interrupt request can only occur when the laser is firing and in the Q-switched mode.

4.10.2.4 Software Modifications

While Phase I experiments have shown the feasibility of real-time hand-off, the processing and calculations to verify the capability were of necessity done in nonreal-time. To effectively demonstrate the hand-off, the prime Phase II goal, certain additions to AMOS computer capabilities and interfacing to real-time communications equipment are required. These additions, plus some minor improvements to the software for processing beam director pointing information (found to be

deficient in the Phase I experiments) are being implemented during Phase II.

4.10.2.4.1 Improved Mount Models

Phase I error analysis showed that the accuracy achievable in laser ranging measurements makes other parameters in the trajectory estimation process influential in the hand-off error volume. For example, angle measurement errors dominate the error ellipsoids in the direction along the target's velocity vector.

During the Phase II program, existing procedures, algorithms and models are being reviewed to ensure that inaccuracies are not being inadvertently included. Truncation errors, insufficient terms included in computations, parameters inaccurately or incompletely defined, outdated coordinate systems, and other factors, are being investigated in an attempt to make the final state vector a more optimized product.

Work during the Fall of 1978 centered around modifications to the AMOS modeling software. Significant changes to the model were completed and first tested by computer simulation. A brief description of the differences between the old and new models for the Cassegrain telescopes follows:

1) The polar axis flexure f_p, is deleted;
2) A new parameter, declination box flexure f_{DB}, is added;
3) The parameters for declination shaft angle offset dependence on polar angle are deleted;

4) The shared parameters, polar shaft angle offset and inclination, are changed to independent parameters for each 1.2 m Telescope;

5) A class of second-level shared parameters for sensors which share the same telescope is created, which includes polar shaft angle bias, inclination and declination axis flexure.

Modifications to model parameter estimation software (AUTOCON3) were made to accommodate the new model. The new program (AUTOCON4) deletes some of the capabilities of AUTOCON3 in favor of simpler, reasonably well-structured software and conversational-style operation. In particular, the following changes were made:

1) Run-to-run coupling by saving the covariance matrix on disk is deleted;

2) All parameters, except shaft angle offsets, are reset at the beginning of each run and the covariance matrix is set to 10^{-8} diagonal;

3) Post update residual RMS is tested before updating the disk mount parameter file;

4) The user must specify which mount he wants to process and may specify marks to be deleted;

5) Much of AUTOCON3 is reorganized into subroutines to improve readability of the listing;

6) Three logical units are defined for messages to

the operator/user, commands from the operator/user, and normal output.

During the latter part of September, the software modifications were evaluated at AMOS. The new mount model subroutine was integrated into the real-time tracking program, transitioned to operational status, and the coefficient estimator was established as part of standard nonreal-time software. Additional software for quick pointing verification test data reduction (POINTEST) was also established.

Four sets of stellar observations from the 1.2 m and the 1.6 m Telescopes were acquired and processed. The hydraulic fluid temperature control systems were in operation for both mounts. Generally, the three temperatures - air, mount and oil - were within one degree of each other and constant throughout the observation periods. The statistics for the post-estimate residuals for the first data set are shown in Table 6. The estimate of astronomical refraction at 45° elevation from the 1.2 m observations was identical to that reached independently from the 1.6 m observations.

Pre- and post-estimate residuals for data set 2 are given in Table 7. The CSP (Classical Sensor Package) parameters determined from data set 1 yielded rather good pointing performance two nights later, judging from the pre-estimate statistics. On this night, the estimator gave 40.2 arcseconds for the refraction coefficient. The difference from the nominal value of 40.6 arcseconds cannot account for all of the 2 arcseconds

TABLE 6 POST-ESTIMATE RESIDUAL STATISTICS DATA SET 1
(20 SEP 78)

SENSOR	Sample Size	Sample Mean ($\widehat{sec}$)	Sample Deviation ($\widehat{sec}$)
B29 POL	58	-0.0	1.3
B29 DEC		-0.1	2.1
B37 POL	61	-0.0	1.9
B37 DEC		-0.0	2.8
18.6 POL	64	-0.2	5.0
18.6 DEC		-0.2	6.4
CSP POL	65	-0.0	2.3
CSP DEC		-0.0	1.7

TABLE 7 PRE- AND POST-ESTIMATE RESIDUALS DATA SET 2
(22 SEP 78)

SENSOR	Sample Size	Before		After	
		Sample Mean ($\widehat{sec}$)	Sample Deviation ($\widehat{sec}$)	Sample Mean ($\widehat{sec}$)	Sample Deviation ($\widehat{sec}$)
CSP	48 POL	-2.2	2.8	0.0	2.3
	DEC	-1.7	1.9	-0.0	1.5
10"	53 POL	33.6	32.3	0.8	13.3
	DEC	100.0	11.7	-0.0	12.6

mean pointing error. The pre-update residuals for the 10-inch acquisition telescope are large because its model parameters were set equal to the CSP parameters. Six iterations were required to reduce the mean error below 1 arcsecond. The field-of-view of the 10-inch telescope is about 1 degree, so the fit (sample deviation) is about 0.4 of 1 percent of the field-of-view per axis. The corresponding number for the CSP is about 1.5 percent. The estimator conservatively assumes that the measurement error statistics are Gaussian, with standard deviation equal to 4 percent of the field-of-view for each axis.

Data set 3 results are presented in Table 8. The mean pointing errors for the CSP are extremely small, but the sample deviations are somewhat larger than the expected measurement noise which suggests that systematic errors remain. The post-estimate sample deviations are very small, and probably represent almost entirely the errors in the measurement process.

The residual statistics for data set 4 are given in Table 9. These results are extraordinary -- the estimator deviations of 1.4 arcseconds were, in the past, unusually good; here this level of performance was achieved before doing the estimate using one day old mount model parameters.

4.10.2.4.2 Automatic Range Gate and Multiple Return Sorting

New software is required to augment the automatic range gate and multiple return capabilities discussed previously. Preliminary planning was accomplished in late 1978. The

TABLE 8 PRE- AND POST-ESTIMATE RESIDUALS DATA SET 3
(25 SEP 78)

SENSOR		Before			After	
		Sample Size	Sample Mean (sec)	Sample deviation (sec)	Sample Mean (sec)	Sample Deviation (sec)
CSP	POL	68	1.1	2.9	-0.0	1.1
	DEC		1.0	2.0	-0.0	0.9
10"	POL	57	7.6	8.9	-0.1	6.9
	DEC		1.0	11.8	1.0	10.7

TABLE 9 PRE- AND POST-ESTIMATE RESIDUALS DATA SET 4
(26 SEP 78)

SENSOR		Before			After	
		Sample Size	Sample Mean (sec)	Sample Deviation (sec)	Sample Mean (sec)	Sample Deviation (sec)
CSP	POL	67	-1.5	1.4	-0.0	1.1
	DEC		-0.5	1.4	-0.0	0.8

software is scheduled for completion in the Spring of 1979.

4.10.2.4.3 Kalman Filter Modifications

Key to the Phase II demonstration of a real-time hand-off is the necessity of processing range and angle observations on-line. At present, the Kalman filter (using the CDC 3500 computer) processes only angles data. To give the added dimension of range, it is necessary to modify the state estimator. Although range data is presently input to the computer it is now only used in data recording. The Kalman estimator has the capacity to handle the additional range input, but modifications to the software are required. Prior to the hand-off demonstration, the Kalman filter will be restructured as described below to incorporate range measurements and to accommodate the error sources which were identified in the nonreal-time Phase I analyses.

The parameters of estimation for the real-time Kalman filter are the elements of the target variational vector $d\bar{X}$. It is necessary to define the transformation, to first order, between the observation error (dD) and the Kalman parameters of estimation ($d\bar{X}$):

$$dD = \left[B \right] \quad d\bar{X}.$$

The transformation matrix $\left[B \right]$ is the first order term of the Taylor series expansion for dD.

The following definitions apply;

$\bar{X}(t) = x, y, z, \dot{x}, \dot{y}, \dot{z}$

target state vector in earth-centered inertial (ECI) coordinates,

$\bar{X}(t) = x_b, Y_b, z_b$

target position vector in beam director coordinates centered at flat,

$R_b = (x_b^2 + y_b^2 + z_b^2)^{1/2}$

target range relative to beam director,

$\bar{X}_{1.6}(t) = x_{1.6}, Y_{1.6}, z_{1.6}$

target position vector in 1.6 m mount coordinates centered at laser receiver,

$R_{1.6} = (x_{1.6}^2 + Y_{1.6}^2 + z_{1.6}^2)^{1/2}$

target range relative to laser receiver,

D = laser/receiver target measurement

$dD = D - (R_b + R_{1.6})$

laser/receiver target measurement error,*

---

* LSB of input data is 4m (i.e. uncertainty = $\pm$2m due to receiver electronics)

$$\bar{X}_r(t) = \{x_r, Y_r, z_r, \dot{x}_r, \dot{y}_r, \dot{z}_r\}$$

reference state vector (ECI),

$$\overline{dX}(t) = \bar{X}(t) - \bar{X}_r(t)$$

target variational vector.

We let $\left[E\right]_b$ and $\left[E\right]_{1.6}$ represent coordinate rotation matrices and $\bar{W}_b$ and $\bar{W}_{1.6}$ represent translation vectors such that:

$$\bar{X}_b = \left[E\right]_b \bar{X} + \bar{W}_b \ ;$$

$$\bar{X}_{1.6} = \left[E\right]_{1.6} \bar{X} + \bar{W}_{1.6}$$

The derivation is then straightforward as follows:

$$R_b = (x_b^2 + y_b^2 + z_b^2)^{1/2}$$

$$R_{1.6} = (x_{1.6}^2 + y_{1.6}^2 + z_{1.6}^2)^{1/2}$$

$$D = (R_b + R_{1.6})^{**}$$

$$dD = \frac{\partial D}{\partial R_b} dR_b + \frac{\partial D}{\partial R_{1.6}} dR_{1.6} = dR_b + dR_{1.6}$$

$$dR_b = \frac{\partial R_b}{\partial x_b} dx_b + \frac{\partial R_b}{\partial y_b} dy_b + \frac{\partial R_b}{\partial z_b} dz_b = \left[H\right]_b \overline{dX}_b$$

** In this equation, D is the calculated value (the notation is not rigorous).

where $\left[H\right]_b = \bar{X}_b / R_b$.

Similarly:

$$dR_{1.6} = \left[H\right]_{1.6} dx_{1.6}$$

where $\left[H\right]_{1.6} = \bar{X}_{1.6} / R_{1.6}$.

Since $\overline{dX}_b = \left[E\right]_b \overline{dX}$,

and $dX_{1.6} = \left[E\right]_{1.6} dX$,

therefore $dD = \left[B\right] \overline{dX}$,

where $\left[B\right] = \left[H\right]_b \left[E\right]_b + \left[H\right]_{1.6} \left[E\right]_{1.6}$.

We now must look at the nature of $\left[E\right]_m$ and $\bar{W}_m$.

We have,

$$\bar{X}_m = \left[D\right]_m \left[C\right]_m \left(\left[A\right] \bar{X} + \bar{U}_m \right) + \bar{V}_m ,$$

where

$\left[A\right]$ = ECI to ECR rotation matrix,

$\bar{U}_m$ = site translation vector,

$\left[C\right]_m$ = ECR to local horizon rotation matrix,

$\left[D\right]_m$ = local horizon to mount rotation matrix,

$\bar{V}_m$ = mount to sensor translation vector.

Therefore:

$$\left[E\right]_m = \left[D\right]_m \left[C\right]_m \left[A\right]$$

$$\bar{W}_m = \left[D\right]_m \left[C\right]_m \bar{U}_m + \bar{V}_m \quad .$$

The matrices $\left[D\right]_m$, $\left[C\right]_m$ and $\left[A\right]$ and the vectors $\bar{U}_m$ and $\bar{V}_m$ are all available in the EROS system.

The site translation vector $\bar{U}_m$ is the position of the site in ECR rectangular coordinates and, therefore, a function of the earth model parameters.

The covariance matrix Q of the measurement D is required as given information describing the assumed known variance of the measurements.

$$Q = \sigma_D^2$$

Phase I measurements, as discussed previously, have shown that σ_R is the order of 2 meters for the AMOS system, where $\sigma_R = 1/2\sigma_D$.

The EROS Kalman processing capability was designed to facilitate relatively easy extensions to new measurements when available. In order to incorporate the above algorithms into the system, two new subroutines must be developed; DOLSR which is the laser processing control task, and LASER which contains the Kalman logic specific to laser measurements. DOLSR will be activated when laser data buffers are dequeued by the EROS CDC 3500 subsystem. It must convert the raw hardware inputs (including multiple returns) into a time-tagged range measurement in CDC 3500 floating point units of seconds and meters. The second subroutine, LASER, is required to calculate the observation error dD and its associated $\left[B \right]$ and $\left[Q \right]$ matrices. This software is scheduled to be operational by June of 1979.

4.10.2.4.4 Hand-off Software

Once the state estimator is upgraded, it will be necessary to interface the resultant state vector outputs to the existing data communication system. This will include transformations to user-agreed coordinates, formatting for range (WTR) compatibility and producing mutually acceptable data rates throughout the observation interval. Initial discussions have taken place with personnel who operate one of the sensors that is a candidate to receive AMOS data during Phase II. These discussions have allowed the efforts involved in this task to be defined. The task is scheduled for completion by June of 1979.

4.10.2.5 Measurements

During the week of 25 September, range and angle data was obtained on three passes of GEOS-C and three passes of LAGEOS. The new model software described previously was utilized. Ranging data showed average shot-to-shot jitter of about 2 meters (i.e., excellent performance). The three GEOS-C passes are summarized in Table 10.

Responsibility for preparing high-accuracy orbits for GEOS-C from Doppler observations has moved from the Naval Surface Weapons Center to the Defense Mapping Agency (DMA) Aerospace Center (St. Louis). The software is the same, but it now operates routinely. Orbit data for all three phases reached AERL 19 days after calling in the request. The DMA orbit determination uses the GEM-10 gravity coefficients and NWL-9Y station coordinates. Each determination spans 2-1/4 days of observations (32 revolutions), with 1/4-day overlap from one determination to the next. Orbits are consistent to the order of 1 meter in the overlap interval. DMA quotes position accuracy as about 1 meter in range and about 5 meters in-track and cross-track.

The metric calibration program is an augmented version of the one used for Phase I. The primary change is an algorithm for correcting calculated path length to account for displacement between the GEOS-C center of mass and the laser retroreflector.

TABLE 10 LASER RANGING MISSIONS DATA SUMMARY
GEOS-C

Rev. No.	Date (UT)	Data Span (UT)	No. of Range Observation	No. of Angle Observations
17900	26.10.78	0501:26 to 0514:16	47	66
17914	27.10.78	0454:14 to 0501:17	45	88
17928	28.10.78	0441:02 to 0447:16	51	51

The correction term is,

$$\Delta R = 1.411 - 0.036 \left(\frac{\gamma}{+0.0524}\right) \cos (\gamma - 0.3922) \text{ meters}$$

where γ is the angle of incidence in radians and

$$\tan \gamma = \frac{R_s \cos e}{R + R_s \sin e}$$

where

R = slant range (observer to target),

R_s = distance from center of earth to observer,

e = target elevation at observer.

The correction term reduces the slant range calculated from the DMA state vectors by the order of 1 meter. The formula is taken from "Prelaunch Testing of the GEOS-3 Laser Retroreflector Array", Minot et al, NASA Tech Paper 1138, January 1978.

In spite of careful efforts to express AMOS coordinates on the NWL-9Y ellipsoid, the range residuals showed a signature characteristic of observer position bias. Figure 56 shows range residuals before and after translating the observer with respect to the target. The shift is the same for all missions.

All three missions respond to the same ad hoc shift in spite of the variation in observation geometry, which suggests that the bias is real. This does not mean that the AMOS site coordinates are wrong, since the shift can be applied to targets position with exactly the same result. The correction term is considered as a factor for use only with DMA GEOS-C orbits.

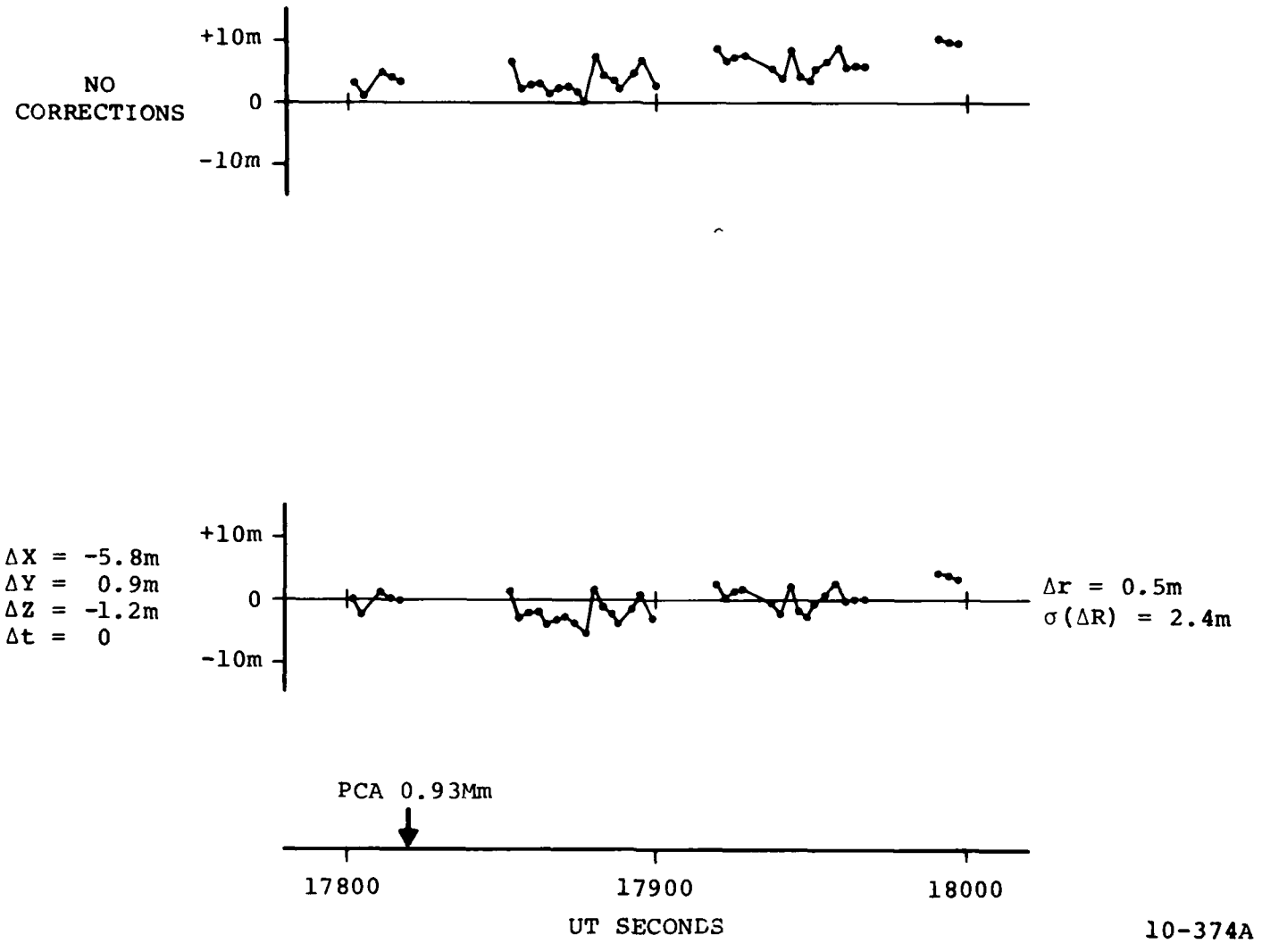

Fig. 56 GEOS-C range residuals.

The results of these measurements confirm the Phase I analysis and justify the conclusion that, once the modifications and upgrades described in previous paragraphs are completed, AMOS will be able to hand-off a ballistic target to a downrange sensor to better than 500 feet, 3σ. This demonstration is scheduled for the Summer of 1979.

AMOS GLOSSARY/ACRONYMS

AATS	AMOS ACQUISITION TELESCOPE SYSTEM
ACONS	AMOS CONTROL SOFTWARE
A/D	ANALOG TO DIGITAL
AERL	AVCO EVERETT RESEARCH LABORATROY
AF	AUTO-FOCUS
AFWL	AIR FORCE WEAPONS LABORATORY
AIDS	AMOS INTERNAL DATA STORAGE
AMOS	ARPA MAUI OPTICAL STATION
AMTA	ADVANCED MULTI-COLOR TRACKER FOR AMOS
ANK	ALPHANUMERIC KEYBOARD
ARG	AUTOMATIC RANGE GATE
ASTEP	AMOS SATELLITE TRACKING EVALUATION
ATN	AMOS TEST NUMBER
BMD	BALLISTIC MISSILE DEFENSE
BMDATC	BALLISTIC MISSILE DEFENSE ADVANCE TECHNOLOGY CENTER
BTU	BUFFER TRANSFER UNIT
CCU	CAMERA CONTROL UNIT
CDC	CONTROL DATA CORPORATION
CDRL	CONTRACT DATA REQUIREMENTS LIST
CI	COMPENSATED IMAGING
CIS	COMPENSATED IMAGING SYSTEM
CSP	CLASSICAL SENSOR PACKAGE
DARPA	DEFENSE ADVANCED RESEARCH PROJECTS AGENCY
DMA	DEFENSE MAPPING AGENCY

AMOS GLOSSARY/ACRONYMS

DOD	DEPARTMENT OF DEFENSE
FACC	FORD AEROSPACE COMMUNICATIONS CORPORATION
FLIR	FORWARD LOOKING INFRARED
FOV	FIELD-OF-VIEW
HP	HEWLETT PACKARD
HSSR	HIGH SPEED SHIFT REGISTER
IC	INTEGRATED CIRCUITS
IID	INTERFACE INFORMATION DOCUMENTS
IR	INFRARED
ISIT	INTENSIFIED SILICON INTENSIFIER TARGET
LBD	LASER BEAM DIRECTOR
LLLTV	LOW LIGHT LEVEL TELEVISION SYSTEM
LSB	LEAST SIGNIFICANT BIT
LTI	LONG TERM INTEGRATION
LWIR	LONG WAVE INFRARED
MIT/LL	MASSACHUSETTS INSTITUTE OF TECHNOLOGY/LINCOLN LAB
MIOP	MISSION INSTRUCTION AND OPERATION PLAN
MOTIF	MAUI OPTICAL TRACKING AND IDENTIFICATION FACILITY
MRC	MULTIPLE RETURN COUNTERS
MSB	MOST SIGNIFICANT BIT
NBS	NATIONAL BUREAU OF STANDARDS
NORAD	NORTH AMERICA AIR DEFENSE
NSWC	NAVAL SURFACE WEAPONS CENTER
PMC	PHOTOMULTIPLIER CIRCUIT

AMOS GLOSSARY/ACRONYMS

PMEL	PRECISION MEASUREMENTS EQUIPMENT LAB
PRR	PULSE REPETITION RATE
RADC	ROME AIR DEVELOPMENT CENTER
RMS	ROOT MEAN SQUARE
RTAM	REAL-TIME ATMOSPHERIC MONITOR
SAE	SHAFT ANGLE ENCODER
SAMSO	SPACE AND MISSILE SYSTEMS ORGANIZATION
SC	SEQUENCE CONTROLLER
SEP	SAMSO EVALUATION PROGRAM
SOI	SPACE OBJECT IDENTIFICATION
TI	TEXAS INSTRUMENTS
TM	TECHNICAL MEMORANDA
TTC	TIME-TAG COUNTER
WTR	WESTERN TEST RANGE

MISSION
of
Rome Air Development Center

RADC plans and executes research, development, test and selected acquisition programs in support of Command, Control Communications and Intelligence (C^3I) activities. Technical and engineering support within areas of technical competence is provided to ESD Program Offices (POs) and other ESD elements. The principal technical mission areas are communications, electromagnetic guidance and control, surveillance of ground and aerospace objects, intelligence data collection and handling, information system technology, ionospheric propagation, solid state sciences, microwave physics and electronic reliability, maintainability and compatibility.